Novel Cross-linkable Polymeric Membranes For Organophilic Ultra- and Nanofiltration

by

Zhaoqing Pei

Thesis submitted to the Department of Chemistry of
Universität Duisburg-Essen, in partial fulfillment of
the requirements of the degree of
Dr. rer. nat.

Approved by the examining committee on

Chair : PD Dr. Ursula Telgheder

Advisor : Prof. Dr. Mathias Ulbricht

Reviewer : Prof. Dr. Jochen S. Gutmann

Date of oral examination: 14.01.2013

Essen, 2012

Abstract

Membrane technology is being applied in more and more processes involving organic solvent, examples are re-use of catalytic species, purification of synthesized products, edible oil processing, solvent recovery and solvent exchange. To meet the requirements of these applications, the membranes are required to have the following properties: they should have the desired selectivity combined with a high permeability, as well as good stability in the organic solvents and under the required conditions of temperature and pressure.

Two novel copolymers that can be applied to prepare solvent resistant nano-/ultrafiltration (SRNF/UF) membranes have been developed: block copolymers of acrylonitrile (AN) and polyethylene glycol (PEG), this block copolymer can be used either directly to prepare ultrafiltration membranes that are resistant to many kinds of organic solvents, or cross-linked via post-treatment and converted to nanofiltration (NF) membranes and they are stable even in extremely aggressive organic solvents; copolymers of AN and 2-acrylamido-2-methyl-1-propanesulfonic acid (AMPS), which can directly form nanofiltration membranes for aqueous conditions, it is also possible to cross-link the membranes via post-treatment thus applicable in non-aqueous conditions or to improve the rejection of salts.

For the synthesis of block copolymers of PAN and PEG, it was unconventional free radical copolymerization initiated by cerium(IV)-PEG redox system. The reaction conditions have been optimized. The composition of the copolymers was characterized by attenuated total reflection infrared spectroscopy (ATR-IR), ^{1}H-NMR, element analysis, and the molecular weight information was studied by gel permeation chromatography (GPC). The free radical concentration in the initiation step was studied with the help of stable free radical. From the compositions of the copolymers and the experiments on the free radicals, the proposed mechanism of the reaction was proved to be true. Furthermore, because of the mechanism of the polymerization, the copolymers were exclusively block copolymers. Membranes from the block copolymers were prepared via non-solvent induced phase separation. Because of low solubility of the block copolymers in dimethylformamide (DMF), dimethyl sulfoxide (DMSO) or N-methylpyrrolidone (NMP), it was not possible to prepare polymer solutions with concentration higher than 16%, therefore, only ultrafiltration (UF) membranes were

formed. From the research on the membrane performance and pore morphologies as well, the concentration had strong influence on the properties of the resulting membranes. Variation of other parameters in the preparation steps was made to find out the optimized conditions for membranes and also to derive membranes with distinct separation performances. The membranes were also tested in several normal organic solvents, and the results showed that the membranes were stable in these solvents; therefore they are applicable in some SRUF processes. After cross-linking as post-treatment, the membranes were stable in almost all the organic solvents including DMF, NMP and so on, so application of the membranes can be greatly broadened. With another post-treatment to convert the membranes to NF types, the membranes became largely densified, the finally resulting membranes were endowed with excellent pure solvents permeability, solvent resistance and good rejection of polymers in both aqueous and organic conditions. Besides, the membranes were also capable to reject salts in aqueous solutions at an acceptable level. It was also possible to adjust the separation properties of the membranes by changing the conversion conditions, therefore, the membranes can be used in most SRNF applications as well as in aqueous NF applications.

For the copolymers of AN and AMPS, they were synthesized via typical free radical polymerization initiated by azobisisobutyronitrile at elevated temperature. The reaction conditions have been optimized. The composition of the copolymers was characterized by ATR-IR, ^{1}H-NMR, element analysis, and the molecular weight information was studied by gel permeation chromatography (GPC). Reactivity ratio of these two monomers were studied in real condition synthesis, and found to be similar to each other and close to 1. Therefore, copolymers tended to be random copolymers. Because of the similar reactivity ratios, it was possible to change the compositions of the copolymers freely, thus to influence the separation properties. It was not possible to prepare polymer solutions with concentration higher than 6%, but the resulting membranes were rather dense even from lower concentration. From the filtration experiments, it was found that all the membranes were dense as well in application. The composition of copolymers also had clear influence on the separation performance and influence of other parameters during the preparation step was also studied to get the optimal conditions for that. The resulting membranes were endowed with both high water permeability and high rejection of PEGs, but the rejection of salts was relatively low, which was probably because of the low charge density in the membranes,

since the charge was provided by sulfonic acid groups in AMPS, and the mole ratio of AMPS in the copolymers was low. In order to improve the salt rejection, content of AMPS have to be increased, and then a cross-linking process would be needed, otherwise the copolymers were water soluble. Therefore, this part of work needs and is worth further research.

This study provides a novel method to synthesize SRNF/UF membranes, and also develops a new type of NF membrane for aqueous condition using conventional method.

This thesis is dedicated to

my wife (Xiaowei Sun)

for her love, endless support and encouragement.

This work was performed during the period from October 2008 to February 2012 in the Institute of Technical Chemistry (Lehrstuhl für Technische Chemie II), Department of Chemistry, Universität Duisburg-Essen, under the supervision of Prof. Dr. Mathias Ulbricht.

I declare that this dissertation represents my own work, except where due acknowledgement is made.

Zhaoqing Pei

Acknowledgements

This thesis could not have been completed without the help and support of many people and organizations that are gratefully acknowledged here.

At the very first, I would like to express my deepest gratitude to my supervisor, Prof. Dr. Mathias Ulbricht for the supervision and support. With his qualified guidance I could have worked out this dissertation. He has offered me not only valuable ideas and suggestions with his profound knowledge and ample research experiences, but also supervised me to think critically and arrange things systematically. Moreover, ha also paid attention to my private life when I lived in Germany with my family during the study.

I would like to give best thanks as well to CSC (China Scholarship Council) for providing me the three-year scholarship to support my PhD study in Germany. I am greatly grateful to Consul Lin Wang for the help of scholarship arrangements and extension.

I would like to thank the group of Prof. Dr. Thomas Schrader (Organische Chemie, UDuE) for the help with the FTIR measurements, S. Boukercha (Anorganische Chemie, UDuE) for the SEM analyses, D. Jacobi (Technische Chemie, UDuE) for the GPC measurement, and V. Hiltenkamp for the elemental analysis.

I would like to thank Dr. Mahendra Kumar (Technische Chemie II, UDuE) for the very valuable discussion and suggestions, and to all members of our research group at Lehrstuhl für Technische Chemie II, Universität Duisburg-Essen, namely, Inge, Claudia, Tobias, Christian, Sven, Qian, Dongxu, Haofei, Nico, Bintasan, Heru, Jun, Nkem, Jing, Falk, Polina, Nadia and Frau Nordmann for the nice discussion and environment.

At last, I would love to express my special thanks to my wife, my parents and parents-in-law for their deepest love, understanding and support, all through my PhD study. Best thanks are also given to my uncle of blessed memory, for his considerate support and endless love.

Table of Contents

List of tables

List of figures

Chapter 1. Introduction

1.1. Background and motivation

Nanofiltration is a relatively recent pressure-driven process, and NF membranes have been used increasingly because of their advantages such as relatively low operating pressures, high fluxes and low operating and maintenance costs [1]. NF membranes were mostly applied as alternative to reverse osmosis membranes for the purification of water by eliminating bivalent or trivalent salts and for the removal of middle to low molar mass molecules from aqueous solutions [2-4].

Nowadays, the demand for the application of NF membranes in non-aqueous systems is increasing rapidly in several strategic fields, They include materials recovery from dyeing industry, separation of active pharmaceutical compounds, residual reactants or solvents in pharmaceutical synthesis, separation of homogeneous catalysts from organic solutions, separation of mineral oil from organic solvents, separation of free fatty acids from vegetable oil and separation of light hydro-carbon solvents from lube filtrates [4-18]. Whereas, the solvent-resistant nanofiltration (SRNF) membranes are required instead of applying the already existing NF membranes for aqueous systems. There are some commercially available SRNF membranes which were designed for specific applications, but some of them were reported to fail in an extended run [4]. A number of novel SRNF membranes are also under development [5, 19-21].

1.2. Objectives of this research

The objective of this project is to produce solvent resistant ultra- and/or nanofiltration membranes based on polyacrylonitrile (PAN), with both high permeability and rejection, and the membranes are expected to have both chemical and mechanical stabilities. To achieve this goal, several investigations in the following will be required:

(i) To investigate the effect of various parameters during the copolymers synthesis on the composition and structure of the resulting copolymers, hence the mechanical and the chemical stability of the membranes.

(ii) To investigate the influence of parameters in membranes preparation on the structure and separation performance of the resulting membranes.

(iii) To find out optimized condition for post treatments to get desired membrane performance.

1.3. Scope of the thesis

There are already several membrane processes applied in the application under organic conditions, which indicates the large potential of pressure driven membrane processes in this field. However, the development of the membrane technology for non-aqueous applications lags behind for the reasons like chemical and mechanical resistance of membranes and modules under organic conditions. Improvements in material and optimization of membrane synthesis could extend the possibilities for wider application. This will be the main scope of this work.

Two types of polymeric membranes were researched and developed:

1) Cross-linked membranes based on block copolymer of PAN and PEG
2) Cross-linkable membranes based on copolymer of PAN and AMPS

In the case of PAN-b-PEG, a study on the synthesis of block copolymers using unconventional water phase precipitation radical copolymerization was first carried out. Detailed characterizations for figuring out the composition and other important properties of the copolymers were performed, which includes ^{1}H-NMR, ATR-IR, element analysis by CHNS analysis and GPC. Influence of different parameters on the resulting copolymers was studied.

Membranes from this block copolymer were then developed. While it is not possible to directly prepare nanofiltration membranes from this copolymer, the performance of the membranes in ultrafiltration processes was first studied. Cross-linking as post treatment was then carried out to enhance the chemical stability and to improve the performance in organic solvents. The cross-linked membranes were tested in extreme conditions to prove the wide applicability in organic solvents filtration processes. After cross-linking, another

post treatment to convert the membranes into nanofiltration type was performed, the eventual organic solvent resistant nanofiltration membranes were derived. The performance of the membranes in organic solvents nanofiltration process was researched.

A second approach was to develop another copolymer based on PAN, and to prepare membranes from this copolymer. Study on the characterizations of the copolymers was necessary, nanofiltration membranes can be directly formed from this copolymer, and the performance in nanoflitraion was evaluated. Influence of various parameters was studied to get the optimized membrane properties which are evaluated with two classic output parameters, namely permeability and retention.

Chapter 2. Theories

2.1 Membrane technology

A membrane is a selective barrier between two phases [22]. Membranes are being applied in a wide and diverse range of occasions, one important example of which is the huge desalination plants spreading all around the world especially in the Middle East for producing drinking water. Depending on the application, different membrane morphologies will be used. A schematic representation of various morphologies is given in Fig. 2.1. Several types of membrane separation mechanisms exist. In membrane applications where the solution diffusion mechanism plays the major role, the membrane material is chosen based on the selective sorption and diffusion properties, membrane morphology will be not the main factor to affect the selectivity but it is still important as regarding to total flux.

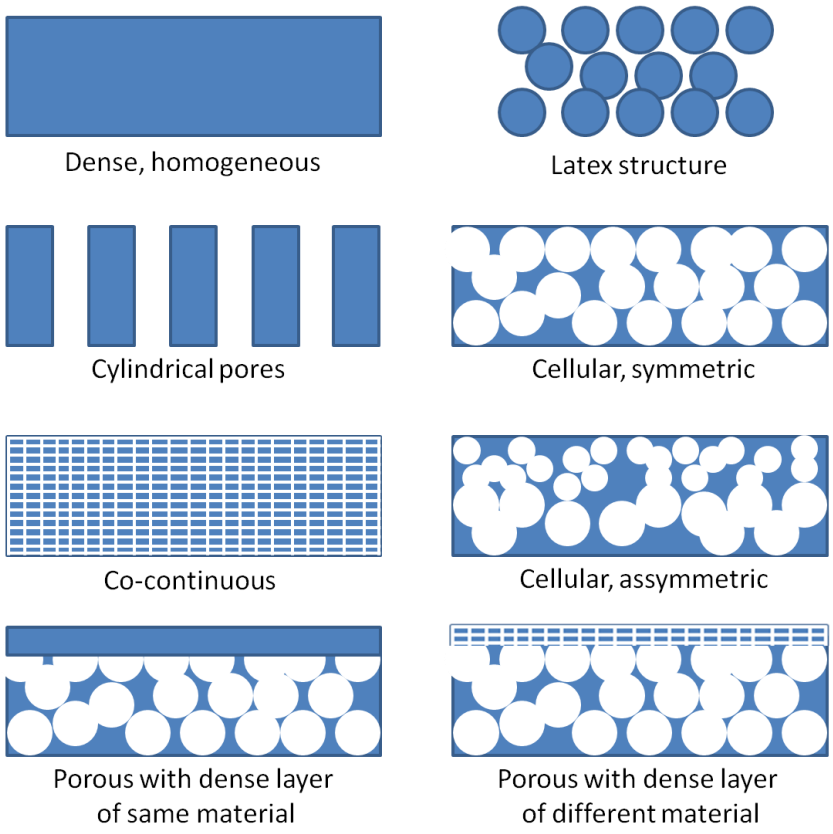

Fig. 2.1 Schematic representation of different membrane morphologies

In all the membrane processes, driving force is essential to deliver the energy to separate the feed molecules; commonly applied driving force includes pressure, electrical potential, temperature, concentration or partial pressure gradient. The most widely used pressure driven processes are generally classified as microfiltration (MF), ultrafiltration (UF) and hyperfiltration, which is normally subdivided in reverse osmosis (RO) and nanofiltration (NF). However, the difference between the processes is not always so sharp, which can be seen from Table 2.1, summarizing the main characteristics of various membrane processes, in which, typical permeability is for solvent mixture.

Table 2.1 pressure driven membrane processes

Membrane process	Typical pressure (bar)	Typical permeability (l/(m^2·h·bar)	Morphology of the selective layer
Microfiltration	0.1-2	>50	Porous
Ultrafiltration	1-5	10-50	Porous
Nanofiltration	5-20	1.4-12	Porous/Dense
Reverse Osmosis	10-100	0.05-1.4	Dense

The membrane efficiency for pressure driven separations is evaluated by the retention (Eq. 2-1) and the permeability (Eq. 2-2):

$$\text{Retention } (\%) = \left(1 - {C_p}/{C_f}\right) \times 100\% \tag{2-1}$$

$$\text{Permeability } (\mathrm{l}/(\mathrm{m}^2 \cdot \mathrm{h} \cdot \mathrm{bar})) = {V_p}/{(A_m \cdot t \cdot p)} \tag{2-2}$$

Where C_p is the solute concentration in permeate [mol/l or wt%], C_f is the solute concentration in the feed solution, V_p is the volume of permeate [l], A_m is the active membrane surface [m^2], t is the permeation time [h] and p is the pressure [bar]. To characterize the membranes, the concept of molecular weight cut-off (MWCO) is often used.

The MWCO is defined as the molecular weight of the solute, which is 90% rejected by the membrane.

2.2 Solvent resistant nanofiltration and ultrafiltration membranes

During the 1990s, green chemistry has come to the fore as a way of developing focus on more atom efficient chemical process [23]. The conventional chemical industry has to face the vision of increasing the efficiency of chemicals especially the solvents engaged in the reaction of in other processes. SRNF as an emerging field can offer a better solution for solvent intensive processes to yield the significant environmental and cost benefits. SRNF was then attracting more attention and getting applied in wider field.

2.2.1 Applications of SRNF/UF membranes

At present, the application of SRNF membranes is mainly focusing on the following processes:

1. Purify organic solvents in order to reuse them. In this case, the separated solute is of no or minor interest.
2. Recover products, inhibitors, catalysts… from reaction media, fermentation broths…
3. Exchange solvents.
4. Combination of 1, 2 or 3.

Normally the membrane process is applied in combination with other separation techniques, like evaporation, distillation and extraction, as the membrane separation itself is almost not capable to isolate completely a product or a catalyst from an organic solution. The organic mixture will be first concentrated and then solvents will be completely removed via an evaporation or distillation step. Only in the case of solvent purifications, as the required product is exclusively the solvent, the membrane processes can be used without any other separation processes. The advantage of using membranes in these processes is to reduce the energy consumption and reduce the discharge of harmful components in the environment.

In the following, different processes involving membrane separations in organic conditions will be illustrated in detail, including catalytic processes, processes in petrochemical industry, in food processing and in the pharmaceutical chemistry.

Catalytic organic processes

Membrane separations are playing an important role in bridging the gap between homogeneous and heterogeneous catalysis. In the membrane process, catalytic species can be separated from solvent and products, and after the separation they can be reused. If the separation was performed by traditional UF membranes, MWCO of which is above 1000 Da, another process for enlarging or immobilizing the homogeneous catalysts is needed. Several routes are following this respect, such as, anchoring the catalyst to solid supports or the synthesis of dendrimeric forms. Other possibilities are the use of catalytic nanoparticles or emulsion systems with catalytic species situated in the dispersed droplets [24]. A review made by Vankelecom described the state of the art in the membrane assisted catalysis field [25].

In some of the syntheses of fine chemicals, where hydrogenation, hydroformylation and C-C coupling reactions are common reactions, off-the-shelf homogeneous catalysts are mainly applied. In most cases, these catalytic transition metal complexes are expensive and toxic, so they have to be separated from the products and be reused again. Therefore, membrane separation processes are attracting growing interest, and in these processes, nanofiltration and reverse osmosis membranes are applied.

Even in some work that initiated in the seventies of last century, the separation of homogeneous transition metal complexes (TMC) from the reaction products and solvents in membrane processes has been done on screening the suitability. The patent of the British Petroleum Company applied cellulose acetate membranes (Sartorius) in the separation of TMC used in the aqueous hydroformylation and dimerisation of olefins [26]. Similar separations were performed with aromatic polyamide membranes [27] and cross-linked PDMS membranes (MPF-50) [28]. As for non-aqueous conditions, Scarpello *et al*. screened several commercial polymeric membranes on their potential to separate the Jacobsen catalyst, Pd-BINAP ((R)-(+)-2,2`-bis(diphenylphosphino)-1,1`-binaphthyl) and Wilkinson catalysts out of different organic solvents [29]. Separation of Pd complexes from a Heck reaction product with dimethylacetamide (DMAc) as solvent with inorganic silicalite membranes was studies by Turlan *et al.* [30].

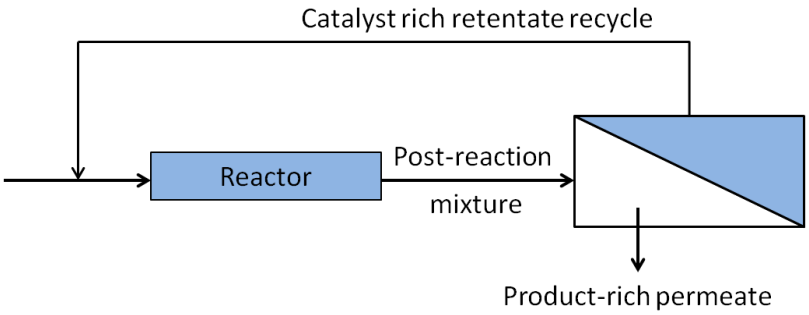

Fig. 2.2 Schematic representation of Semi-continuous process

A semi-continuous process operated by Nair *et al*. which is schematically represented in Fig. 2.2 allowed the catalyst concentrated retentate resulting from membrane filtration to be pumped back to the reaction batch for a subsequent reaction [31]. Another continuous approach was introduced by De Smet *et al*., which combined catalyst separation with a continuous stirred tank reactor [32].

Processes in petrochemical industry

Membrane technology has also been applied in the petrochemical industry, especially in refining lubricants and gasoline.

I) Dewaxing process

In order to achieve desired properties for the resulting lube oil, a lube refining process is needed, commonly referred to as dewaxing, in which a mixture of volatile organic solvents is applied to remove paraffin was from a waxy intermediate. In the conventional dewaxing process, it is always involved with high energy and cooling water demands and a significant exhaust of organic solvents. To de-bottleneck these processes, membrane technology has been introduced.

As shown in Fig. 2.3, in traditional dewaxing process, paraffin wax crystallizes during the chilling of feed mixture that is composed of waxy feed and solvents. The chilled feed mixture is then sent to the rotating drum dewaxing filters to separate the wax mix and lube oil filtrate. Both of them contain certain content of solvent, and then the solvent is removed and recycled by a combination of successive vaporization and distillation operations. The lubricating oil is then derived. Because of the vaporization and distillation steps and large amount of solvent applied, this process is highly energy intensive.

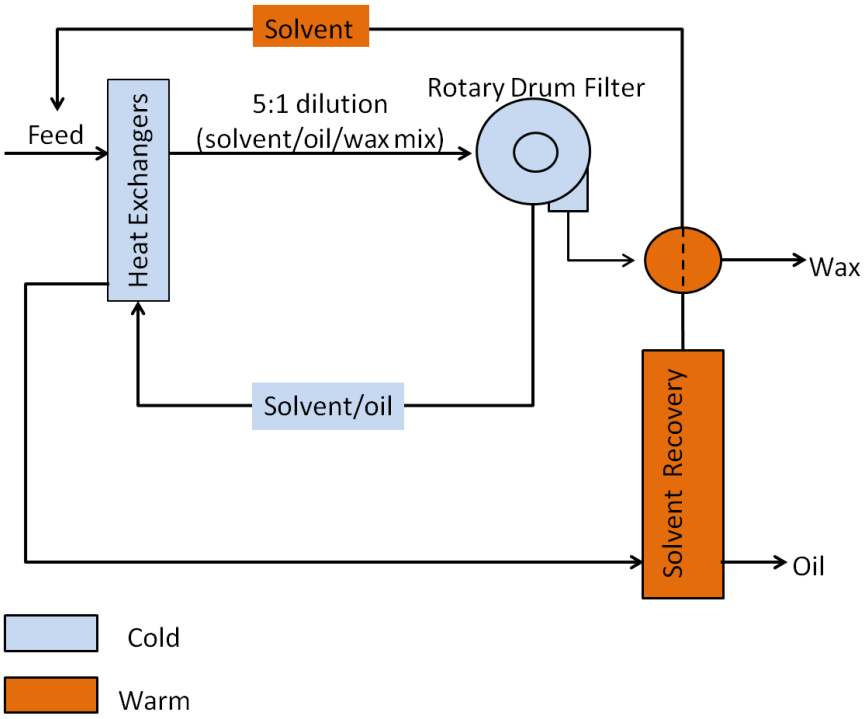

Fig. 2.3 Conventional chilled solvent dewaxing

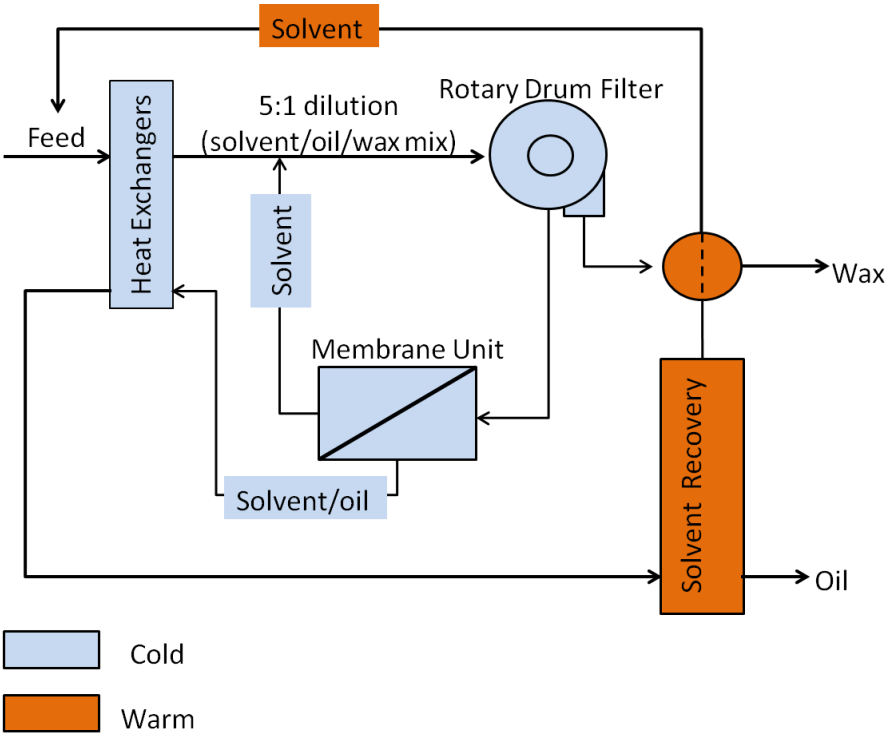

Fig. 2.4 Solvent dewaxing with membrane separation (adapted from [38])

In the late eighties of last century, several groups initiated research to apply membrane technology to separate the dewaxing solvents from the lube oil in conventional processes. Exxon filed several patents concerning membrane development, basically describing the utility of some membrane materials, such as cellulose acetate (CA) [33], polyamides (PA) [34] and especially polyimide (PI) [35,36]. Eventually, the process based on membrane technology to recover these solvents was developed [37,38,39]. Fig. 2.4 represents the dewaxing process with membrane separation. The lube oil filtrate is filtrated through PI NF membranes, resulting in more than 95% rejection of lube oil, and cold solvent with a purity of more than 99%. The purified solvent can be directly recycled to the chilled feed stream. The concentrated lube oil solution is then treated as in conventional process yielding the pure lube oil.

As large content of cold solvent can be recycled, the storage of lube oil solutions needs much less refrigeration capacity. Therefore, the lube oil production is increased by 25%, at the mean time, the yields are improved and total energy cost is significantly decreased.

II. Removal of sulphur

Membrane technology has been also applied in the process of removing elemental sulphur from gasoline. By treating a sulphur containing gasoline with NaOH, alcohols and organomercaptan compounds, insoluble polysulfides are formed, and then insoluble polysulfides can be easily removed by ultrafiltration or even microfiltration [40].

Applications in food processing

In most cases, processes in the food industry are under aqueous condition, whereas, in some special condition, like in vegetable oil industry and the synthesis of amino acids and their derivatives, which are used as food additives, organic solvents are also applied.

I. Edible oil processing

Virtually there are two processes to obtain oil from seeds: 1, the oil is pressed out of the seeds, like the production of soybean oil and sunflower oil; 2, oil is extracted with a solvent, mostly hexane, seeds that have oil content below 25% are economically suitable for this process. After extraction, the obtained oil micelles contains not only edible oil but also the solvent, phospholipids, free fatty acids, carbohydrate fractions, proteins and pigments. All

these components must be removed. In classical processes, addition of high amounts of water and chemicals like NaOH, phosphoric acid and bleaching earth are always needed [41], besides, as high temperature treatments are normally applied, the consumption of energy is also high. Therefore, membrane technology is introduced in edible oil processing: the removal of phospholipids and pigments, extraction solvent recovery and deacidification of the oil. With the help of membrane technology, thermal treatment is not necessary anymore, as a result, the thermal damage to the products is minimized, besides water, energy and chemicals consumption is reduced.

II. Degumming process

Degumming process is the most studied process. The main apparent purpose is to remove phospholipids, because of their amphiphilic characteristics, reversed micelles in apolar solvents are formed by trapping the more polar components inside. The molecular weight of these micelles is around 20,000, which makes it easy to separate them from the oil and the solvent, so in these processes, ultrafiltration membranes are applied. Lever Brothers patented the application of ultrafiltration membranes in the removal of phospholipids from soybean oil in hexane. The phospholipids content was reduced to 23 ppm with a polyacrylonitrile membrane (IRIS 3042, Rhone-Poulenc, MWCO 50 kDa). Besides, even the color of the crude soybean oil was reduced and the content of metals such as calcium, iron and magnesium were decreased, free fatty acid content was not changed. Finally the silicone membrane was selected as the best membrane, even though a certain degree of selectivity for triglyceride was also detected with this membrane, and the permeability of this membrane was also a bit lower [42]. Another work made by Gupta mentioned the addition of ammonia to neutralize the crude oil, resulting in increased free fatty acid retention [43].

One problem of high resistance for the passage of viscous miscella in spiral wound modules with 0.3 mm to 3 mm thick spacers that happened in the filtration was reported by several works [44, 45]. In the membrane process, the miscella could be concentrated up to 200 times, so although the rejection of phospholipids could be more than 99%, quite high content of oil stayed in the retentate stream, which is not good for the recovery of oil. So Koseoglu *et al.* suggested a higher concentration factor or the use of continuous processes to recover more oil [45].

Another important problem in the degumming process is the fouling of the membrane which is caused by the retained micelles of phospholipids. To solve this problem, Ochoa *et al*. investigated the fouling resistance of polyvinylidenefluoride (PVDF), polyethersulfone (PES) and polysulfone (PSf) membranes, and found out that PVDF had a considerably better fouling resistance [46].

III. Recovery of extraction solvents

Another interesting application of membrane technology in the edible oil processing is the recovery of the extraction solvents. In conventional processes, this is done by distillation, which occupies 50% of the total energy cost in edible oil processing. Besides, considerable amount of solvents could be exhausted in the environment during the distillation process. The introduction of nanofiltration and reverse osmosis process can greatly overcome the drawbacks of the conventional processes. Similar to the membrane process in de-waxing, after filtration through the membranes, the concentrated oil fraction still needs purification with distillation to remove the solvent, but much less energy is required.

As the solvents used in the process are not so aggressive, i.e. isopropanol, ethanol and hexane, it is also possible to apply some membranes designed for aqueous conditions directly in this process. Köseoglu *et al*. reported the performance of some commercial RO and UF membranes in the separation of cotton seed oil from solvents [47]. All the tested membranes had acceptable performance in isopropanol and ethanol, but as regards to hexane, most membranes were either damaged or showed a low permeability. Cross-linked PDMS membranes had good performance in the hexane, which were reported by Schmidt *et al*. [48] and Stafie *et al*. [49].

Processes in pharmaceutical industry

One evident application is the concentration of antibiotics or pharmaceutical intermediates out of organic solvents or aqueous solutions containing organic solvents. A typical example is in the synthesis of 6-aminopenicillinic acid (6-Apa). After the formation of 6-Apa, the particular composition of the reaction solution is 0.37% 6-Apa, 16% methanol and 2% methylene chloride. The content of 6-Apa were concentrated to 4% in commercial scale with the help of a commercial NF membrane [196].

In the synthesis of pharmaceuticals, reactions are often involved in several steps, and for each step, the optimal solvent may differ, therefore, solvent exchange is necessary in most pharmaceutical synthesis chains, keeping in mind that the yield per reaction step should be as high as possible and the content of the impurity as low as possible. Because most intermediates are thermally labile, athermal processing is required and high vacuum is necessary in the conventional distillation. Furthermore, when solvents with high boiling points have to be exchanged with low boiling solvents, distillation becomes even impossible. Membrane separation of the high molecular weight product of interest from the low MW by-products, reactants and solvents seems to be an interesting alternative. Practically, NF membranes are applied to retain compounds with molecular weights between 250 and 1000 Da. In the membrane process, solutions are filtered through the NF membrane, then diluted with another solvent, repeated for several times to achieve the desired concentration. The process is proven for an erythromycin solution in ethyl acetate, exchanged with methanol.

In a continuous mode, the volume of solution is also reduced with a classical nanofiltration process. However, during the membrane filtration, methanol was continuously added to the solution until the ethyl acetate concentration was low enough [50].

Livingston tested the concept with solutions containing tetraoctylammoniumbromide (TOABr) and tetrabutylammoniumbromide (TBABr) dissolved in toluene or methanol. Toluene was exchanged with methanol and the methanol with ethyl acetate [51].

2.2.2 Preparation of SRNF membranes

The majority of SRNF membranes are either composites comprising a separating layer on a membrane support, or integrally skinned asymmetric membranes made of polyimides [52], which are schematically represented by the last two graphs in Fig. 2.1. To increase the chemical and thermal stability of the membranes, chemical cross-linking has been widely used and shown appreciable effect [53,54], although this is often at the expense of a decrease in permeability [55-57].

Synthesis of composite membranes

Composite membranes are generally defined as membranes consist of two layers that are made from different polymer materials. The choice of support materials, together with the

procedures to optimize them in order to get a proper performance of the resulting composite will be discussed. In essence, several methods to deposit a thin and defect free selective layer on the support layer were developed, such as interfacial polymerization and dip coating will be also discussed in detail.

I. Support materials

One of the advantages of the composite membranes is the good chemical, mechanical and thermal stability offered by the support layer. In most cases, the support membrane is an asymmetric UF membrane, with an average pore size around 0.1 μm. PSf UF membranes are frequently used supports [58-65], besides PI [66-69], PAN [70], polycarbonate (PC) [71] and PVDF [72] as well as some inorganic membranes can be used alternatively. Some other materials such as polypropylene (PP) [73] and nylon 6,6 [74] are also applied for supports. When coating the selective layer onto the porous support, because of capillary force, the coating solution can intrude into the pores of the support, thus results in drastic decrease in permeability. In order to solve this problem, several routes have been developed. One solution is to fill the pores with a fluid that is immiscible with polymer solution [75]. Pore protectors like paraffin, mineral oils [73] or glycerol are reported also in some publications. A third route is to pre-coat the supports with low molecular weight polymers, such as polyethylene glycol (PEG) [76] or polysiloxanes [77, 78].

As membranes are used in organic solvents, the supports also have to be stable in them. So some inorganic materials are also applied, alumina supports that have good stability in almost all the organic solvent, were used in the preparation of polyphospazene composite [79]. Using TiO_2 mesoporous material as support was also reported, but NaCl solution as pore fillers have to be introduced to prevent pore blocking caused by the coating polymers, after the formation of the composite membrane, NaCl was removed by water [80].

Normally a heat treatment is applied after the coating process, to induce the cross-linking reaction of the selective layer. The pores of the supports tend to collapse at elevated temperature, resulting in a decrease in permeability through the supports [81]. Introduction of pore protectors is also able to prevent pore collapse during the heat treatment [77, 82].

II. Interfacial polymerization

A comprehensive overview of thin film composite membranes was reported by Petersen in 1993 [83]. And during the last decades, there was less academic attention paid on this field.

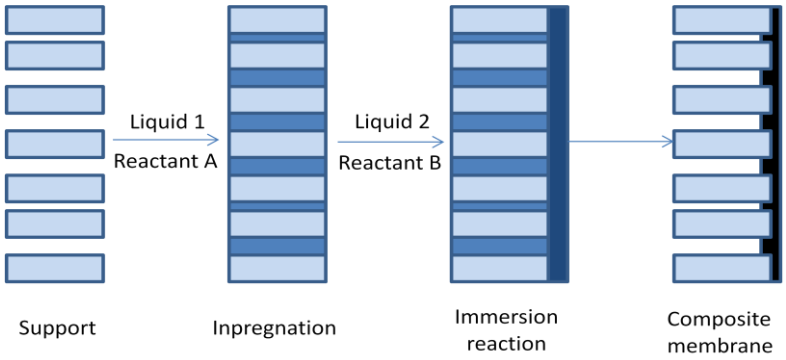

Fig. 2.5 Schematic illustration of the interfacial polymerization

Interfacial polymerization has become a very important and useful technique for the synthesis of thin film composite RO and NF membranes. As shown in Fig. 2.5, porous membrane is first immersed in solution 1 that contains reactant A, the excess of the solution is removed, followed by contacting the saturated support with a second solution that contains reactant B, then polymerization takes place at the interface between two solutions. For instance, low temperature polycondensation of 3,3'-diaminodiphenylsulfone (3DDS) and terephthaloyl chloride (TPC) can be performed in DMAc solution, which can be used in this system. As a sequence, a thin polymer layer is formed on top of the porous support. The composition and morphology of the membranes depend on different parameters, such as concentration of the reactants, their partition coefficients and reactivity ratio, kinetics and diffusion rates of the reactants, presence of by-products, competitive side-reactions, cross-linking reactions and post-reaction treatment.

III. Dip coating

A relatively simple membrane preparation technique is to coat polymer solutions on a support. Several coating techniques were developed including a simple lamination of two layer, spin coating, dip coating and plasma deposition. When the viscosity of the coating solution is high enough, the solution can be casted on the support by a casting knife. Fig. 2.6 represents a dip coating procedure frequently used in the industry.

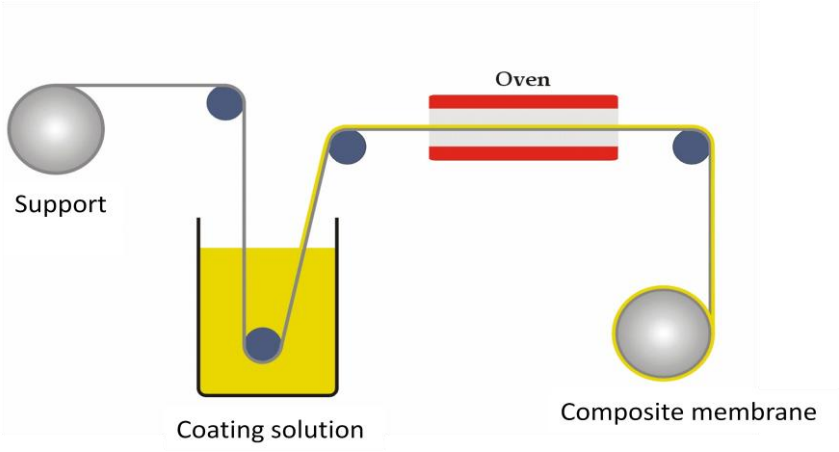

Fig. 2.6 Schematic representation of a dip coating setup used in industry

Because of the simplicity of setups and applications, lots of polymers have been studied as coating polymers for application in organic processes, for instance, chitosan [84-86], polyvinyl alcohol [73,81,87,88], polyacrylic acid [71,89,90], polydimethylsiloxane [77,78,91,92], polyethyleneimine [93-96], polyphenyleneoxide [97], polyphosphazene [79,98-100] and poly(aliphatic terpenes) [101].

Generally, elastomeric polymers are superior to glassy polymers, because during the solvent evaporation step, the glassy polymers pass from the rubbery to the glassy state, which induces stress and possibly cracks.

During a dip coating process, there are several parameters to control, the most important one of which is the thickness of top-layer. The top-layer is an equilibrium state of a film deposited on a support resulted from a balance between viscous forces, surface tension and gravity. The thickness d (m) depends on the coating velocity v (m.s^{-1}), the viscosity η (kg.m^{-1}.s^{-1}) and the density ρ (kg.m^{-3}). Then it can be calculated via the Navier-Stokes equation:

$$d = \frac{2}{3} \times \sqrt{\frac{\eta \times v}{\rho \times g}} \qquad (2\text{-}3)$$

where, g is the gravity constant (9.807 m.s^{-2}) [102].

Higher viscosity of the casting solutions leads to thicker top-layers, thus lower fluxes but normally the retentions are not affected obviously. The viscosity of polymer solution

depends on the molecular weight of the polymer, temperature and the concentration of the solution, additives, *etc*. Influence of solution concentration on the permeation rates was reported on a polyacrylic acid coating on a polycarbonate support [71]. Higher viscosity also prevents the intrusion of the solution into the support. As the molecular weight of the dissolved polymer has strong influence on the viscosity of the solution, thus on the thickness of the coated film, increasing the molecular weight of polyethyleneimine (PEI) lead to higher dye retentions for PEI/PSf-composite membranes [96]. The solvent that dissolves the polymers affects the properties of the resulting membranes as well, because it has direct influence on the viscosity of the solution. This influence was investigated for PVA coatings on Psf-supports [81]. In an appropriate solvent, the polymer coils extend, therefore, the intrusion of polymer solution into supports is reduced as a result of larger size of the polymers [102].

After the formation of a membrane, normally a cross-linking process is then performed to increase the stability of the membrane and sometimes also leading to better separation performance. In general, cross-linking will make the membrane denser, less permeable and more selective. The degree of cross-linking is then an important factor that affects the membrane properties, which is determined by type of cross-linking agent, its concentration, reaction time, temperature, *etc*. Much effort has been made to develop cross-linked composite membranes from polymers like polyethyleneimine (PEI) [96,103], polyphenyleneoxide (PPO) [97,104], polyorganosiloxanes [105-107].

Preparation of integrally skinned asymmetric membranes

Instead of composite membranes, it is also possible produce membranes with a thin selective layer and porous substrate from the same polymer, which is named integrally skinned asymmetric membranes. The development of this asymmetric membrane made a major breakthrough first for NF/RO membrane synthesis [108], later for gas separation. The synthesis of this type of membranes is mainly based on the “phase inversion” process, which refers to the controlled transformation of a cast polymeric solution from a liquid into a solid state. The process relies on the phase separation of polymer solutions producing porous polymer films.

Phase separation mechanisms are generally subdivided in three main categories based on the conditions that induce demixing. By changing one of these conditions at one particular side of the film, asymmetric boundaries are formed on the polymer film which can be seen in the resulting structure. By changing the temperature at the interface of the polymer solution, solubility of the polymers in the solution is altered and demixing can be induced (thermal induced phase separation or TIPS). The original polymer solution can also be subjected to a reaction which causes phase separation (reaction induced phase separation or RIPS). The most used technique is based on diffusion induced phase separation (DIPS). In this technique, by contacting a polymer solution to a vapor (VIPS) or liquid (non-solvent, NIPS), or by evaporating the volatile solvent from the solution (EIPS), diffusional mass exchange will lead to a change in the local composition of polymer film and demixing takes place [109]. Often combinations of various methods are applied to achieve the desired membrane [110].

I. Influence of polymers

Asymmetric membranes from many types of polymers have been already developed. The polymer characteristics have an important influence on the membrane performance and the stability of membranes.

At first, most obviously, the polymer characteristics can affect the chemical and thermal stability of the membranes. A crystallized polymer will be better to gain higher stability of the asymmetric membranes. Also rigid main chains consisting of aromatic and/or heterocyclic groups without any flexible group lead to higher stability, such as polyphenyleneoxide and aromatic polyamides. Existence of resonance structures in the main chain increases the stability furthermore [109]. Examples for such polymers are polyimides, polybenzimidazoles and polyoxadiazoles. Bulky side groups can decrease the possibility of main chains to rotate thus enhance the stability. For example, polyacrylonitrile, the high polarity of the side groups (-CN) results in better interaction between the chains, therefore, these polymers are less soluble and chemically more stable.

Another influence, and also most important for the membranes, is the influence on the membrane performance. Higher hydrophilicity of a polymer can obviously lead to an increase in flux of polar solvents through the membrane prepared from it, either due to

better wetting for porous membranes or higher sorption/diffusion for dense membranes. Examples for this phenomenon were illustrated by comparing the water flux of membranes prepared from CA and cellulose acetate butyrate (CAB, 17% butyryl content). Accompanied with higher water flux, the salt rejection was also lower [111,112].

Polarity of the membranes will also affect the separation performance. Introducing charged groups can improve the hydrophilicity of the membranes, thus water flux is higher, and salt rejection that is based on Donnan exclusion also gets higher. Membranes from polyamide (PA) with varied amounts of carboxylic groups were studied to check the influence of polarity and charge effects [113,114,115].

The polymer structure has also influence on the membrane performance. Membranes prepared from highly-branched polymers are expected to have higher fluxes, as the distance between different chains is higher. In case of relatively rigid polymers, such as PA and poly(amide hydrazide) (PAH), higher molecular weight lead to lower fluxes and higher retentions. This was explained by the fact that longer chains establish more secondary hydrogen bonds between the imino and carbonyl groups, which would cause densification of the membrane and dense barrier layer leads to longer solution diffusion time [116].

II. Basic principles

The thermaldynamical aspects of immersion precipitation are normally illustrated by the (polymer/solvent/non-solvent) three phase diagram as shown in Fig. 2.7.

The initial cast solution is situated in the stable region of the diagram outside the two curves. There are two ways for the solution to induce phase separation. For path A, polymer solutions situated in the region between the bimodal and the spinodal are metastable. They will phase separate into a polymer lean and a polymer rich phase according to the nucleation and growth mechanism. The second path B in Fig. 2.7 represents the “spinodal demixing” (SD), which occurs when the demixing path crosses the critical point, going directly into the unstable region, instead of well defined nuclei, two co-continuous phases are formed.

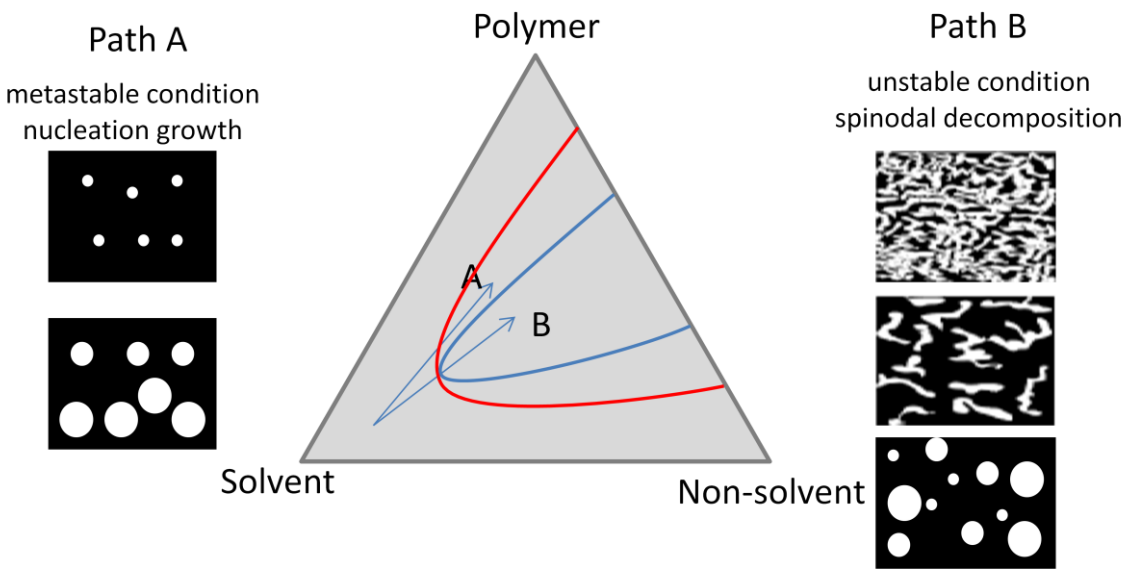

Fig. 2.7 Mechanism of phase separation during membrane formation

As regarding to the integrally skinned asymmetric membranes, it is important to have different processes to form skin layer and sub-layer. The morphology of the sub-layer is more important for the determination of flux and mechanical stability of the resulting membrane. In this context, very important features are the so-called macrovoids that means finger-like pores, as they severely limit the compaction resistance of the membrane.

When the rate of inward diffusion of non-solvent into the polymer poor phase exceeds that of the outward solvent diffusion, macrovoids structure forms, as more non-solvent enters, the wall will deform and expand in the form of a tear. The main driving force for the non-solvent to enter the developing pore is the osmotic pressure. As the content of solvent decreases continuously, at a certain point, the pore wall will vitrificate or crystallize, and pore wall is then completely formed. In the opposite conditions, when the diffusion coefficient of the non-solvent is low, when osmotic pressure is low or when a lot of small, stable nuclei are formed, sponge-like membranes will be formed.

The ultimate membrane morphology is determined by the thermodynamic characteristics of the polymer solution combined with the kinetic aspects of diffusion [109,117]. Therefore, the following parameters could have strong influence on the morphology: 1, characteristics of polymer; 2, composition of the cast solution; 3, post-casting treatment; 4, coagulation bath; 5, post-treatment of membrane. The influence of parameters 2-5 will be discussed in the following section.

III. Composition of cast solution

Besides the polymers, the most important component in the casting solution is the solvent. The interaction between the solvent and the non-solvent are of great importance, when the interaction is low, more sponge-like structures will be formed [115]. The polymer concentration and addition of additives affect the morphology and separation performance of the ultimate membranes as well.

A direct way is to increase the polymer concentration in the casting solution. The inward diffusion is then reduced because of the higher polymer concentration at the polymer/non-solvent interface upon immersion, and the demixing is delayed, resulting in denser skins with increased thickness, sub-layers with lower porosities and lower fluxes [109,117,118].

Adding additives in the polymer solution is also an effective method to obtain distinct membranes. Addition of volatile solvents can greatly enhance the evaporation effect after casting process even at room temperature, then a relative dense skin layer is formed. Ethylether and tetrahydrofuran (THF) were added to (S)PPESK/N-methylpyrrolidone (NMP) solutions [118,119] to prepare membranes with retentions and fluxes within the NF range. White *et al.* [39,120] added THF in the PI/NMP solution, by evaporating THF under a convective airflow at controlled temperatures, they derived membranes with dense selective layer.

Addition of non-solvents or 'bad' solvents is also used to control the morphology of the membranes and affect the formation of a defect free skin layer significantly. At first, increasing the content of non-solvent or bad solvent lead to macrovoids structure, but when the content is increased further, after a certain limit, the film will reach metastable state and a lot of stable polymer-lean nuclei will emerge. Then phase separation will take place quickly and equally throughout the film, thus hindering growth of nuclei and formation of macrovoids [117]. Furthermore, the osmotic pressure is also reduced when non-solvent is added into the polymer solution [121].

There are several pore forming additives applied in the membrane preparation to improve the separation performance. LiCl or $LiNO_3$ was added into polyamide hydrazine (PAH) casting solutions resulting in a higher flux without reducing selectivity [122-124]. Addition of $Mg(ClO_4)_2$ increased the porosity of asymmetric CA or CAB membranes, but the selectivity

was also reduced [111]. Besides, organic additives are also frequently used. As maleic acid (MA) enhances the solubility of cellulose triacetate (CTA) polymers, it is added to CTA casting solutions to increase the porosity and permeability of the membranes. Polymeric additives are also widely applied, such as sulfonated poly(ether ether ketone) (SPEEK) [125], PEG [126], PPO [127] and so on.

IV. Evaporation step

Before immersing the casted film into non-solvent, or putting them into oven, an additional evaporation step can be also applied, which is normally achieved by forcing a convective airflow along the cast film or by allowing the solvent to evaporate freely in the open air. The evaporation of solvents leads to a higher polymer concentration in outer surface of the cast film. The higher concentration of polymer in this region leads to a dense layer, named the skin layer.

Evaporation time is an important parameter in this process, as increasing evaporation time leads to decrease in permeability and increase in rejection. This was illustrated for membranes prepared from PA [113,128], PAH [116,122-124,129,130], CA [111,112] and PPESK [131]. But decreased selectivity was also found in the preparation of PAH membranes, when evaporation time was increased to longer than 50 min at 110 °C, which was attributed to the onset of crystallization process [124,130]. Besides, evaporation temperature is also very important for the performance of ultimate membranes [116,122].

V. Coagulation bath

As discussed in composition of casting solution, the interaction between solvent and non-solvent is highly important in the membrane formation process. Good interaction will lead to a high exchange rate. Thus porosity is higher, for example, the solvent/non-solvent pair NMP/water leads to a porous structure.

The interaction between solvent and coagulation bath can be changed by adding additives in the coagulation bath. Adding poor coagulants to the coagulation bath can reduce the exchange rate, for example, addition of alcohols to the water coagulation bath for the casting solution of sulfonated PVDF in DMF, results in denser membranes [132]. Beerlage indicated the same effect when coagulating PI/DMF films in alcoholic media. The

membranes quenched in ethanol and isopropanol had denser morphologies and lower ethanol fluxes [133].

Alternatively, addition of the same solvent as in the polymer solution to the coagulation bath leads to a similar effect. This reduced the exchange rate because of a reduced osmotic pressure and thus decreased the porosity [109]. It is also reported that addition of oligomeric or polymeric substances to the coagulation bath can influence the exchange rate. For example, poly(ethylene oxide) (PEO) was added to the water bath for the poly(ether ketone)/sulfuric acid casting solution, by increasing the amount of PEO, the porosity and the MWCO of the membrane was reduced [134].

VI. Cross-linking

One important characteristic of the SRNF/UF membranes is the stability in different organic solvents. Chemical cross-linking is an important way to enhance the stability.If the polymers carry functional groups, or functional groups can be introduced, it is possible to perform cross-linking reactions with multifunctional compounds that are called cross-linkers.

PAN is widely used in SRNF/UF processes, because of the stability in various organic solvents, but after an extra cross-linking it becomes even insoluble in aprotic solvents. Hicke *et al.* reported a novel membrane prepared from a PAN copolymer, namely poly(acrylonitrile-co-glycidyl methacrylate) (PANGMA). After the formation of the membrane, treatment with ammonia resulted in a solvent-resistant membrane [135], mechanism of which is shown in Fig. 2.8.

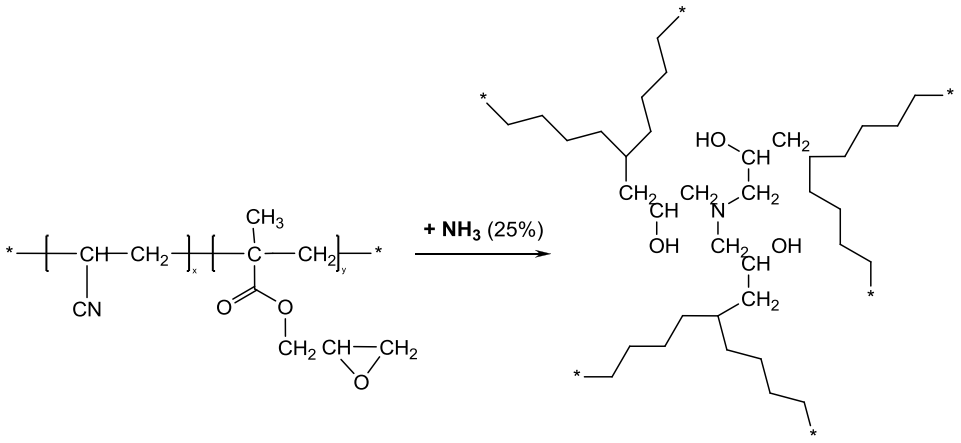

Fig. 2.8 Cross-linking of poly(acrylonitrile-co-glycidyl methacrylate) by treatment with ammonia (adapted from [135])

Besides, physical cross-linking is also applied. Takezo *et al.* followed a more physical approach, by plasma-treatment of a PAN membrane with an electrical discharge in He or O_2 gases [136].

2.3 Redox polymerization

2.3.1 Introduction

Actually all free radical chain reactions require a separate initiation step, in which a radical species is generated in the reaction mixture. Some types of chain reactions are initiated by adding a stable free radical directly to the reactants, whereas the free radical should have little or no tendency to self-combine. Even in this situation, a separate initiation step is still involved because these stable radicals are mostly inorganic ions or metals.

Therefore, according to the way how the first radical species is created, radical initiation reactions can be divided into two following general types: (1) homolytic decomposition of covalent bonds by energy absorption; (2) electron transfer from ions or atoms containing unpaired electrons followed by bond dissociation in the acceptor molecule.

A very effective method of generating free radicals under mild conditions is by one-electron transfer reactions, the most effective of which is redox initiation. This method has found wide application for initiating polymerization reactions [137,138] and has industrial importance, e.g. in low temperature emulsion polymerizations [139].

For the homolytic cleavage of covalent bonds of most practical thermal initiators, the bond dissociation energy required is in the range of 125-160 kJ/mol, and compounds with values out of this range give either too slow or too rapid rate of generation of radicals at the generally used polymerization temperatures. This narrow range of dissociation energies limits the types of useful compounds to those containing fairly specific types of covalent bonds, for example, oxygen-oxygen, oxygen-nitrogen and sulfur-sulfur bonds. Besides the very short induction period (almost negligible), a lower energy of activation (40-80 kJ/mol) allows the redox polymerization to be carried out under milder conditions than thermal

polymerization. This lowers the possibility of side chain reactions giving high molecular weight polymers with a high yield.

2.3.2 Metal ion oxidants in redox initiation

A lot of reducing agents like alcohols, thiols, ketones, aldehydes, acids, amines and amides were used in combination with oxidizing metal ions to participate in general single-electron transfer reactions for free radical polymerization. Metal ions used mainly for this purpose are Mn(III) (and Mn(VII)), Ce(IV), V(V), Co(III), Cr(VI) and Fe(III).

Cerium(IV) ion has been used for the oxidation of many organic compounds, in the form of cerium(IV) ammonium nitrate (CAN), cerium(IV) ammonium sulfate (CAS), cerium(IV) sulfate (CS) and ceric perchlorate and the mechanism of such reactions has been well established.

Reducing agents combined with cerium (IV) are alcohols, aldehydes, acids and amines. Earlier investigations revealed the fact that the rates of vinyl monomers were in the order of: ceric perchlorate > ceric nitrate > ceric sulfate which is in the order of oxidation power of mentioned species.

Ceric ion forms complexes with anions such as sulfate, nitrate and hydroxyl in aqueous solution whose relative concentrations have been found to be function of hydrogen ion, respective anion concentration and ionic strength. Increase of ligand concentration, X = SO_4^{2-} and NO_3^- depress the rate of polymerization due to formation of less reactive cerium (IV) species, CeX_n than Ce^{4+} and $Ce(OH)_n$.

The mechanism and kinetics of polymerization involve ceric ion alone [140] and also in combination with reducing substrates such as alcohols [141-147], diols [148-150], polyols (glycols, sorbitol, mannitol) [151], aldehydes [152] and ketones [153], and amines [154] etc. with different monomers, acrylamide, acrylonitrile and methylmethacrylate etc.

In previous studies, it was generally suggested that for the ceric salts initiated vinyl polymerization, both ceric ions and primary free radicals participate in the initiation process while the termination occurs exclusively by the interaction of propagating chain radicals and ceric ions, or mutual combination of growing chain radicals. On the cerium (IV)--2-

chloroethanol redox pair initiated polymerization of acrylamide under nitrogen [144], it was reported that ceric ion was not able to initiate the acrylamide polymerization under the experimental conditions of the study that is reported by other workers [155-161]. In this study, it was reported that cerium (IV) ion forms a complex with 2-chloroethanol which on decomposition produces free radicals via single-electron transfer process, which is represented in Eq. (2-4). It was found that the rate of polymerization is directly proportional to the concentration of 2-chloroethanol, dependent on the square of monomer concentration at lower concentration and inversely proportional to the concentration of cerium (IV) ion. The disappearing rate of ceric ion was found to be independent of monomer concentration and directly proportional to the concentration of ceric ion and 2-chloroethanol. As shown in Eq. (2-5) to Eq. (2-7), following reaction steps were proposed by making a conclusion that ceric ions do not participate directly in the initiation process and termination occurs exclusively through the oxidative termination of ceric ion only. The square dependence on monomer concentration also rules out the possibility of mutual termination of growing chain radicals.

$$\mathrm{Ce(IV) + ClCH_2CH_2OH \rightleftharpoons \underset{\text{Complex (C)}}{[Ce(IV)\text{-}ClCH_2CH_2OH]} \xrightarrow{k_d} \underset{\text{(R)}}{ClCH_2\dot{C}HOH} + Ce(III) + H^+} \tag{2-4}$$

Initiation

$$M + R^{\cdot} \overset{k_i}{\rightarrow} RM_1^{\cdot} \tag{2-5}$$

Propagation

$$RM_1^{\cdot} + M \overset{k_p}{\rightarrow} RM_2^{\cdot} \tag{2-6}$$

$$RM_{n-1}^{\cdot} + M \overset{k_p}{\rightarrow} RM_n^{\cdot} \tag{2-7}$$

There are several termination possibilities depending on cerium(IV) concentrations and other factors as shown in Eq. (2-8) and Eq. (2-9):

Termination by cerium (IV)

$$RM_n^{\cdot} + Ce(IV) \overset{k_t}{\rightarrow} RM_n - Ce(III) + H^+ \tag{2-8}$$

Coupling termination

$$RM_n\dot{M} + \dot{M}M_nR \overset{k_o}{\rightarrow} R - M_n - M - M - M_n - R \quad (2\text{-}9)$$

It was found that molecular weight of polymer decreases on increasing the concentration of ceric ion (cerium ammonium nitrate, CAN) and increases on increasing the concentration of acrylamide and 2-chloroethanol [157,158].

In the acrylonitrile polymerization by cerium (IV) (CAN)-primary alcohol in nitric acid under nitrogen, by the application of Taft's correlation, it was suggested that the mechanism is free radical mechanism [144].

$$Ce(IV) + R - CH_2OH \leftrightharpoons [Ce(IV) - CH_2OH - R] \rightarrow \dot{R}CH - OH + Ce(III) + H^+ \quad (2\text{-}10)$$

Similar to polymerization of acrylamide, increase in cerium (IV) decreases the molecular weight and increase in alcohol concentration decreases the molecular weight of polymer.

2.3.3 Factors affecting redox polymerization

There are several factors that can influence the redox polymerization processes, but specifically for the polymerization initiated by metal ion oxidants, the following parameters will be discussed, including the effect of solvent and retardants, effect of alkali metal salts and oxygen.

I. Effect of solvent and retardants

It was reported that addition of 5% (v/v) aliphatic alcohols and DMF to the mandelic acid-permanganate redox system in the acrylamide polymerization lead to increase in induction period and a decrease in the yield [162]. And the sequence of the influence is in the order of

EtOH > MeOH > DMF > Isopropanol

The reasons for this phenomenon might be: 1, addition of water-miscible organic solvents to the reaction medium decreases the area of shielding of a strong hydration layer in aqueous medium, resulting in the termination of growing chain; 2, due to transfer of macroradical

chains to these solvents, the propagation rate decreases and therefore polymerization rate is also observed to decrease. During chain transfer reaction, it is possible to generate a solvent radical that is not able to initiate the polymerization reaction, therefore the yield decreases as well. The order of the retardation effect of the solvents is following:

MeOH > EtOH > PrOH > BuOH

Besides, some amount of the catalyst might be consumed in the presence of these solvents, which can also lead to the results above.

Complete inhibition was observed when adding retarders/chain transfer agents (methylamine) to the reaction system for polymerization of N-vinylpyrrolidone [162]. Carbon tetrachloride and benzene brought decrease in percentage in polymerization due to increased chain transfer. Addition of benzene caused 10 times decrease in molecular weight of the polymer. In the polymerization of methylmethacrylate (MMA) initiated by Ce(IV)-alcohol system [163], the order of decrease in the conversion was found as below:

MeOH > EtOH > Acetone

In addition to ethanol and methanol, in the polymerization of AN initiated by thioacetamide-permanganate system, acetic acid and formic acid (in the presence of 10%) depressed the initial rate and maximum conversion as well [164], which is probably due to: 1, solvation of the radical end of the propagating chain (cage effect) which hinders the propagation process; 2, increase in the regulated rate of production of primary radical which render the termination rate relatively fast as compared to the growth rate [165,166].

II. Retardation effect of alkali metal salts

In the same reaction system [164] as above, addition of Na_2SO_4, $ZnSO_4$ and KCl caused a decrease in the initiating rate and maximum conversion, which was assumed to be a result of increase in ionic strength of the medium. But in the case of $CuSO_4$, the retardation of rate was related to an increase in the rate of linear termination of polymer chains by the Cu(II) ion. The addition of Na^+ into the same reaction system resulted in a decrease in the rate due formation of complex with Mn(III) which act as poor source of the primary radicals responsible for the initiation of polymerization.

The effect of the ionic radii of the alkali metal ion is another possible factor [167] in the reduction of the polymerization rate, as the ionic radii increases, the effect of alkali metal chloride that suppress the polymerization rate and the maximum conversion also increases. The retardation effects of these salts are in the order of

None > LiCl > NaCl > KCl > RbCl > NH_4Cl

III. Effect of oxygen

Oxygen plays several roles in radical polymerization reaction, depending on the experimental conditions, it may act as initiator, inhibitor or retarder in these reactions [168]. In the unique case of high pressure radical polymerization of ethylene, it inhibits the initiations [169]. Unlike its role in initiation [170,171] the retarding or inhibitory action of oxygen in such reactions was not understood well, not withstanding the well-known peroxide scheme [172]. Furthermore, the peroxide based inhibition effect of oxygen in radical polymerization is dependent on temperature, as the peroxides decompose at elevated temperatures, generating additional radical that may initiate polymerization.

The inhibition effect of oxygen in the radical polymerization of styrene initiated by Co^{2+}-BH_4 redox system was explained by the formation of 1-phenyl ethanol [173]. Oxygen may react with the primary radical to give peroxide radicals:

$$R^{\cdot} + O_2 \rightarrow R - O - \dot{O} \qquad (2\text{-}11)$$

If the peroxide radicals are not as reactive as the primary radicals, the oxygen will act as an inhibitor or retarder of polymerization, in the opposite condition, oxygen may act as an initiator itself.

Chapter 3. Experiment techniques

3.1 Materials

Acrylonitrile (AN), 2-hydroxylethylmethacrylate (HEMA) and AMPS were purchased from Sigma-Aldrich. Poly(ethylene glycol) (400, 600, 4000) were purchased from FLUKA. Cerium ammonium nitrate, glutaraldehyde were purchased from Sigma-Aldrich. DMF, ethanol, hexane, ethyl acetate, heptane, acetonitrile, chloroform and dichloromethane were purchased from VWR. Malonyl dichloride, oxalyl chloride and terephthaloyl dichloride were purchased from Acros. Sulfuric acid was purchased from Fisher chemicals. All the chemicals purchased were analytical pure (≥98%). Ultrahigh purified argon gas was purchased from Messer Griesheim GmbH. Water purified with a Milli-Q system from Millipore was used for all experiments.

3.2 Copolymer synthesis

3.2.1 Copolymer of PAN and PEG

PEG was first fully dissolved in distilled water in a three neck flask equipped with magnetic stirring and argon inlet and outlet. The flask was kept in a 1 ◦C thermal stable water bath and the solution was then deoxygenated by filling with argon. Then, cerium salts dissolved in distilled water were injected into the PEG aqueous solution, after a certain time for the pre-action of PEG and cerium ammonium nitrate (t_b), followed by the injection of acrylonitrile monomers under vigorous stirring. Copolymerization then began and was allowed to proceed for another 4 hours, after which block copolymers were obtained and precipitated in distilled water for 24 hours, during which distilled water was changed for three times to remove the residue un-reacted PEG. Copolymers gained were filtered and dried at 50°C in

vacuum to a constant mass. The amount of cerium salts used was based on the principal that mole ratio of ceric salts to hydroxyl groups is 1.1 to make ceric ion moderately excessive.

The expected mechanism of the polymerization is as following Fig. 3.1:

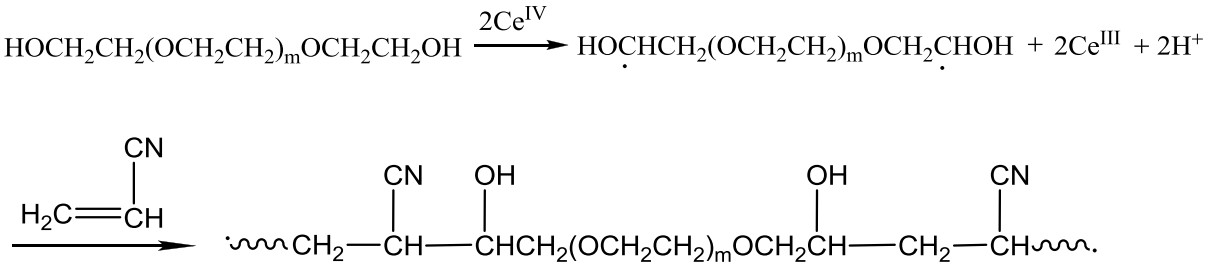

Fig. 3.1 Proposed polymerization mechanism of PAN-b-PEG-b-PAN

3.2.2 Copolymer of PAN and hydroxylethyl methacrylate (HEMA)

Azoisobutyronitrile (AIBN) was first dissolved in dimethylformamide in a three neck flask equipped with magnetic stirring and argon inlet and outlet. The flask was kept in 60°C water bath, and argon flow was used to deoxygenate the solution. Then HEMA was injected into the solution, followed by the injection of acrylonitrile monomers. Then the reaction began and progressed for 10 hours. The solution of the copolymers in DMF was applied in a rotate evaporator to get more concentrated, and then copolymers were obtained by precipitation using water as non-solvent. The polymerization reaction is a typical free radical polymerization, mechanism of which is shown in Fig. 3.2.

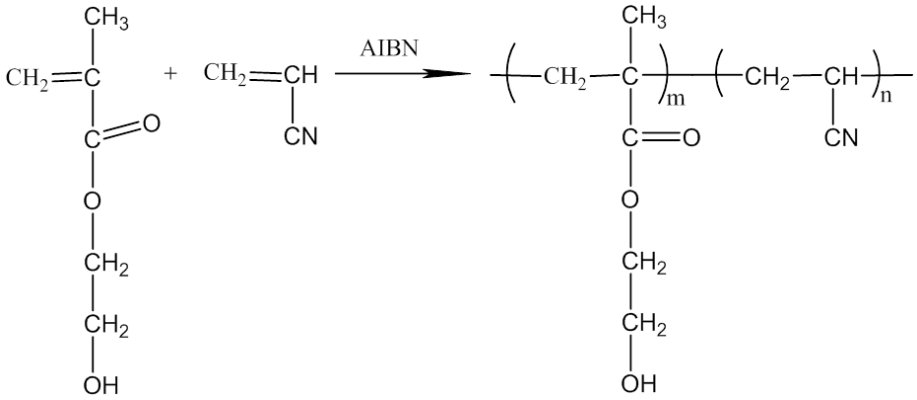

Fig. 3.2 Copolymerization of AN and HEMA initiated by free radical

3.2.3 Copolymer of PAN and 2-acrylamido-2-methyl-propanesulfonic acid (AMPS)

Acrylonitrile and 2-acrylamido-2-methyl-propanesulfonic acid with different weight ratio were first fully dissolved in water, it was kept at 60°C with water bath, after purging with argon for 10 minutes, azo-isobutyronitrile as initiator was added into the solution, the reaction was allowed to process for different durations under rigorous stirring, after a certain reaction time, the water bath was removed, and the reaction solution was left in the flask for another 24 hours with stirring. The copolymers were obtained and dipped in distilled water for 24 hours, within which, the water was changed for several times. Then copolymers were filtered and dried at 40°C in vacuum to a constant weight.

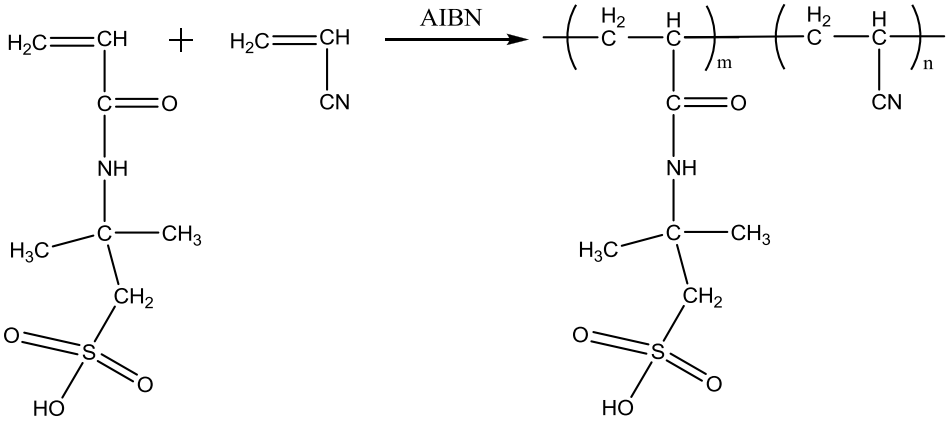

Fig. 3.3 Typical free radical polymerization of AN and AMPS

3.3 Characterization of the copolymers

3.3.1 ATR/FTIR

FT-IR spectra of the copolymers were observed by using the instrument Varian 3100 Fourier Transform Infrared spectroscopy (FT-IR) Excalibur series equipped with a horizontal ATR unit. A total of 64 scans were performed at a resolution of 4 cm^{-1} using a diamond crystal; the temperature was 21±1°C. Pro 4.0 was used to record the different spectra versus the

corresponding background spectra. The quantitative composition was estimated from relative peak ratios.

3.3.2 ^{1}H-NMR

^{1}H-NMR spectra of the copolymers was evaluated on a Bruker DMX300 spectrometer (300 MHz) using DMSO-D6 as solvent at 25 °C. TopSpin 1.3 was used to record the spectra.

3.3.3 Element analysis

Element analysis was operated on CHNS analyzer to calculate the weight content of C, H, N and S in the copolymers. The element analyzer is used for simultaneous determination of carbon, hydrogen, nitrogen and sulphur content present in organic, inorganic and polymeric materials. Samples are sent into a quartz tube at 1020°C with constant carrier gas flow and high purity oxygen is used to achieve complete oxidation of thermally resistant substances. The combustion gas mixture is driven through an oxidation catalyst (WO_3) zone, and subsequently through a copper zone that reduces nitrogen oxides and sulphuric andydride (SO_3) and retains the oxygen in excess. The resulting components of combustion mixture are detected in a sequence of N_2, CO_2, H_2O, and SO_2 by thermal conductivity detector.

3.3.4 Gel permeation chromatography (GPC)

GPC was performed to get the information about the molecular weight, in which, DMF+0.01M LiBr was used as eluent, PMMA for calibration, and the columns were applied as following coupled with a Waters refractive index detector:

SDplus 10^2 Å, 10 µm, 300/8 mm, 50- 5 000 (g/mol)

SDplus 10^3 Å, 10 µm, 300/8 mm, 1 000 – 70 000 (g/mol)

SDplus 10^5 Å, 10 µm, 300/8 mm, 10 000 – > 1 000 000 (g/mol)

3.3.5 Determination of amount of free radicals

The amount of free radicals generated in the initiation step was calculated with the help of stable free radical: 2,2-diphenyl-1-picrylhydrazyl (DPPH). First, DPPH was dissolved in a mixture of acetone and water with a volume fraction of 3:2, at the meantime, PEG 400 and ceric salts with same composition as the copolymer synthesis were dissolved in distilled water, after a certain period (t), the reaction solution was added into the DPPH solution, when the color of DPPH solution turns from dark violet and black to transparent, the volume of reaction solution used was recorded, and the concentration of generated free radicals (C_{gr} [mol/l]) was calculated via the following equation:

$$C_{gr} = \frac{V_{sr} \times C_{sr}}{V_{rs}} \tag{3-1}$$

where, V_{sr} [l] is the volume of the stable radical solution, C_{sr} [mol/l] represents the concentration of the stable radicals, and V_{rs} means the volume of used reaction solution.

3.4 Membranes and films preparation

3.4.1 Films

Casting solution was made by dissolving PAN-b-PEG-b-PAN block copolymer in N,N-dimethylformamide (DMF) solvent for 1 day with gentle stirring to form a homogeneous solution with a concentration of 12.5% (wt%). Films were prepared by casting the solution with a casting knife on a clean and smooth glass, the thickness and the casting speed was 200 µm and 20 mm/s respectively. Subsequently, the film was dried in vacuum with temperature of 40 °C for another 12 hours to evaporate the solvent; it was then immersed in water to remove the film from the glass support.

3.4.2 Membranes

Casting solutions were made by dissolving PAN-b-PEG-b-PAN block copolymer in DMF for 1 day with gentle stirring to form a homogeneous solution with different concentrations (10%, 12%, 15% and 16%). Membranes were prepared by casting the solutions on a glass plate with different thicknesses (200 µm and 300 µm), the casting speed was 20 mm/s. Then the

membrane was directly immersed in coagulation bath for 20 minutes, followed by drying with different methods: drying in the air and drying with solvent exchange (ethanol and hexane in sequence).

Copolymers of AN and AMPS were dissolved in NMP with different concentration at room temperature. After fully dissolved, the solution was filtered with dense filter paper under 5 bar, and then degassed with vacuum. Polymer solutions were casted on clean glass plates or PET non-woven support with thickness of 300 µm and the casting speed was 15 mm/s, followed by immersing the casted solution into different coagulation bath.

3.5 Properties of membranes and films

3.5.1 Swelling test of the films

Dry films with a known weight m_0 were immersed into different solvents and were allowed to equilibrate for 96 h at room temperature. Each sample was weighed from time to time until no weight change was observed, after which these films were taken out from the solvents and weighed (recorded as m_∞) after the solvent was wiped out with tissue paper. The value of swelling degree is calculated according to the following equation.

$$SD = \frac{m_\infty - m_0}{m_0} \times 100\% \tag{3-2}$$

3.5.2 Thickness of membranes

The thicknesses of membranes and films were measured by Coolant Proof Micrometer IP 65, Mutico Co. Japan, and at least five measurements from different position of the membrane were averaged.

3.5.3 Pore morphology

The top surface and cross-section morphology of the membranes were observed by using a Quanta 400 FEG (FEI) environmental scanning electron microscopy at standard high vacuum conditions. A K550 sputter coater (Emitech, U.K.) was used to coat the outer surface of the sample with gold/palladium. The pore size was estimated by a single electric meter in the photo treatment software, for each membrane, at least 10 pores were measured, and average value was calculated.

3.5.4 Contact angle

Static contact angles of water on membranes were measured by captive bubble method using an optical contact angle measurement system (OCA 15 Plus; Dataphysics GmbH, Filderstadt, Germany) at 21 °C. The volume of air bubbles used was always 5 µL. All the values were average of at least 5 measurements taken at different locations of the membrane surface.

3.5.5 Separation experiment

Pure solvents flux measurements were conducted in a standard Amicon cell as well as a self-made stainless steel nanofiltration cell with an active membrane area of 9.1×10^{-4} m^2 and a feed chamber volume of 100 ml. In the latter module, membrane discs were supported by a porous stainless steel disc and sealed with solvent resistant O-rings. Varied argon pressures and solvents were applied at room temperature. For each membrane, solvent and driving pressure, tests were repeated at least three times to make sure the stability and reproducibility of membrane performance.

Dead-end filtrations were carried out in the self-made nanofiltration cell using 2 g/L aqueous solutions of PEG or Dextran with different molar masses as feed. For the rejection measurements in non-aqueous solutions under nano-filtration condition, 2 g/L solutions of polystyrene (PS) oligomers in different organic solvents were applied as feed.

All the rejection measurements were performed under magnetic stirring at 500 rpm with a Teflon-coated magnetic stirrer suspended 3 mm above the membrane. For each test, permeate samples were collected and weighed in every four minutes to get a detailed changing in flux and to determine permeability (P, $l/m^2\cdot bar\cdot h$). For the determination of

rejection (R, %), PEG and Dextran concentrations were calculated via total organic carbon (TOC) measurement using a TOC-Vcpn system from Shimadzu (Japan). PS concentrations were analyzed using a Gilson high performance liquid chromatography (HPLC) system with a Gilson 118UV-Vis detector. Separation of the oligomers was achieved by an ACE 5-C18-300 column. A mobile phase of 35 vol% analytical grade water and 65 vol% tetrahydrofuran was used with 0.1 vol% trifluoroacetic acid. The UV detector was set at a wavelength of 264 nm. At present, although other properties such as solute-polymer interactions can affect the membrane separation performance [174], the selection of membranes is still based upon the molecular weight cut-off (MWCO), which is defined as the molecular weight of the solute which is 90% rejected by the membrane. It is also used to characterize the membranes in this study.

3.6 Cross-linking

Different cross-linking methods for PAN-b-PEG-b-PAN were performed to find out the optimized process.

1, Malonyl dichloride, the total amount of hydroxyl functional group in the copolymer membrane, and K_2CO_3 were measured out in a 1:2:3 molar ratio. The malonyl dichloride was first dissolved in dichloromethane (1% v/v), and the membrane was placed in a three neck flask along with the K_2CO_3 powder with a little content of dichloromethane, then the solution of malonyl dichloride in dichloromethane was added dropwise. The reaction mixture was maintained at room temperature under argon for a total reation time of 12 hours. The mechanism is shown in Fig. 3.4.

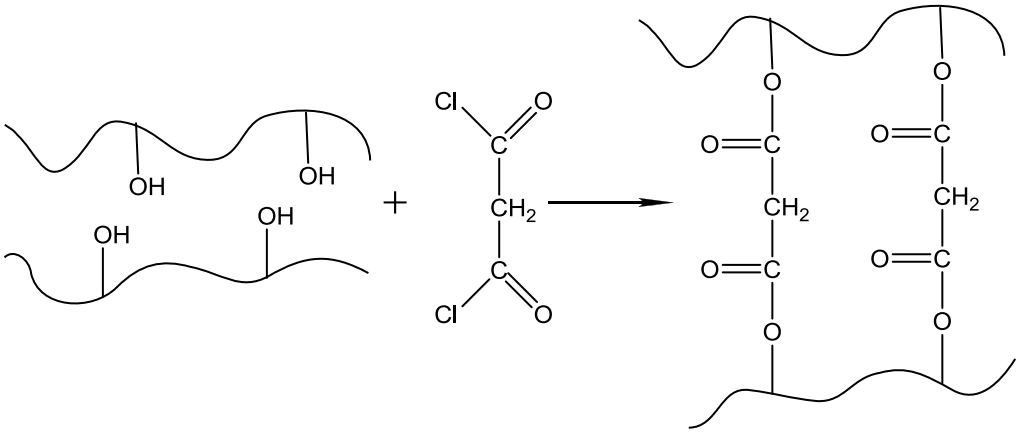

Fig. 3.4 Proposed reaction between cross-linker and membrane

2, First, glutaraldehyde aqueous solution with 25% (wt) was diluted to 0.25 mol/L with MilliQ water, the pH value of the solution was adjusted to 3 by adding sulfuric acid (H_2SO_4), following that, membranes was dipped into the solution, the reaction was allowed to proceed at 60°C for 3 hours. The mechanism of the reaction was expected to be the following Fig. 3.5:

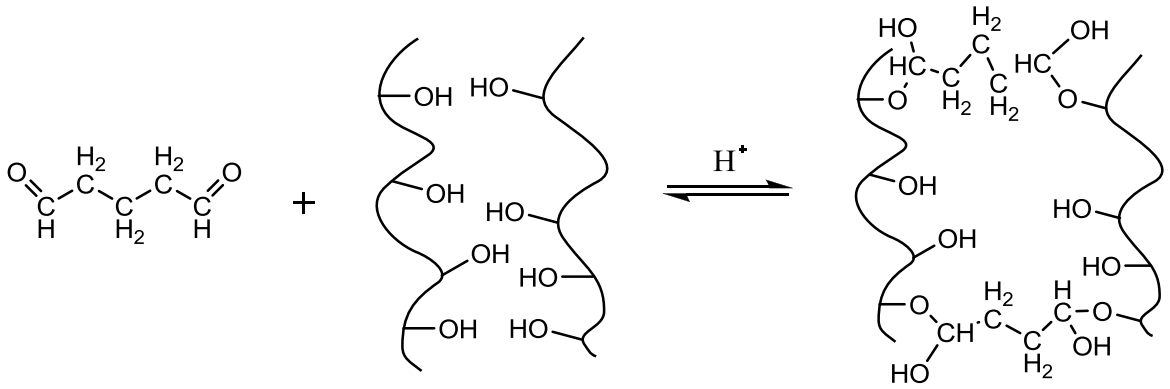

Fig. 3.5 First-step reaction of the cross-linking process using glutaraldehyde as cross-linker

After this process, the color of the membrane turned from light red and brown to totally transparent, which could be a symptom of successful cross-linking, because the color of membrane was probably due to the ceric IV ion that was coupled with carbon connected with hydroxyl group in PEG segments, after successful cross-linking, all the hydroxyl groups reacted with aldehyde groups, then the ceric ion lost the coupling effect as well, as a result, the membrane turned to totally transparent. Meanwhile, the solvent resistance of the

membranes was also enhanced. They became stable in polar aprotic solvents such as DMF or DMSO for long period.

Hemiacetal was formed after this step, whereas, in the following conversion process, NaOH will be used to treat the membrane, and hemiacetals are not stable enough in base solutions, so it is necessary to convert the hemiacetals to acetals, which was achieved via the following process, PEG 400 was first dissolved in water to form 2 g/L solution, then the pH value was tuned to 3 with H_2SO_4, the membranes were dipped in the solution, the reaction took place at 60°C for 3 hours, condenser tube was used to facilitate back flow of water. Fig. 3.6 illustrates the second-step cross-linking reaction.

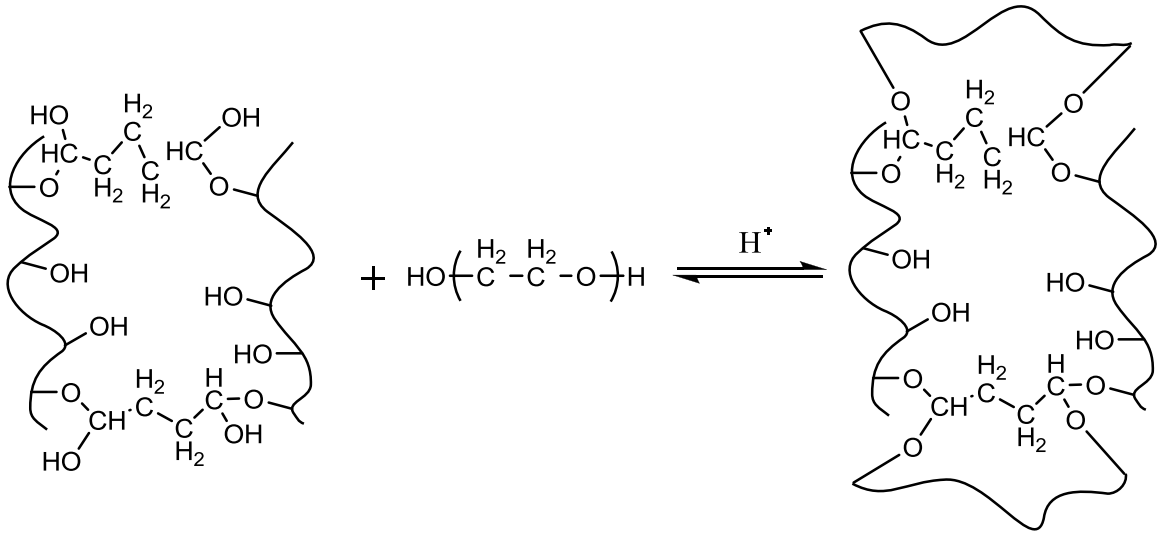

Fig. 3.6 Second-step reaction of cross-linking process

3.7 Conversion to nanofiltration membranes

The membranes after cross-linking were soaked in $ZnCl_2$ aqueous solution with different concentrations (15%, 30%, 45% and 60%) for 72 hours. After saturation with the $ZnCl_2$ solution, the membranes were heat treated in oven at 110°C till completely dry. Followed by, the membranes were allowed to cool to room temperature in the open air. By soaking the membrane in a very dilute HCl aqueous solution (pH = 3–4), $ZnCl_2$ was removed. The

membranes were then hydrolyzed with 1 M NaOH at room temperature for a controlled period. After the reaction, the hydrolyzed membrane was treated with 1 M HCl at room temperature overnight. Following that, the membranes were infiltrated with a dilute NaOH solution (pH = 8–9) to convert it into a NF membrane with highly dense pore surface functional groups (–COONa, –CN and –$CONH_2$).

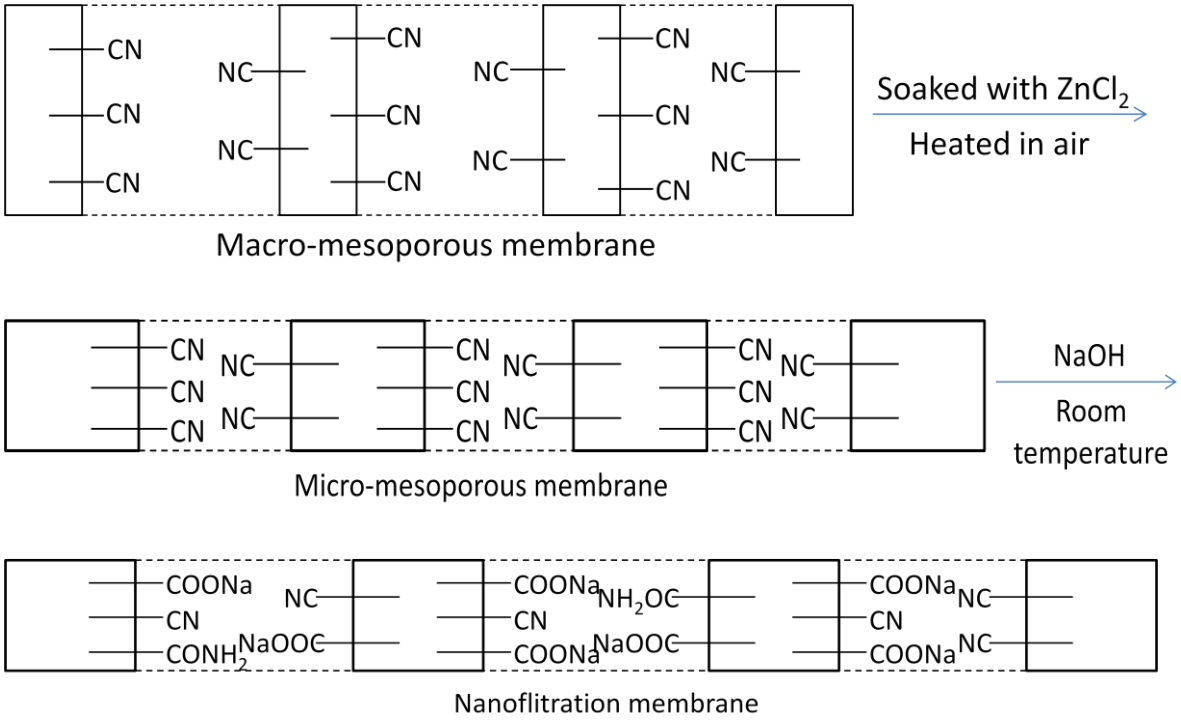

Fig. 3.7 Conversion of membranes for application in nanofiltration

Chapter 4. Results and discussion on copolymers of PAN and PEG

The experiment results obtained and discussion on them are divided into three following paragraphs: (i) copolymer characterization in part 4.1, (ii) swelling tests on films in part 4.2, (iii) characteristics of membranes formed from these copolymers before and after cross-linking and conversion process in chapter 4.3 to 4.6.

4.1 Characterization of block copolymers

It is well understood and also discussed before that the properties of polymers have much influence on the performances of the ultimate UF or NF membranes, especially the mechanical and chemical stabilities, which can affect the resistance to various solvents. Therefore, it is of great importance to characterize the block copolymers in details in this study. The copolymers were characterized with respect to molecular weight and polymer composition. As regarding to composition, it has the main influence on the chemical properties and also affects the cross-linking procedures, thus it was mainly focused. The fraction of each segments were calculated via three different characterization methods: ^{1}H-NMR, FT-IR/ATR and element analysis.

4.1.1 NMR, IR, Elemental analysis and GPC results

To get an optimized composition of the block copolymer, a series of variations were actualized, which includes molecular weight of PEG, content of PEG, content of ceric salts and pre-reaction time for the PEG and ceric salts (t_b). The following data will show the effect of each parameter, and the most significant difference was caused by the pre-reaction time and molecular weight of PEG. Whereas, when the cross-linking process as post treatment is taken into consideration, the PEG with lower molecular weight will be preferred, so the characterizations were prior focused on the difference of pre-reaction time. In all the experiments, copolymers were derived and then characterized in details.

Table 4.1 Composition and parameters used in the copolymerization

	A01	A02	A03	A04	A05	A06	A07	A08
Water (ml)	90	90	90	90	90	90	90	90
PAN (g)	7	7	7	7	7	7	7	7
PEG (g)	3	3	3	2	4	3	3	3
(MW)	(600)	(6000)	(400)	(400)	(400)	(400)	(400)	(400)
Ceric salts (g)	3.216	0.373	4.522	3.014	6.046	4.522	4.522	4.522
Reacting time (hour)	4	4	4	4	4	4	4	4
T_b (min)	30	30	30	30	30	0	10	20
Yield (%)	65	70	58	62	59	60	58	61

As the characteristic peak due to vibration of CN group is fairly obvious and not affected by other groups, it is quite convenient to characterize the copolymer with IR spectrum. Fig. 4.1 shows the IR spectrum of the block copolymers. From Fig. 4.1, absorption bands (cm^{-1}) of 3507, 2877 and 1113 are assigned to ν(O-H), ν(CH_2) and ν(C-O-C) in the PEG block respectively, and another three characteristic absorption bands (cm^{-1}) of 2243, 2939.3 and 1453.3 are assigned to ν(CN), $\nu_{as}(CH_2)$ and σ(CH_2) in the PAN block in the block copolymer. From the IR data, the absorbance of CH_2 group in PEG segment and CN group can be calculated via Beer-Lambert law with the equation as following:

$$A = -log_{10}\left(I/I_0\right) \quad (4\text{-}1)$$

where, *A* means the absorbance, I_0 and *I* represents the intensity of incident and transmitted light respectively. Table 4.2 shows the absorbance of CN peak and CH_2 peak in PEG segment, and the relative ratio of these two peaks as well.

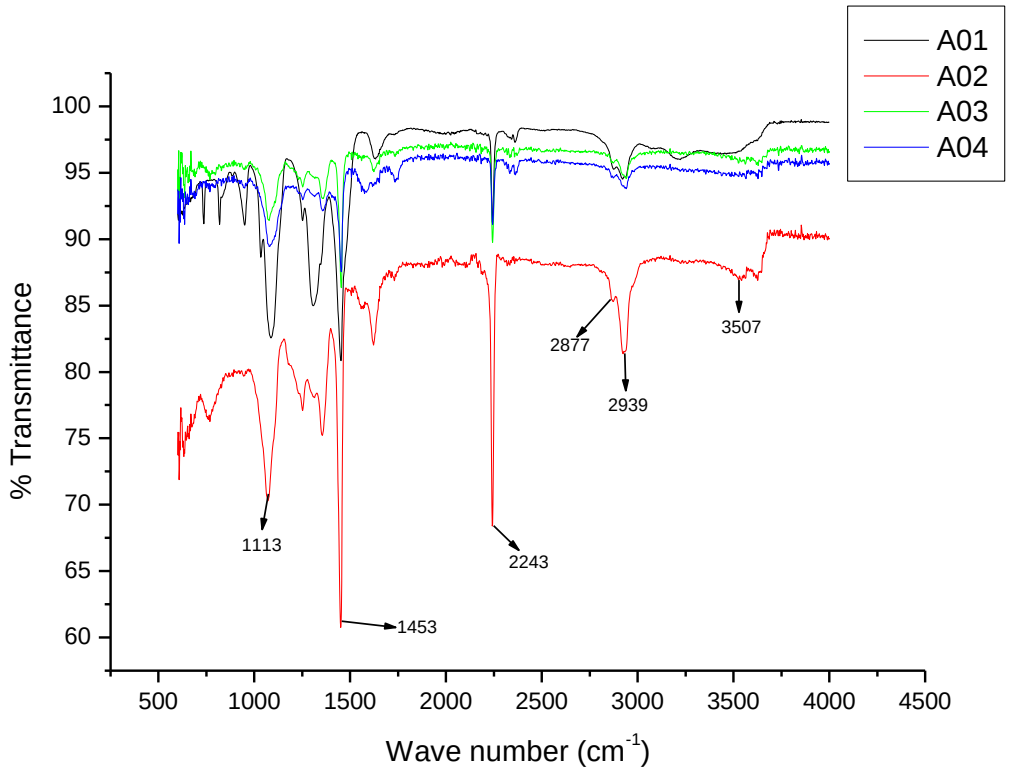

Fig. 4.1 FT-IR spectra of block copolymers with different composition

Table 4.2 Relative ratio calculated from IR results

	A01	A02	A03	A04	A05	A06	A07	A08
Absorbance of CN	3.2	11.9	3.7	4.3	2.1	0.44	2.1	2.9
Absorbance of CH_2 in PEG	1.3	4.4	1.0	1.1	0.8	0.17	0.7	0.8
Relative ratio of CN to CH_2	2.46	2.7	3.7	3.9	2.6	2.6	3	3.6

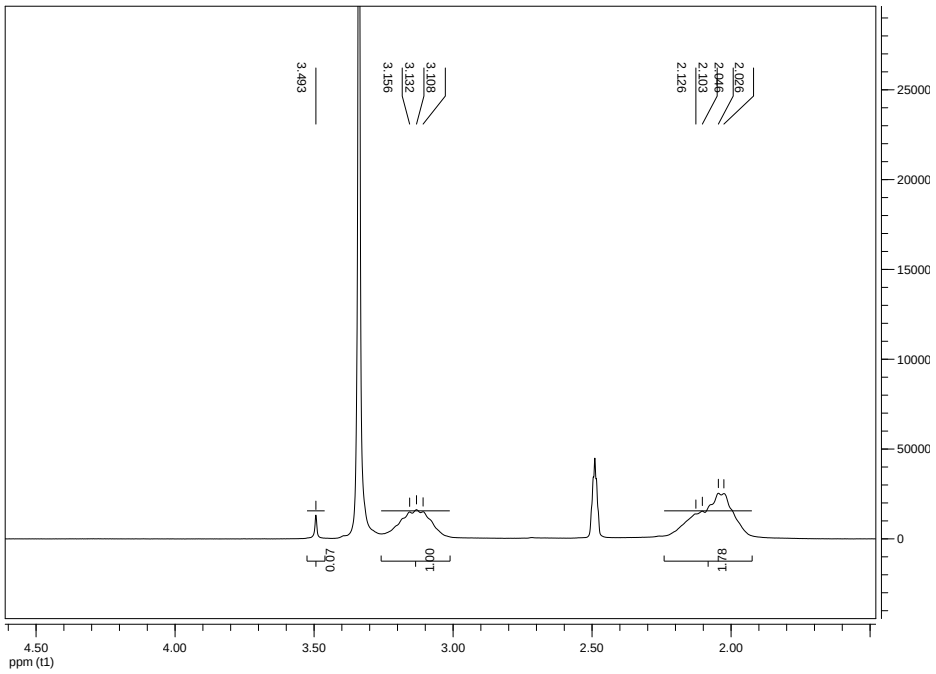

Fig. 4.2 ^{1}H-NMR spectra of the block copolymer from A07

Fig. 4.2 illustrates the ^{1}H-NMR spectrum of the block copolymers. It can be observed clearly from the spectrum that chemical shifts at 2.03 and 3.17 ppm are attributed to the hydrogen in CH_2 and CH in the PAN segments, the appearance of chemical shift at 3.51 ppm is due to the $–CH_2CH_2O–$ group of PEG, and chemical shift at 2.51 ppm is because of the solvent DMSO-D6. By integrating the area under the peaks at 2.03 ppm and 3.51 ppm, absolute ratio of AN molecules to repeating units in PEG segments ($-CH_2CH_2O-$ group) can be calculated, then contents of every element were derived, which are shown in Table 4.3.

Table 4.3 Content of elements based on the NMR results

	A01	A02	A03	A04	A05	A06	A07	A08
C (%)	67.71	64.35	67.75	67.79	67.68	67.55	67.68	67.72
N (%)	25.98	19.38	26.13	26.19	26.02	25.8	26.02	26.08
O (%)	0.6	9.7	0.42	0.33	0.59	0.91	0.59	0.5
H (%)	5.71	6.57	5.7	5.69	5.71	5.74	5.71	5.7

Table 4.4 illustrates the content of each element in the block copolymer derived from element analysis compared with the theoretical values which is calculated from the mass ratio of PEG and AN added in the reaction solution.

From the data of three different characterization methods, obvious evidences for PEG segments in the copolymer were found. As PEG itself was already polymer before the copolymerization, there are alternating blocks of AN and PEG in the copolymer, conclusions can be made that block copolymers were successfully synthesized.

Table 4.4 Content of each element from element analysis

	A06	A07	A08	A03	Theoretical value
C (%)	65.4	66.2	65	66.2	63.17
N (%)	24.6	25.1	25	25.6	18.49
O (%)	3.2	1.5	1.4	1.3	11.62
H (%)	5.8	5.6	5.6	5.6	6.72

Furthermore, information of the molar mass of the block copolymers is also of great importance to the solubility in solvents and pore forming properties. Generally, for the formation of appropriate membranes, the polymers are required to have molar mass between 6000 and 300,000 g/mol. So it is essential to characterize the copolymers with molar mass as well as the molar mass distribution. Table 4.5 shows the molar mass of the block copolymers from GPC, in which M_n means number average molar mass, M_w represents weight average molar mass, and PDI for poly-dispersity index. In the data formula, it can be seen that, the PDI is relatively high as comparing to conventional free radical polymerizations, which is normally around 2.5. This is mainly due to the unconventional initiation step, in ideal condition, it is expected to generate free radicals at both ends of PEG molecules, whereas in reality, there is also high possibility to initiate at only one terminal. Comparing with the theoretical values, the synthesized polymers have relatively lower oxygen content, which means the mole ratio of PEG in the copolymer is lower than that in

the feed. It is also connected with the unconventional initiation step, as the free radicals disappear with time, it is possible that some of the PEG chains have no generated radicals in either end. Then the stable PEG will not participate in the reaction, so certain amount of PEG are still left in the reaction solution.

Table 4.5 Molar mass information from GPC

	A05	A06	A07	A02
M_n (g/mol)	2.20E+04	5.70E+04	6.60E+04	6.50E+04
M_w (g/mol)	1.20E+05	3.30E+05	3.40E+05	3.40E+04
PDI	5.5	5.8	5.2	5.2

In the quantization data of IR and NMR spectra and element analysis results, the copolymers prepared from PEG 6000 that was named with A02 had extremely high content of oxygen as comparing to other polymers, which is mainly due to its higher chain length that results in longer PEG segments in the block copolymer. Whereas, the A02 copolymer also has higher molecular weight and low solubility results from the former factor, it was even not able to form completely homogeneous solution with 10 wt%. Similar situation also took place on the copolymer made from PEG 600 named with A01, the highest concentration can be got from this group of copolymer was lower than that from PEG 400. Besides, in the post treatment, cross-linking will happen exclusively between hydroxyl group at the end of PEG segments and functional group in the cross-linker. So longer length of PEG segment will reduce the cross-linking density, which is a negative factor for the solvent resistance, therefore, copolymers with lower PEG molecular weight were chosen for the following series of comparisons and further studies.

4.1.2 Influence of pre-reaction time

In this redox polymerization, complexes were first formed between ceric ion and PEG, then free radicals were generated on the decomposing of the complexes (as described in general introduction, p. 26), therefore the time for the reaction between PEG and ceric salt (pre-reaction time) is required and it has high possibility to affect the composition of the copolymers. So the influence of pre-reaction time on the copolymers was studied based on the results given above.

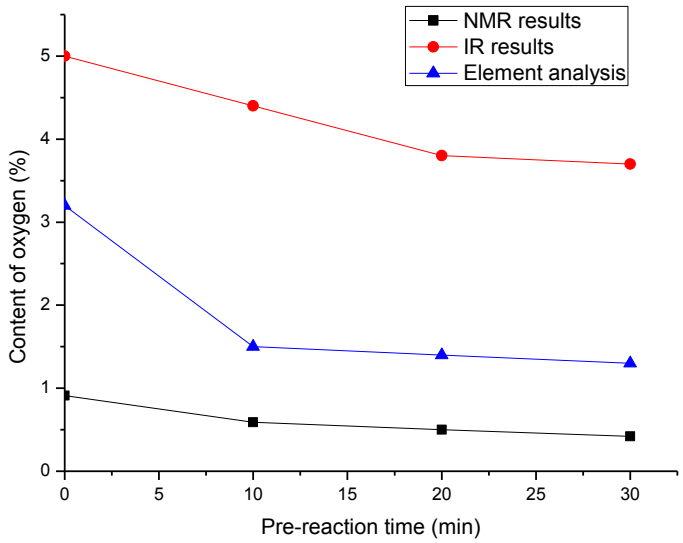

Fig. 4.3 Influence of pre-reaction time on content of oxygen

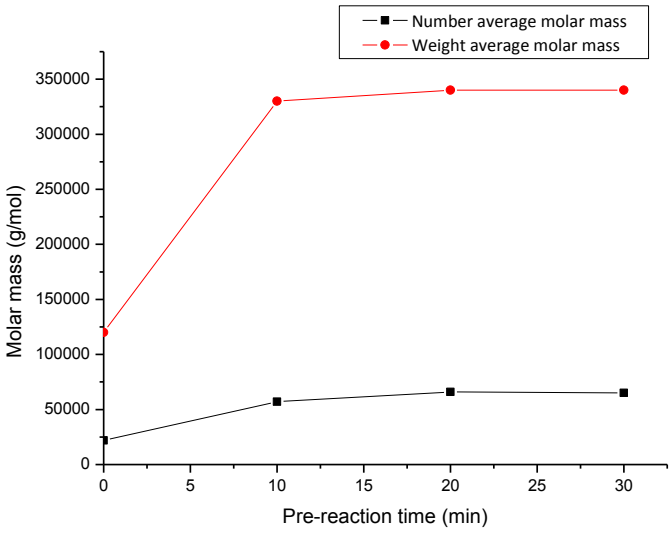

Fig. 4.4 Effect of pre-reaction time on molar mass

From Fig. 4.3 and Fig. 4.4, clear conclusions can be made, that with the increasing of the pre-reaction time, both M_n and M_w increased obviously, whereas the M_w increased more significant that M_n, and the content of oxygen in the block copolymer decreased on the contrary. This can be explained with the following theory:

the polymers that have short chains will contribute more to the M_n, and long chain polymers contribute more to the M_w, when longer pre-reaction time was applied, some of the free radicals were already deactivated, hence less PEG molecules participated in the reaction which results less content of oxygen in the copolymer, and less initiator groups will lead to less but longer chains, which results significant increasing of M_w and slight increase of M_n.

To confirm this hypothesis, stable free radicals were introduced to track the concentration of free radicals generated in the pre-reaction versus time (cf. Experimental part, section 3.3.5). Fig. 4.5 shows the mechanism of the reaction between DPPH and free radicals. In Table 4.6, the volumes of the used reaction solution were recorded.

By coupling with another free radical, covalent bound was formed, then the color of solution changed obviously and the UV-vis spectrum shifted from pink curve to the yellow one, which indicates that all the DPPH have already coupled with other radicals. From the already known DPPH concentration and the recorded reaction solution volume used, the concentrations of free radicals after different pre-reaction time can be calculated, which is also included in Table 4.6.

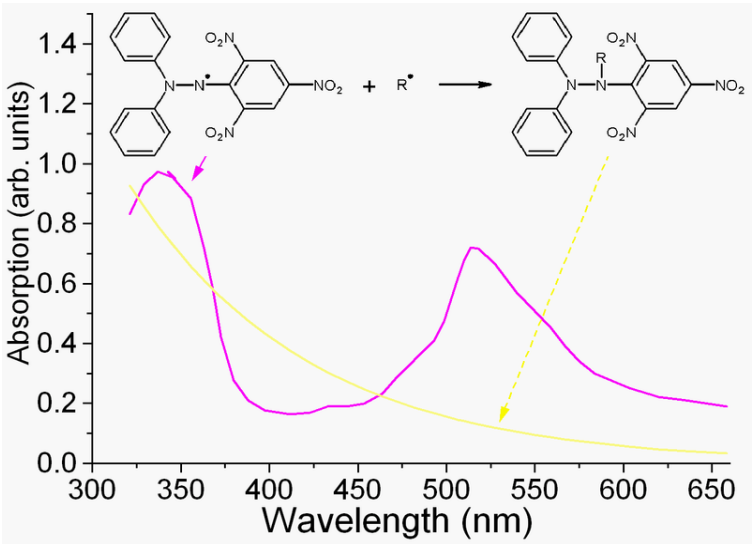

Fig. 4.5 Mechanism of stable free radicals conversion and the corresponding change in UV-vis spectra

Table 4.6 Volume of reaction solution used and calculated free radical concentration

Time (min)	Volume of used reaction solution (ml)	Calculated free radical concentration (mol/l)
0	0.375	1.35e-2
5	0.385	1.32e-2
10	0.390	1.3e-2
20	0.501	1.01e-2
30	0.530	0.96e-2
40	0.551	0.92e-2

Then the dependence of free radical concentration on the pre-reaction time is clearly illustrated in Fig. 4.6. With longer pre-reaction time, the concentration of starting radicals decreased clearly. This is mostly because, free radicals were generated simultaneously after the addition of all the reactants, but with increasing time, even if the radicals didn't initiate

any polymerization, the content and concentration of the existing free radicals decreased continuously, which is mostly because of the coupling effect. Therefore, it is better to use no pre-reaction time, which means AN monomers should be added into the reaction solution immediately after the addition of PEG and ceric ammonium nitrate.

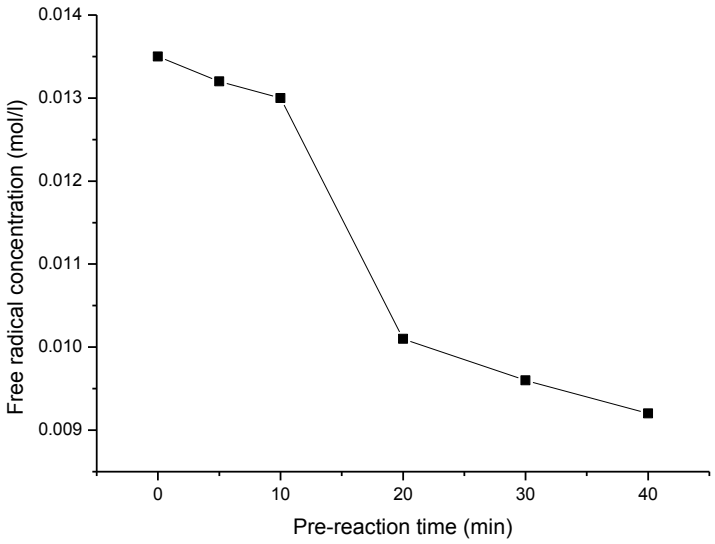

Fig. 4.6 Dependence of free radical concentration on the pre-reaction time

4.1.3 Influence of solvent

Problems of solubility happened when repeating the experiments to produce large amount of copolymers for membranes. Some copolymers could be dissolved neither in DMF nor in NMP even with fairly low concentration. Comparing every condition between these copolymers with distinct solubilities, essential condition that affected the properties of the copolymers was found to be the solvent used in the synthesis. In the following Table 4.7, three kinds of solvents with increasing conductivity were applied and the copolymers derived were characterized as before.

Table 4.7 Solvents used in the copolymerizations

	A09	A10	A11
Solvent	MilliQ Water	Deionized water	NaCl aqueous solution
Conductivity (μS/cm)	0.7	3.0	6.0

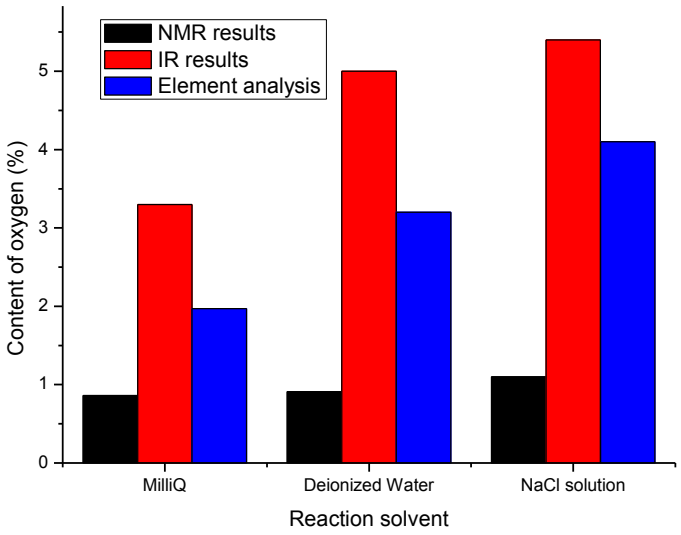

Fig. 4.7 Influence of reaction solvents on composition of copolymers

Compared with the copolymers synthesized in deionized water, the copolymers from MilliQ water have much higher weight average molecular weight. But the difference in number average molecular weight is not so significant, which is seen in Fig. 4.8. Besides, when it comes to the comparison on the copolymer composition (here the content of oxygen was applied to illustrate), as shown in Fig. 4.7, from NMR results, there was almost no difference. But as for the results from IR and elemental analysis, copolymers from MilliQ water have lower oxygen content, which means also lower content of PEG. This is because in the unconventional copolymerization, the polymer PEG acts only as initiator, and the propagation of copolymers was exclusively contributed by AN. Therefore, larger molar mass is directly connected with lower PEG fraction, thus lower oxygen content. But in the NMR measurement, polymers with extremely large molar mass can't be fully dissolved in the solvent DMSO-d6. So there is little distinction in the NMR samples from different copolymers,

as for the measurements that is not involved with solvents and solubility, the results are more reliable, and also closer to the theoretical analysis.

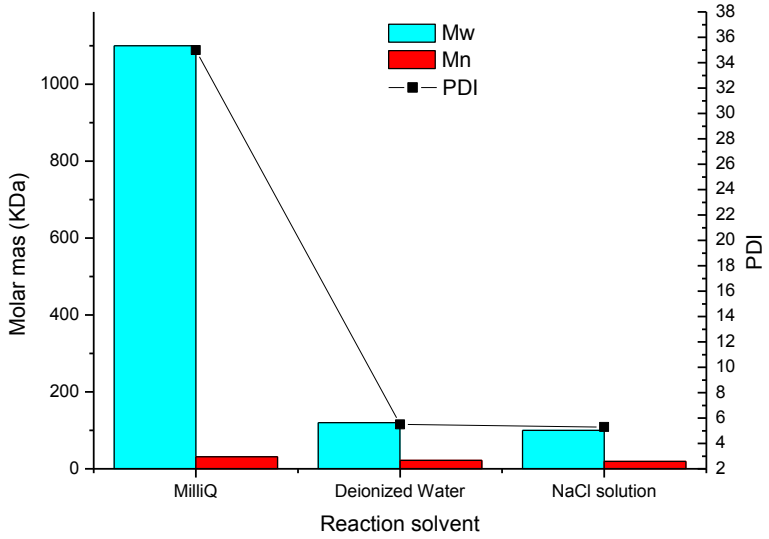

Fig. 4.8 Effect of synthesis solvent on molar mass and PDI

When NaCl solution substituted distilled water as the reaction solvent, there is no clear difference either in molar mass information from Fig. 4.8 or in the copolymer composition from Fig. 4.7. Furthermore, the solubilities of the copolymers are also close to each other.

If the conductivity of the real reaction solution is taken into consideration, addition of ceric salts can greatly change the conductivity, and then the difference between these three conditions will be largely minimized, even can be ignored. Therefore, conductivity is still not proved to be a crucial parameter that can influence the composition or molar mass of the copolymer. The effect of solvent on the resulting copolymers is jet not clear, but the most appropriate solvent for this study is deionized water.

4.1.4 Summary

Block copolymers of PAN and PEG were successfully synthesized via water-phase precipitation copolymerization using Ce(IV)-PEG as a redox initiator system. It is possible to tune the content of PEG, the molar mass of the copolymer, and to change the molar mass of PEG segment, thus to tune the properties of the resulting membranes. Optimized condition

and composition were worked out to synthesize appropriate copolymers to be used for film and membrane studies.

4.2 Swelling properties of films

Swelling behavior of a nanofiltration membrane is of great importance, since so-called "channels" could be created in the dense layer of the membrane due to excessive swelling, then the permeability and rejection can be significantly changed. Besides, in membranes there are large free spaces (pores), which will lead to higher solvent uptake, so the calculated swelling degree will be higher than the real value for the polymer, therefore, swelling behavior was studied on films. Table 4.8 shows the swelling degree of the films in different organic solvents.

Table 4.8 Swelling properties of the films

	Chloroform	Toluene	Acetonitrile	Acetone	Water
m_0 (mg)	11.33	11.01	10.87	15.9	8.05
m_∞ (mg)	11.38	11.3	11.01	16.03	8.25
Swelling Degree (%)	0.44	2.6	1.3	0.82	2.5

From this group of data, it can be seen that the films were endowed with good swelling resistance, whereas the introduction of PEG that is quite soluble in water can make the polymer more hydrophilic, thus a relatively higher swelling degree in water. For the swelling behaviors in these organic solvent, it can be explained by Hansen solubility parameters (HSP) [195]:

· δ_d The energy from dispersion bonds between molecules

· δ_p The energy from dipolar intermolecular force between molecules

· δ_h The energy from hydrogen bonds between molecules

· R_0 Interaction radius of the substance being dissolved

$$(R_a)^2 = 4(\delta_{d2}- \delta_{d1})^2+(\delta_{p2}- \delta_{p1})^2+(\delta_{h2}- \delta_{h1})^2 \quad (4\text{-}2)$$

$$RED = R_a/R_0 \quad (4\text{-}3)$$

·RED < 1 the molecules are alike and will dissolve

·RED = 1 the system will partially dissolve

·RED > 1 the system will not dissolve

The possible range of Hansen solubility parameters of the copolymer can be simulated with the help of the software HSPiP [195], as shown in Fig. 4.9.

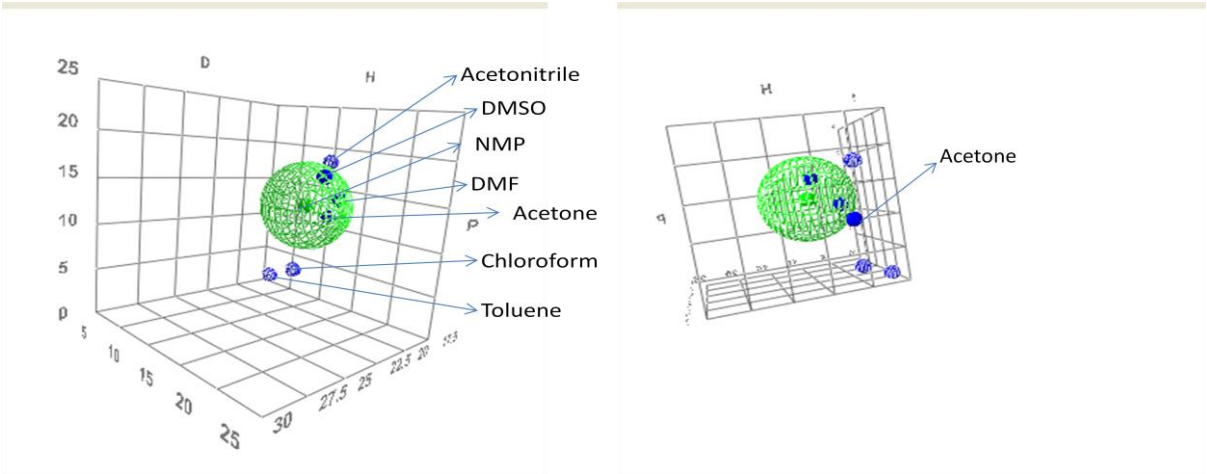

Fig. 4.9 Simulation of Hansen Solubility Parameters with HSPIP

In this 3D diagram, every blue dot represents a kind of solvent. Based on the solubility of copolymers in different kinds of solvents and swelling degree in the non-solvents, a certain mark between 1 and 5 was given for each solvent, as a level to evaluate the interaction between solvent and copolymer, in which, 1 means copolymers are soluble in this solvent, and 5 represents the lowest swelling. In the 3D diagram, these values will be seen as the distance between two different molecules. The farther the distance is, the less solubility or

swelling degree is. From these values, the crude possible range of HSP of copolymers was simulated and graphed in the axis as the green sphere. When the dot of solvent stays inside the green sphere, the copolymer will be possibly soluble in this solvent, the solvent outside the sphere can probably not dissolve, but only induce swelling, and the farther the distance, the less swelling.

4.3 Influence of concentration and drying methods

Drying is the first treatment of the membranes. As the membrane is still in swelling state, the pore structure is yet not stable and could be reformed during the drying process, so it is very important and necessary to investigate the influence of drying methods.

4.3.1 Thickness

In this part of experiments, membranes were casted with the thickness of 200 µm, then thicknesses before and after drying methods were measured. As presented in Table 4.9, in which water means drying directly from water, whereas solvent exchange stands for drying after treating with ethanol and hexane in sequence.

Table 4.9 Thicknesses and shrinkages of the membranes

Polymer concentration (%)	Water			Solvent exchange		
	Before (µm)	After (µm)	Shrinkage (%)	Before (µm)	After (µm)	Shrinkage (%)
10	80.75	63.5	21.36	81	77.5	4.32
12	83	62.75	24.40	88.5	82.5	6.78
14	91.25	66.63	26.98	91.75	84.88	7.49
16	92.33	67.35	27.05	93.15	86.05	7.62

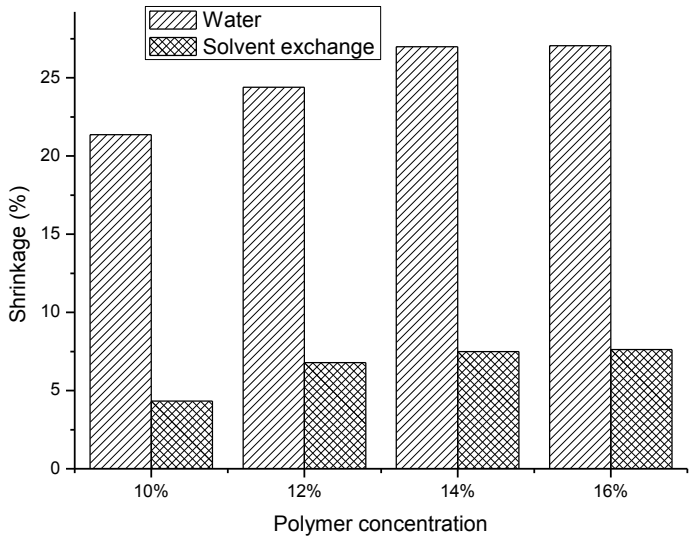

Fig. 4.10 Influence of drying treatment and polymer concentration on the shrinkage of membrane thickness

All the membranes were casted with thickness of 200 µm, but after the non-solvent induced phase separation (NIPS), all the thicknesses decreased by certain content. Increase in polymer concentration decreases the reduction. This is because that, solutions with higher concentration has also higher viscosity, which will prevent the solution from spreading between the steps of casting and immersion into water. In the phase separation process, larger content of polymers that leads to lower free volume is good for the membranes to maintain the structure. So that when water penetrated into the polymer solution to mix with the solvent and then took the solvent out from the solution by diffusion effect, there was less reduction in the volume of the casted solution film. Therefore the thickness didn't change so significantly.

After the drying treatment, the thicknesses of the membranes decreased again, because the copolymers has relatively high swelling degree in water, but the membranes from solvent exchange treatment showed much lower reduction, which indicates that the morphology of the membrane was changed during the drying process, so it is necessary to check the pore morphology via Scanning Electron Microscopy (SEM).

4.3.2 Pore morphology

Membrane surface and cross-section morphologies were visualized by using SEM. As shown in this series of images, all the membranes have asymmetric structure consisting of a thin fine porous selective layer and much thicker porous sub-structure,

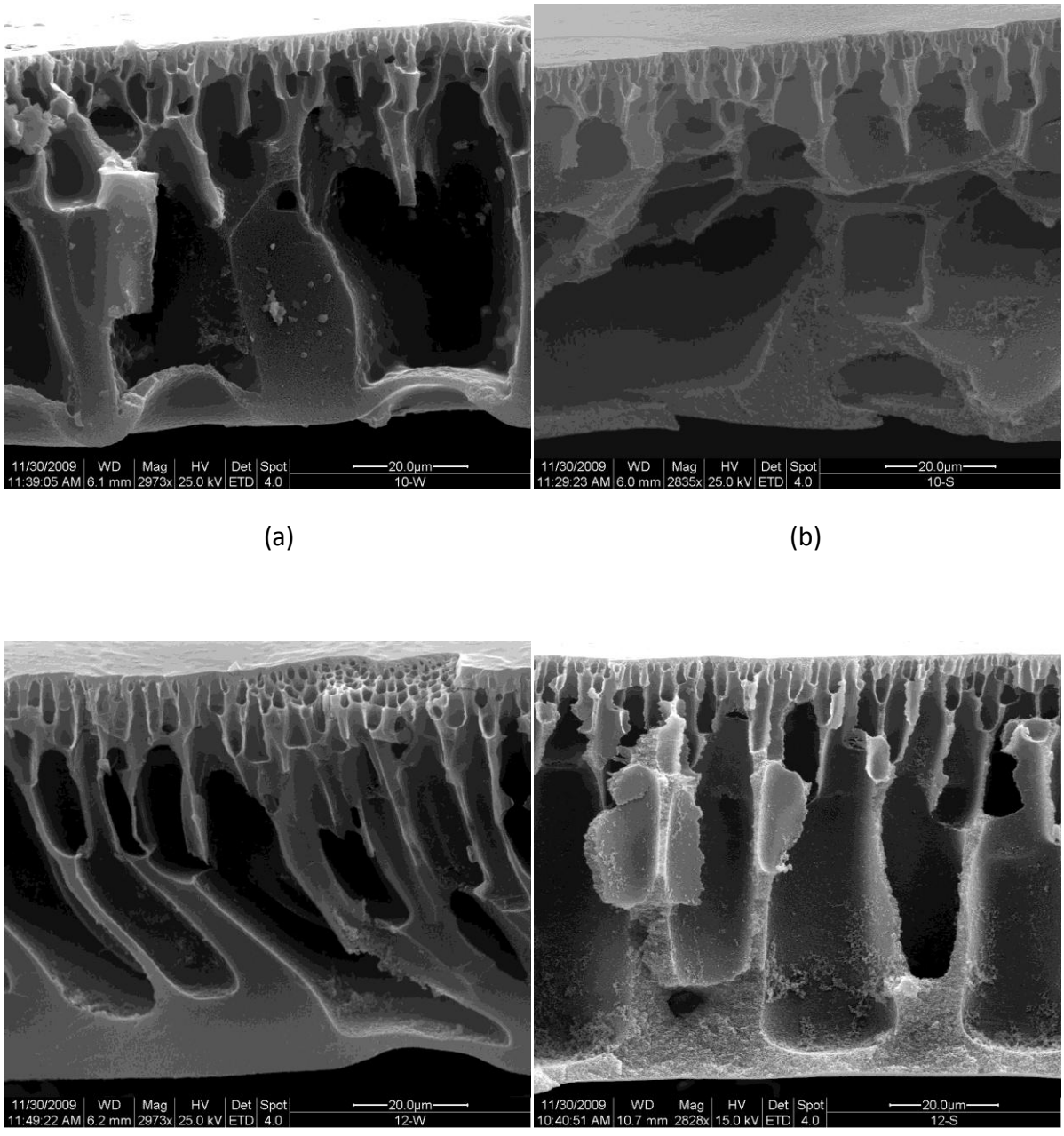

Fig. 4.11 SEM cross-section images of membranes from the block copolymer: (a) concentration 10%, drying from water; (b) concentration 10%, drying with solvent exchange; (c) concentration 12%, drying from water; (d) concentration 12%, drying with solvent exchange.

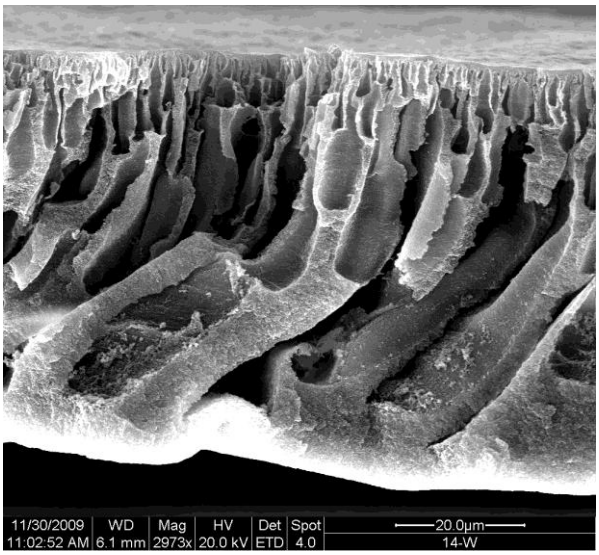

(e)

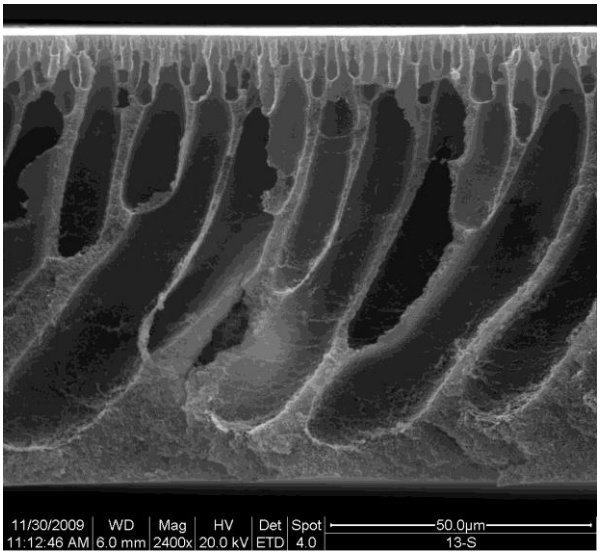

(f)

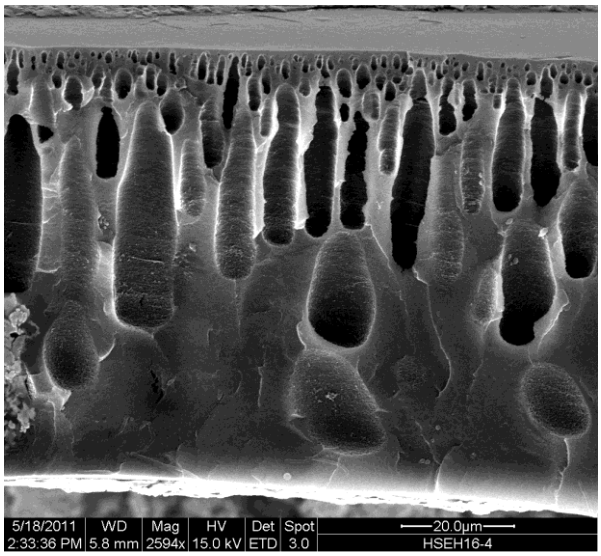

(g)

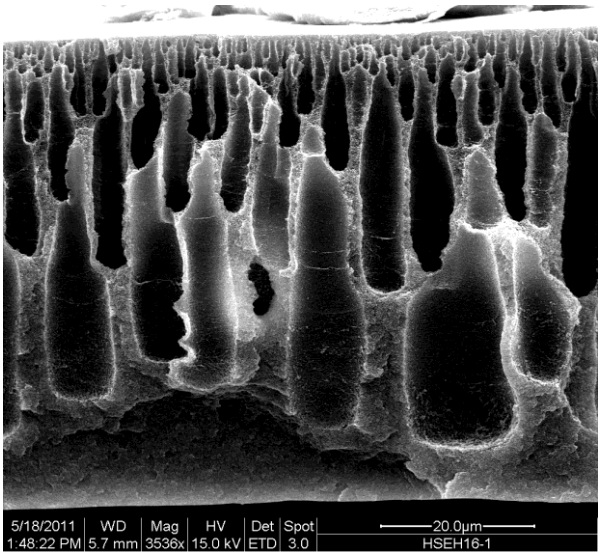

(h)

Fig. 4.11 SEM cross-section images of membranes from the block copolymer: (e) concentration 14%, drying from water; (f) concentration 14%, drying with solvent exchange; (g) concentration 16%, drying from water; (h) concentration 16%, drying with solvent exchange.

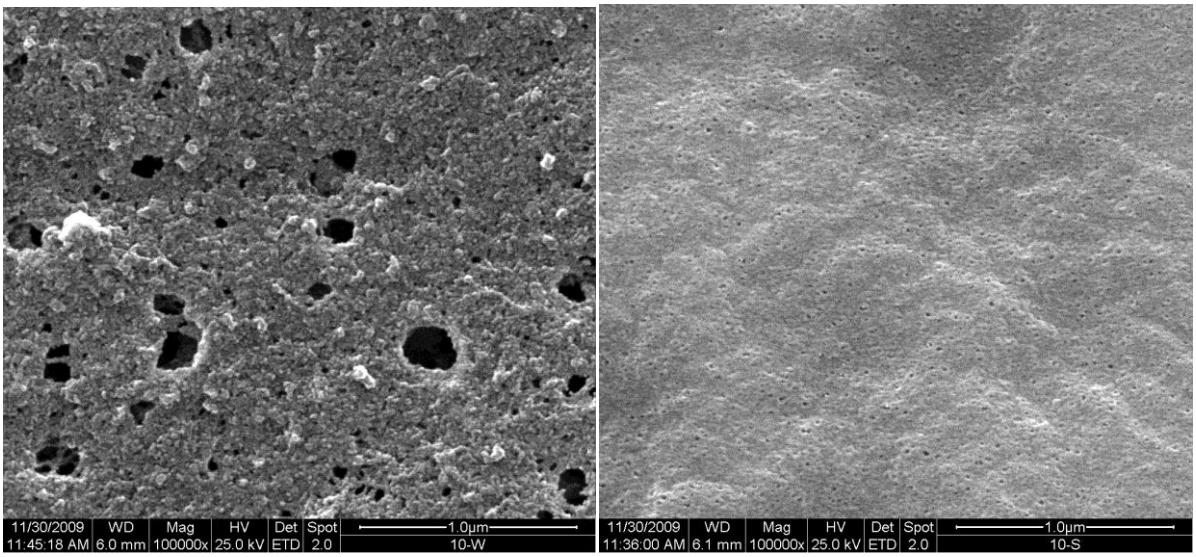

(a) (b)

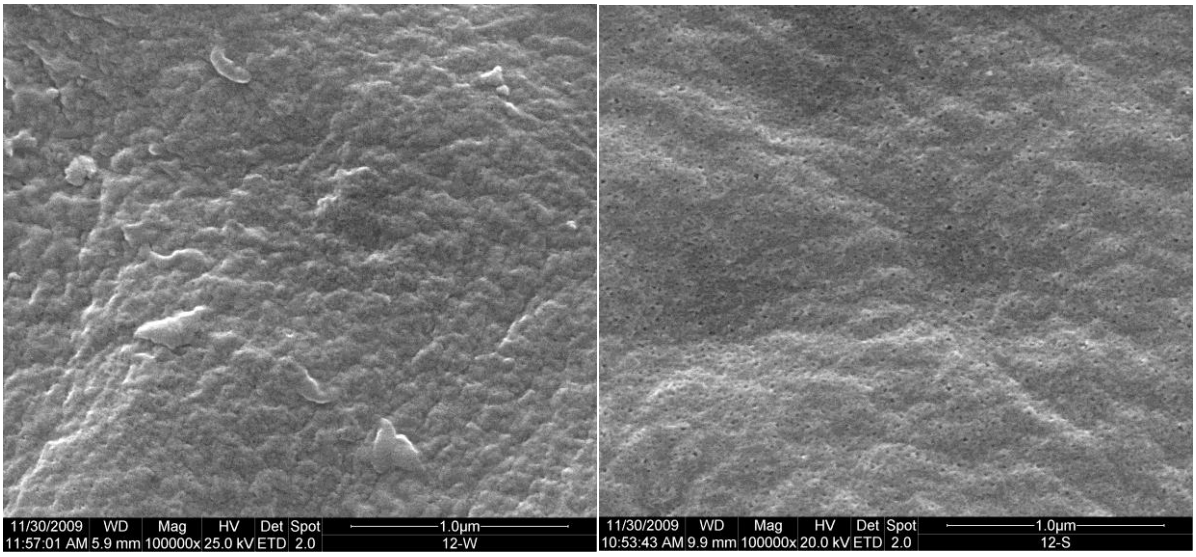

(c) (d)

Fig. 4.12 SEM surface images of membranes from the block copolymer: (a) concentration 10%, drying from water; (b) concentration 10%, drying with solvent exchange; (c) concentration 12%, drying from water; (d) concentration 12%, drying with solvent exchange.

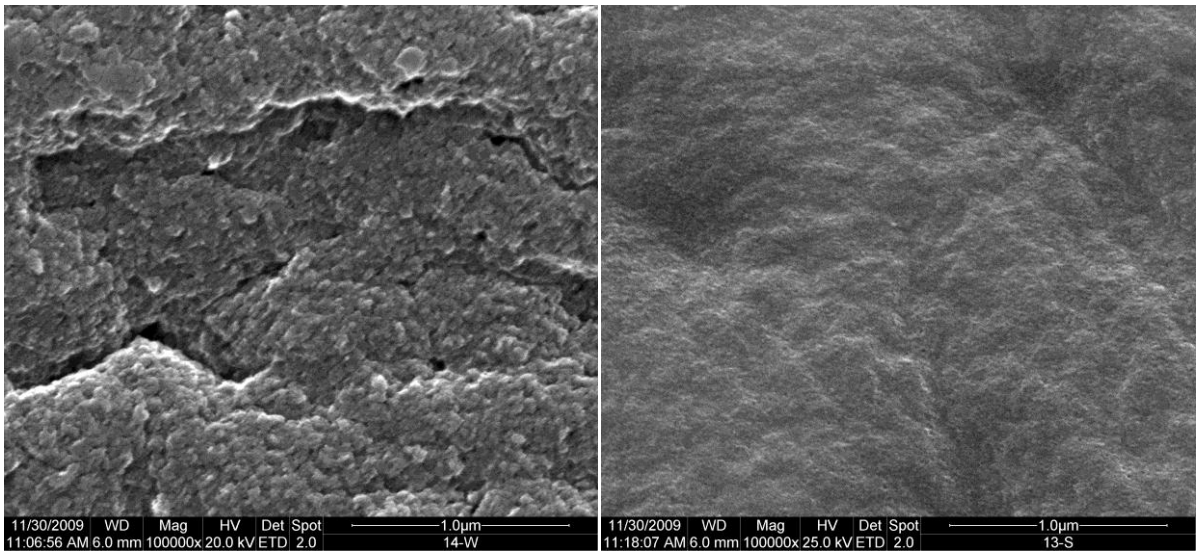

(e) (f)

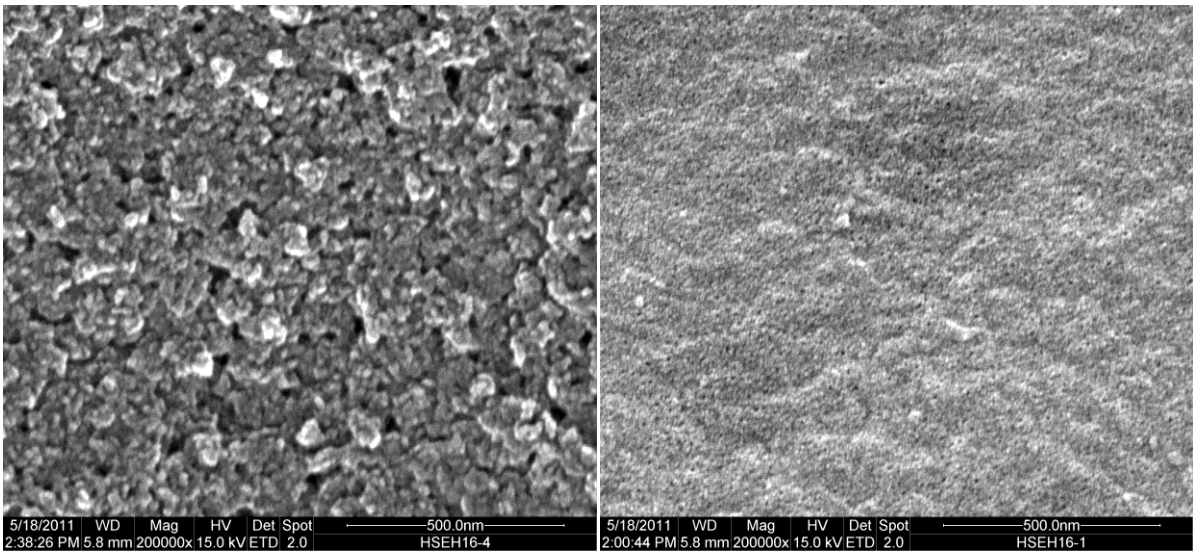

(g) (h)

Fig. 4.12 SEM surface images of membranes from the block copolymer: (e) concentration 14%, drying from water; (f) concentration 14%, drying with solvent exchange; (g) concentration 16%, drying from water; (h) concentration 16%, drying with solvent exchange.

As shown in Fig. 4.11, with increasing concentration of the polymer solution, the difference between the selective layer and sub-structure tends to decrease, thus more regular and finger-like pores are formed. Effect of concentration on the pore structure can be also observed in the surface images in Fig. 4.12, higher concentration leads to smaller surface pores. The effect of concentration is mostly explained with free volume: in the polymer solution, the solvent occupies much volume, with increasing polymer concentration, the

volume occupied by the solvent decreases. In the phase separation process, as the non-solvent is miscible with the solvent, the mixing of solvent and non-solvent will lead to a diffusive flow of solvent that bring the solvent outside the polymer solution. By the meantime, the polymer structure also tends to collapse to a certain extent, but much volume that was occupied by the solvent was remained to form pores, thus porous membranes were formed. With same solvent and non-solvent, the diffusive flow of solvent outside the solution has similar speed in different concentrations, so the collapse of the polymer structure is also similar, therefore, concentration is the only factor that influences the pore structures, higher concentration leads to lower solvent-occupied-volume, eventually resulting smaller pores and denser membrane structures. This can also explain the reduction of the membrane thickness that was found in section 4.3.1.

It can be also found that, for the membranes dried directly from water, the pores were reformed or even broken, especially in the membranes with lower concentration, i.e. in Fig. 4.11 graph (e). Whereas for the membranes treated with solvent exchange, the pores were maintained regular. In the surface images, differences between two drying methods are more obvious and more distinct, the membranes from solvent exchange shows smooth surface and regular pore distribution other than the rough surface and irregular pores of the membranes dried from water. Besides, difference in pore size between various membranes is clearly shown in the surface images, the pores are getting smaller with increasing concentration.

As the membrane has a relatively large swelling degree in water, in the swollen state, membranes have larger free volume that is occupied by water. After the drying treatment, the absorbed water was compressed out, which leads to a reduction in both thickness and pore size. But comparing with drying directly from water, in solvent exchange procedure, as PEG is soluble in all the exchanging solvents, when the solvent is changed from good solvent -- water to relative poor solvent -- hexane, the PEG segments suffer a slow rearrangements of the polymer chains. This slow procedure will probably lead to crystallization of the PEG segments, and the semi-crystal segment is prior to completely amorphous polymers in mechanical stability. So it is better for maintaining the pore structure. Therefore, as shown in the SEM images in Fig. 4.11 and Fig. 4.12, for the membranes from solvent exchange, the pores are not so brittle and easy to be broken as the membranes dried directly from water.

On the other hand, the semi-crystal structure has much less free volume as compare to the totally amorphous structure, and in the dense selective layer, reduction in free volume plays a more important role than the collapse of pore walls. From the SEM images, surface pore sizes of the membranes from concentration of 16% were estimated, the average pore sizes of membranes from water and solvent exchange were 36 nm and 10 nm respectively, which indicated that there should be great variance in the filtration properties. Therefore, drying with solvent exchange will result in denser structure and smaller pore sizes.

4.3.3 Separation performance

The membranes were tested in the filtration process to check the performance. As mentioned above, after the drying treatment, the pore sizes of the membranes were greatly changed, thus difference in filtration properties could be found. Therefore, all the filtration experiments were carried out on both wet and dried membranes. In this part, all the membrane samples were named with symbol of their properties, in which, HSEH means membranes dried with solvent exchange, and HOSH stands for membranes dried in the air after the filtration process of organic solvents, and 10%, 12% means the concentration of the polymer solution they were prepared from.

Fig. 4.13 shows the effect of the polymer concentration and drying treatment on the performance of unmodified membranes. Water permeability was observed to decrease with increasing polymer concentration. A slightly higher MWCO was also achieved at a lower polymer concentration. Besides, water permeability was found to decline a lot after the drying process, the MWCO decreased as well, but the reduction of MWCO was not as significant as that of permeability. In Fig. 4.14, the organic solvents permeability also showed strong dependence on polymer concentration, it decreased with increasing concentration. Among the organic solvents, ethyl acetate was found always to have the highest permeability, hexane and heptanes were also used in the filtration tests, but there were almost no flux at all for both solvents.

Table 4.10 Permeability of water through membranes

	Permeability ($L/m^2 \cdot h \cdot bar$)			
	HSEH10%	HSEH12%	HSEH14%	HSEH16%
Pressure	1 bar	1 bar	1 bar	1 bar
Wet	4182	2340	1010	661
Dry	204	176	140	88

Table 4.11 Permeability of solvents through membranes

	Permeability ($L/m^2 \cdot h \cdot bar$)		
	HOSH16%	HOSH14%	HOSH12%
Pressure	0.5 bar	0.5 bar	0.5 bar
Water	576	756	2749
Ethanol	429	564	2339
Ethyl acetate	994	1300	5402
Acetonitrile	505	594	3053
Hexane			
Water (dried in air)	88	142	196

After the drying treatment, all the membranes got much lower permeability than before, which is clearly shown in the two tables; this proved the conclusion from SEM measurements that were discussed in section 4.3.2. Besides, both the pore size and the permeability of the membranes from concentration of 16% after drying are in the reasonable range of ultrafiltration. Therefore, this group of membranes is decided to be used for further experiments.

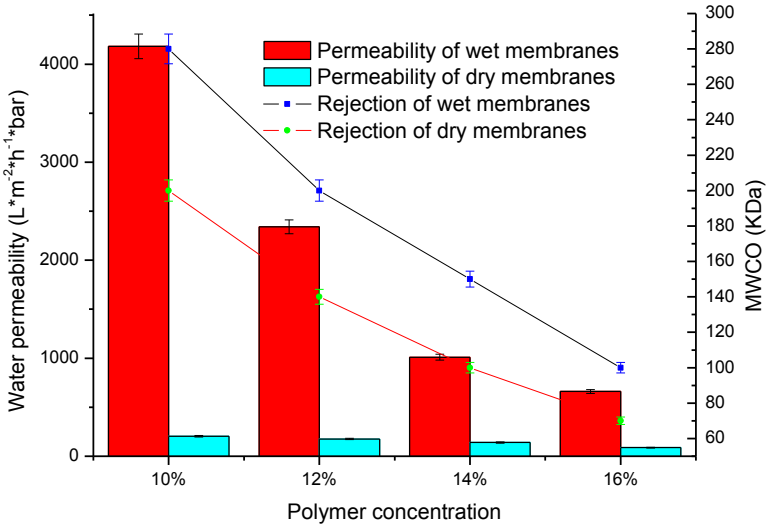

Fig. 4.13 Permeability and molecular weight cut-off of the membranes

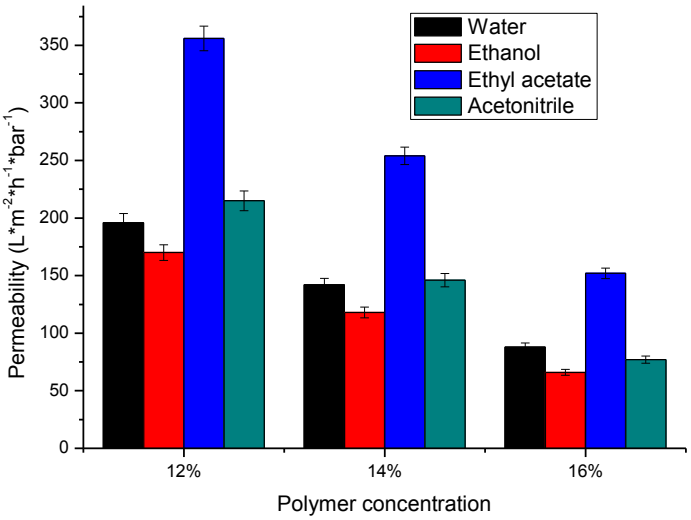

Fig. 4.14 Organic solvents permeability of the dry membranes

In the ultrafiltration process, pore flow model is often used to describe the transport. The pore flow model assumes that the mass transport occurs by pressure driven convective flow through the pores of the membranes. Unlike the solution-diffusion model, the membrane material is not an active participant at the molecular level in the pore flow mechanism. For liquids, the flux through a porous membrane can be described by the Hagen-Poiseuille equation for viscous flow:

$$J = \frac{n\pi r_p^4 \Delta p}{8\eta A \tau l}$$

(4-4)

where J is the liquid flux, n for the number of pores, r_p the pore radius, Δp the pressure difference across the membrane, η is the viscosity of the liquid, A is the membrane area, τ the membrane tortuosity, l the membrane thickness. For a certain membrane, difference in flux of all the solvents was only due to the viscosity of the solvents. Therefore, the dependence of solvent permeability on the viscosity was studied to check the applicability of pore flow model in this study, thus to explain the difference in permeabilities of different solvents.

Table 4.12 Viscosities and permeabilities of different solvents

Solvents	Ethanol	Ethyl acetate	Acetonitrile	Water
Viscosity (mPa*s)	1.2 (20°C)	0.426 (25°C)	0.343 (25°C)	1.002 (20°C)
Permeability (l/(m^2*h*bar))	66	152	77	88

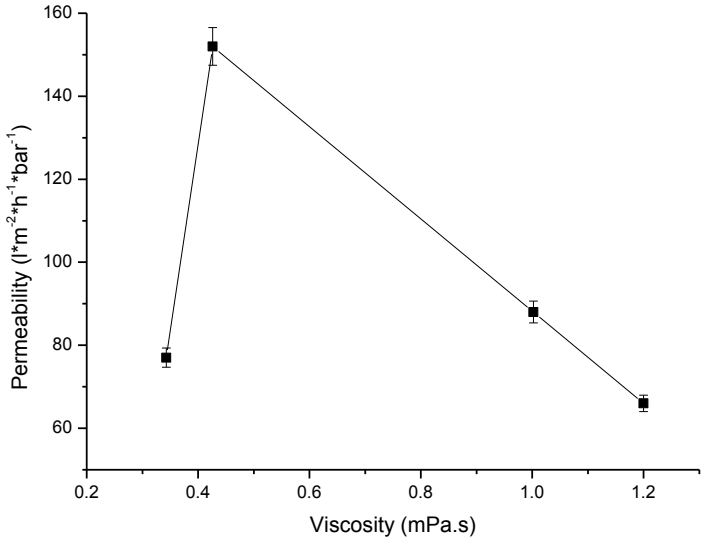

Fig. 4.15 Influence of viscosity on the pure solvent permeability

In Fig. 4.15, there is a clear tendency from the second dot, that with increasing viscosity, the pure solvent permeability decreased, and the permeability is closely vice proportional to the viscosity which fits the Hagen-Poiseuille equation quite well. The only exception happened to acetonitrile, which had lowest viscosity, but didn't have the highest permeability. As the pores in ultrafiltration membranes have much larger size than the diameter of the solvent molecules, the interaction of solvent and membrane could not affect the viscous flow of solvent through the membrane pores effectively, therefore the reason for the abnormally low permeability of acetonitrile is still not clear. Besides, the permeability shows linear relation to the viscosity.

4.3.4 Summary:

After the comparison of various membranes treated with different drying methods, the membranes from polymer concentration of 16% have the most appropriate pore sizes, and treatment with solvent exchange is better to maintain the properties of the membrane and to control both the pore size and pore structure. As for the filtration properties, the membranes from 16% polymer solution were endowed with relatively high permeability and reasonable MWCO. But after drying treatment, the permeability of membranes declined from 661 to 88 L/(m^2*bar*h), and the reduction in MWCO was from 100 kDa to 70 kDa, which was not so significant as the reduction in permeability. Therefore, it is better to store the membranes in water other than dry them. Besides, the separation performance in non-aqueous condition was proved to be stable, and the pore flow model seems to dominate the transport through the membranes.

4.4 Influence of coagulation bathes

As discussed in section 2.2.2, in the phase separation process of membrane production, the interaction between solvents and coagulation bathes is crucial for the membrane properties. Therefore, changing composition of solutions or non-solvents are widely used to modulate the interaction thus to control the properties of resulting membranes. In this study, only the composition of non-solvent was adjusted.

In the following tables and figures, the symbols of the samples refer to different polymers and coagulation bathes, A26 means the polymer that the membranes were made from, W refers to water as coagulation bath, WIP1/1 and WIP1/2 corresponds to mixture of water and isopropanol in a volume ratio 1:1 and 1:2 respectively.

4.4.1 Thickness

Thickness is an indicator of the inner structure, for the membranes prepared from same polymer solution and casted with same thickness, after different formation processes, they were given different thicknesses. As polymers are completely not soluble in the coagulation bath, no polymers can be washed out from the casted film, so lower thickness means that the polymers are more concentrated to occupy the free volume as compare to the higher thickness. Therefore it is probably an indicator of the denser pore structure. In this part of experiments, all the membranes were casted with thickness of 300 μm.

Table 4.13 Thicknesses of membranes derived from different coagulation bathes

Membrane	A26-W	A26-WIP1/1	A26-WIP1/2	A35-1-W	A35-1-WIP1/1	A35-1-WIP1/2	A35-2-W	A35-2-WIP1/1
Thickness(um)	176	126	105	150	103	98	180	132

As seen in Table 4.13, the thickness of membranes decreased with increasing content of isopropanol in the coagulation bath. The reason for that phenomenon is the slowed down mixing speed of solvent and non-solvent, which is because isopropanol is less polar than water.

4.4.2 Pore morphology

Thickness is directly connected with pore morphology. As there was no weight loss during the membrane formation process, lower thickness should lead to denser pore structure. Therefore SEM images were taken to study the influence.

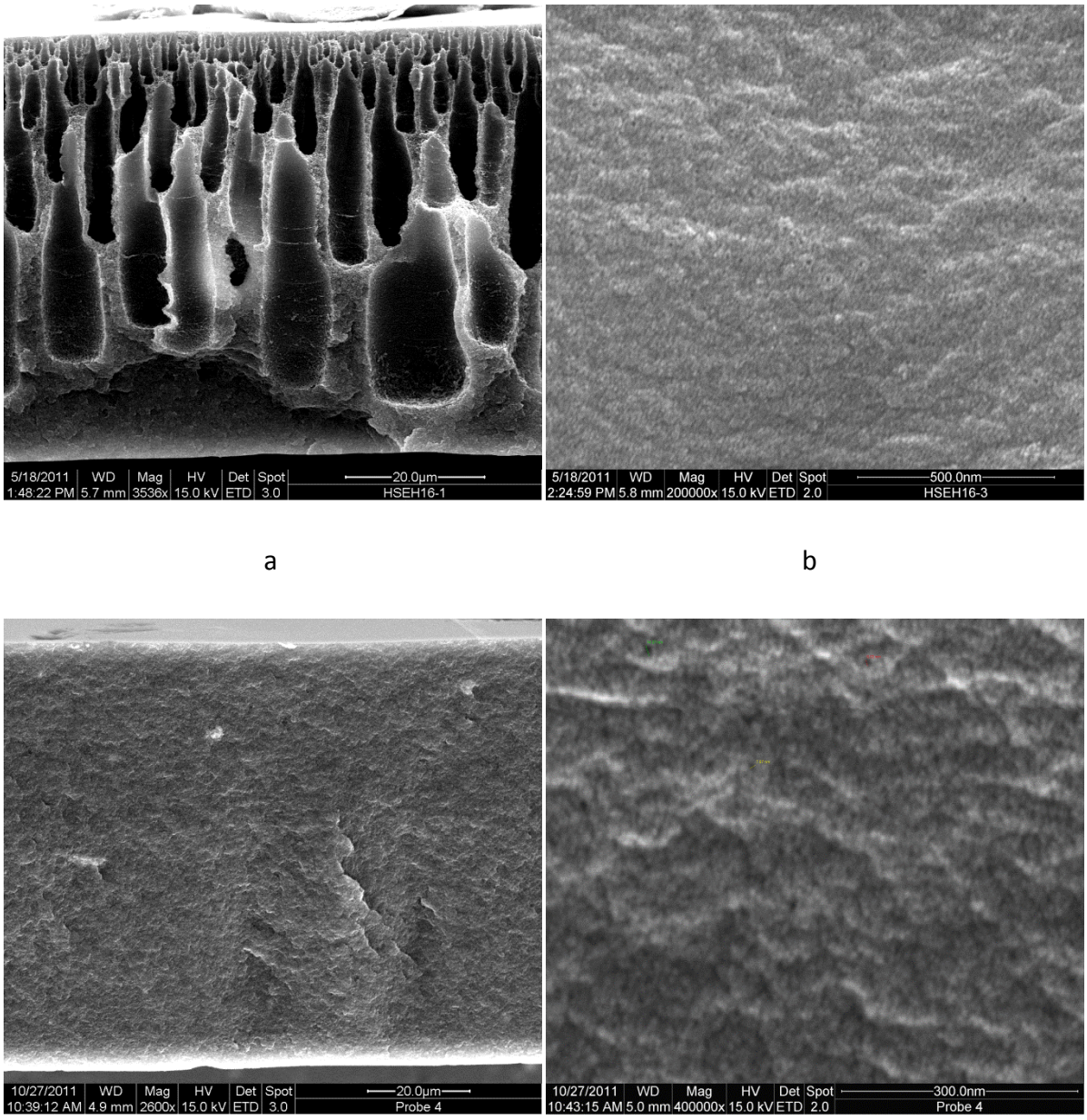

Fig. 4.16 SEM images of membranes derived from different coagulation bathes: (a), cross-section of membrane derived from water; (b), surface view of membrane derived from water; (c), cross-section of membrane derived from WIP (1/1); (d), surface of membrane from WIP (1/1)

Isopropanol may reduce the miscibility of coagulation bath and the solvent which is NMP here, because of its low polarity. So when isopropanol is added, the mixing of solvent and non-solvent is delayed, which can be easily seen in the preparation. If water is used as non-solvent, the mixing of solvent and non-solvent is very fast. So when the casted film was immersed in water, the inflow of water was occurring in parallel. The convective inflow of

water into the liquid polymer/solvent film left its footpath in the casted film, resulting in polymer-free regions. Whereas, the diffusive mixing of water and solvent led to the precipitation of the polymer chains. After the formation of membranes, the polymer-free regions became macrovoids and polymer-rich regions formed the pore walls as seen in Fig. 4.16 (a). As for the membranes derived from WIP(1/1), because of the delayed mixing, solvent can't be brought out of the casted film as fast as before, the phase separation process can be considered as a slowed concentrating process. The concentration in the polymer solution phase is increasing continuously, the polymer chains have possibility and time to distribute to maintain the homogeneous polymer solution. Therefore the volume of the polymer solution decreased with time. At last, as shown in Fig. 4.16 (c), membranes are formed with denser and homogeneous structure, the thickness is also lower than that from water.

4.4.3 Separation properties

Fig. 4.17 shows the effect of coagulation bath on the physical property and separation performance of unmodified membranes. With increasing content of isopropanol in the coagulation bath, the rejection also got higher, which is shown in Fig. 4.18. It is observed that, MWCO decreased much more significantly than permeability. This is due to more homogeneous structure of the membranes, with increasing content of isopropanol, there were no more pores with macrovoid structures in the membrane, the free volume tends to distribute more homogeneous to form a structure similar to sponge-like instead. In this figure, the membranes were prepared from polymer solution with concentration of 16%.

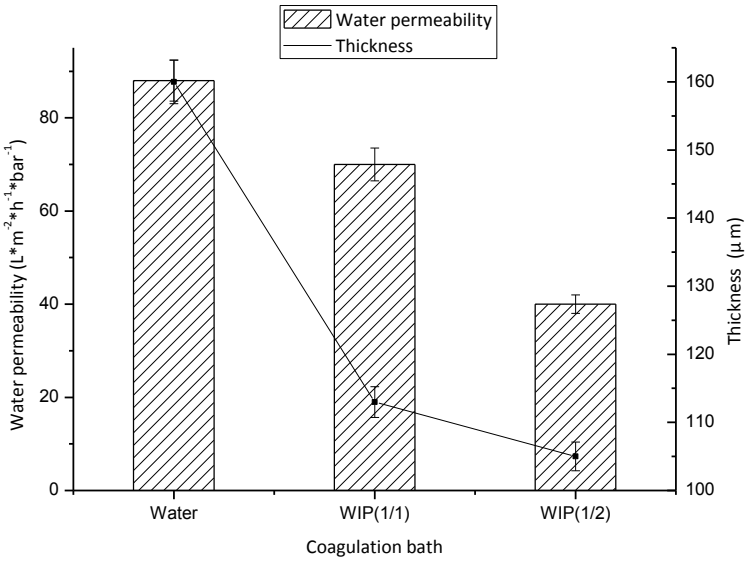

Fig. 4.17 Water permeability and thickness of membranes made from different coagulation bathes (membranes from 16% polymer solution)

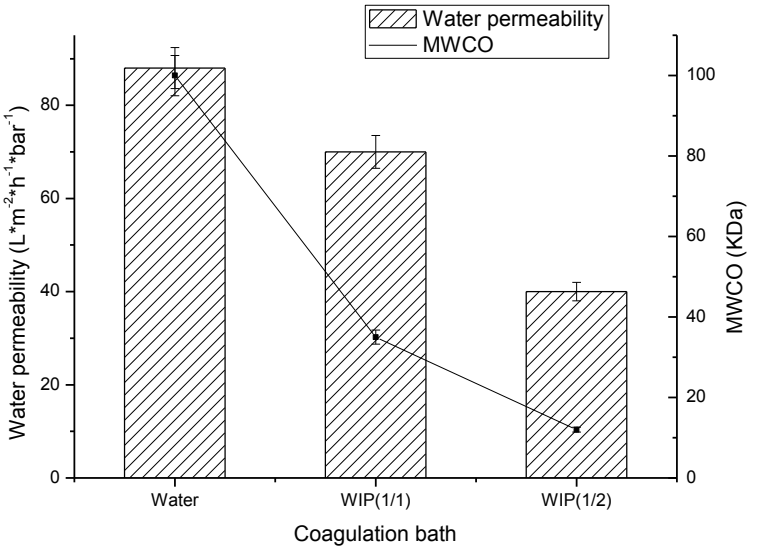

Fig. 4.18 Separation properties of membranes made from different coagulation bathes

Furthermore, membranes from WIP (1/1) and WIP (1/2) have both the sponge-like structure (cf. Fig. 4.16), so even the membranes from WIP (1/2) are denser; they do not have much better rejection properties in comparison with that of WIP (1/1) and water.

4.4.4 Summary

Because of the interaction between solvent and coagulation bath, addition of less polar solvent in the coagulation bath can lead to denser structure of the resulting membranes, thus lower permeability and better rejection properties. Whereas, compared with membranes from the coagulation bath with 50% isopropanol, membranes from 66% isopropanol was endowed with much lower pure solvent permeability but relatively less reduction in molecular weight cut-off. Therefore it is not a perfect way to reach better separation performance by continuously increasing the content of isopropanol in coagulation bath.

4.5 Effect of cross-linking

One of the most important properties for the organic solvents nanofiltration membranes is the solvent resistance, chemical cross-linking is a commonly applied method to enhance the solvent resistance cf. Theory part (section 2.2.2). Whereas, during the cross-linking process, especially when the cross-linking reaction took place on the already-formed membranes; the cross-linking reaction could remodel the pores or change the separation performance of membranes. So it is necessary to investigate various properties after cross-linking.

4.5.1 Solvent resistance

Immersion tests were carried out on non-cross-linked (M0), cross-linked with the first method (M1), cross-linked with only the first step in the second method (M2-1) and fully cross-linked (M2-2) membranes to determine the stability in different kinds of polar aprotic organic solvents, cf. Experimental part (section 3.6). The following Table 4.14 shows the physical phenomenon of the membranes after immersion in the solvent for 96 h.

Table 4.14 Stability of membranes in different solvents

Membrane	Solvent	Observation
M0	NMP	Immediately dissolves
	DMF	
	DMSO	
M1 (Malonyl dichloride)	NMP	Insoluble, but strong swelling
	DMF	
	DMSO	
M2-1 (Glutaraldehyde)	NMP	Stable for short term, swells after 2 days
	DMF	
	DMSO	
M2-2 (Glutaraldehyde and PEG)	NMP	Completely stable
	DMF	
	DMSO	

It was found that M0 dissolved in the tested solvents immediately, which is unremarkable given that the polymer is known to be soluble in several polar aprotic solvents, and the membranes themselves were derived from the solution in DMF or NMP. As for the membranes cross-linked with malonyl chloride (M1), they are not soluble in these solvents despite large swelling. Whereas, after the first-step cross-linking with glutaraldehyde, the membranes M2-1 showed good solvent stability in short term, after two days, there was a certain content of swelling. For the completely cross-linked membranes M2-2, they were endowed with excellent solvent stability and remained un-dissolved in various polar aprotic solvents. Membranes from M1 and M2 are all resistant to strong solvents, the different swelling degree are probably due to different cross-linking density.

The cross-linking reaction was carried out on the already formed membranes; therefore, to achieve the best cross-linking efficiency, it is better to perform the process when membrane is under strongly swollen state. As shown the swelling test in paragraph 4.2, the membrane has the largest swelling degree in water, so the best condition for the cross-linking reaction is in aqueous solution.

The first method, as the cross-linker malonyl dichloride can be hydrolyzed in water, which is described as the following mechanism in Fig. 4.19, is not feasible.

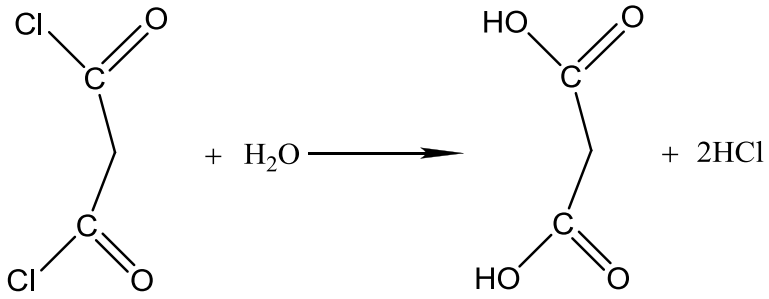

Fig. 4.19 Hydrolysis of malonyl dichloride in water

So the reaction was carried out in toluene, in which membranes have the largest swelling degree except water. The result of swelling test indicated that the cross-linking reaction indeed happened, but the cross-linking density could be not high enough. It is widely applied to functionalize hydroxyl-containing polymers or oligomers with unsaturated anhydrides or acyl chlorides in the presence of a proton scavenger, triethylamine (TEA or Et_3N) [175-179]. But yellowish or dark brown precipitates are always formed during the reaction in this method, and they are practically rather difficult to be removed completely. L. Cai and S.F. Wang [180] performed the reaction between TEA and different unsaturated anhydrides or acryl chlorides in order to demonstrate the formation of complex, and found out that the complex between TEA and acryl chlorides is unavoidable and the complexation competes with the esterification of hydroxyl-containing polymers. Besides, K_2CO_3 was recommended to replace TEA in such reaction. Whereas K_2CO_3 is insoluble in toluene, combined with low swelling degree of membranes in toluene, the cross-linking density is not expected to be high enough, which can be proven in the solvent resistance tests.

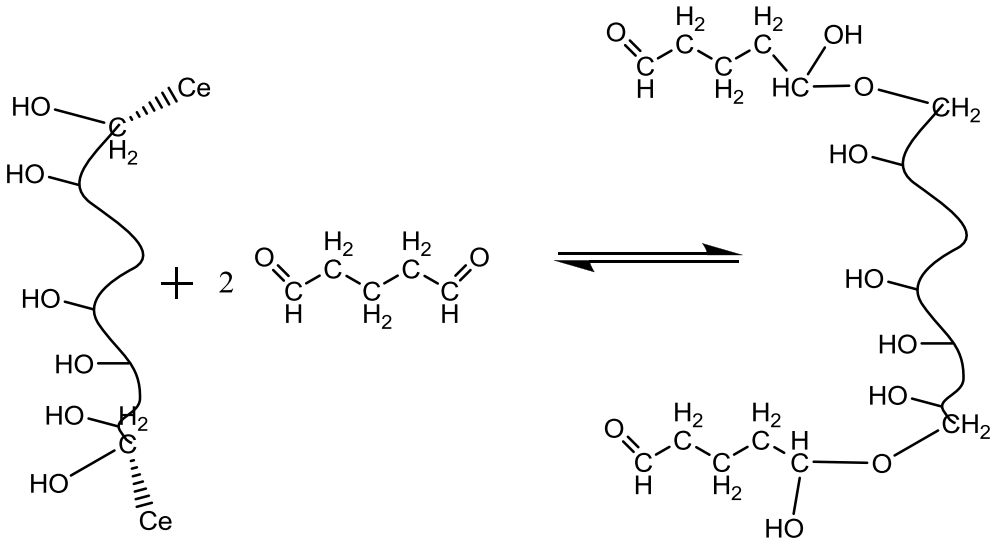

Fig. 4.20 Mechanism for the decolorization of the membrane

For the second method, reaction can be performed in water. After the cross-linking reaction the color of the membrane turned from light yellowish orange to totally white, it indicated the successful cross-linking. Because the color in the membrane was probably from Ce (IV) that is still in the complex with the carbon connected with hydroxyl group, after the reaction between hydroxyl group and aldehyde, the carbon lost the ability to complex with Ce (IV), then the membrane turned back to pure white. It can be described as the following mechanism in Fig. 4.20. After two-step cross-linking, the membrane became completely stable in any solvents, which confirmed again that the cross-linking was successful.

4.5.2 Characterization via FT-IR/ATR

Membranes cross-linked with malonyl dichloride

After cross-linking, the membrane was first evaluated by IR, in the IR spectra as shown in Fig. 4.21, reduction of OH group which is a broad peak around 3500 cm^{-1} and appearance of new ester group (1750 cm^{-1}) indicated that the reaction between the cross-linker and the base membrane has taken place. The appearance of a new peak at 1750 cm^{-1} was due to the stretching vibration of C=O double bond, and it was an evidence of the newly-formed ester group. Besides, the decline of the OH group at around 3500 cm^{-1} proved that the OH group in PEG segments has successfully reacted with the cross-linker which was malonyl dichloride here. These two changes in the IR spectra could be clear evidences of successful reaction between cross-linker and membrane. But in the solvent resistance tests, the membranes

were under strong swelling in polar aprotic solvents although not soluble, which demonstrated again that although the cross-linking reaction happened, the cross-linking density was not high enough.

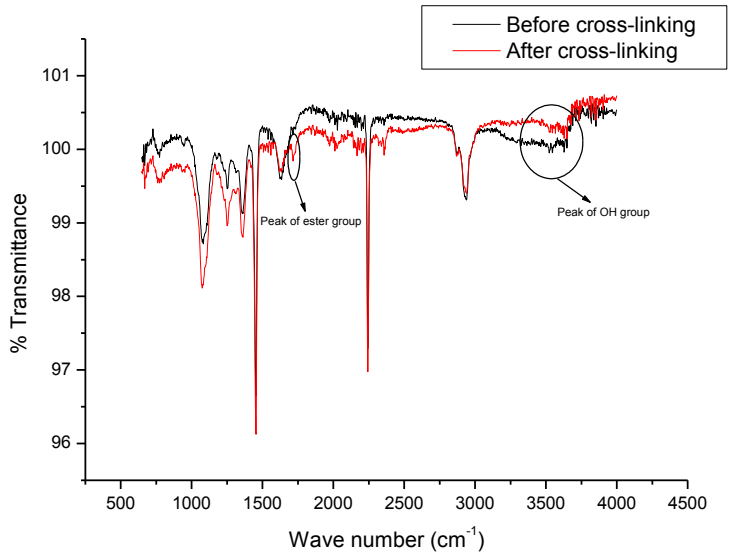

Fig. 4.21 IR spectra of a membrane before and after cross-linking with malonyl dichloride

Membranes cross-linked with glutaraldehyde

In Fig. 4.22, there was a light increase of the peak at 1750 cm^{-1} which is due to the stretching vibration of C=O double bond, which indicated the successful introducing of glutaraldehyde into the membrane. Besides, there were no other obvious changes in the IR spectra, because the second cross-linker PEG-400 already exists in the membrane material, and the unreacted hydroxyl group in PEG-400 remained the peak at around 3500 cm^{-1} at the level similar to original membrane.

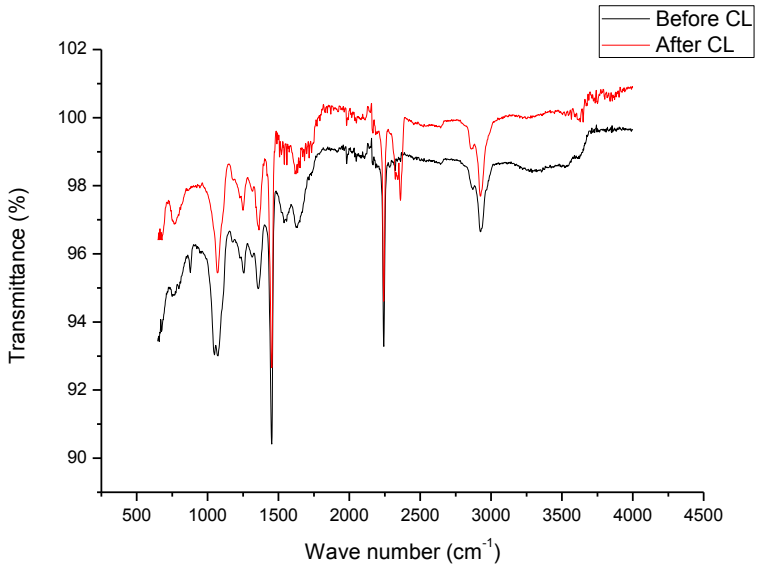

Fig. 4.22 IR spectra of a membrane before and after cross-linking glutaraldehyde and PEG

4.5.3 Pore morphology

After the solvent resistance test, the membranes were immersed in water again, to wash out the solvents absorbed in the membranes, also to stabilize the membranes that were strongly swollen in these strong solvents. Afterwards, the morphology of the membranes was observed again in SEM.

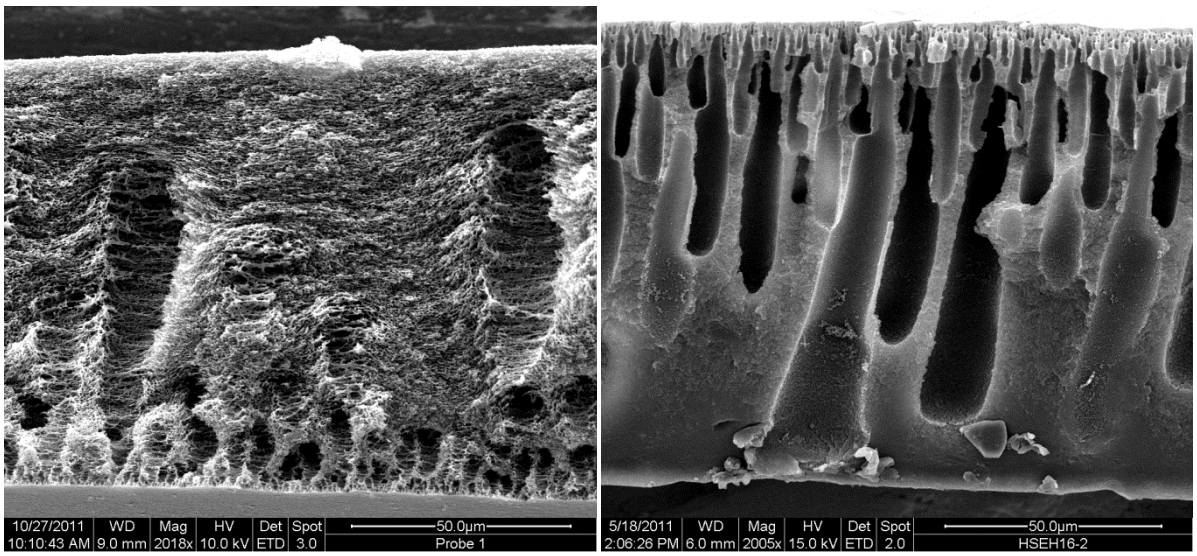

a b

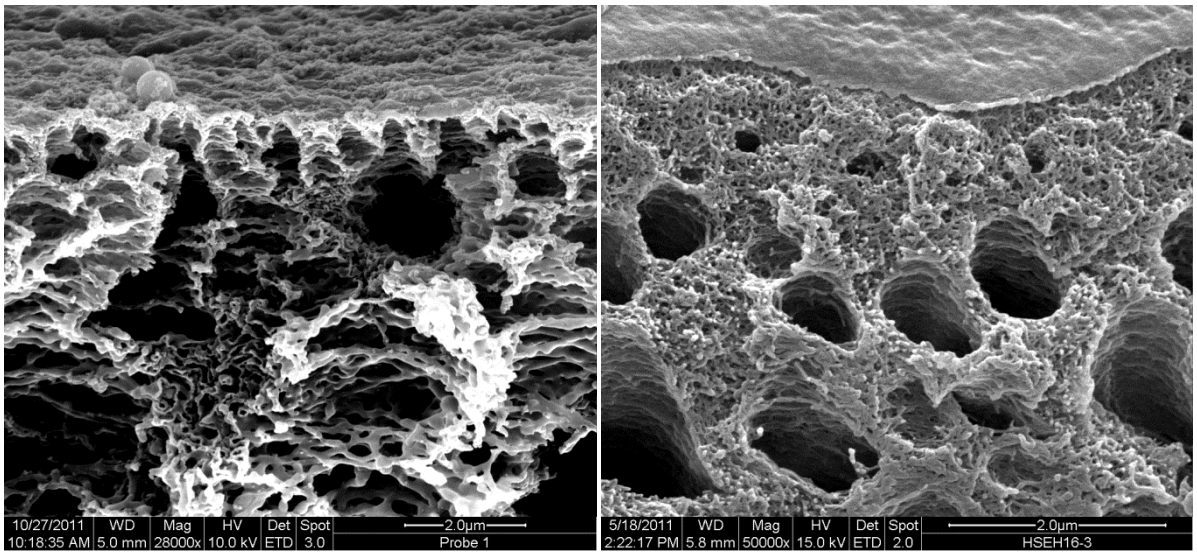

Fig. 4.23 SEM images of membranes cross-linked via different routes: a, membranes cross-linked with malonyl dichloride (M1);
b, membranes cross-linked with glutaraldehyde and PEG (M2)

In Fig. 4.23, clear difference can be found between M1 and M2. After cross-linking with malonyl dichloride (first method), although membranes were not soluble in DMF any more, there were strong swelling in polar aprotic solvents. Therefore the membranes were significantly reformed, when they were precipitated in water again to form stable membranes, the morphology of the membranes was greatly changed from asymmetric to relatively homogeneous structures. Whereas, for the M2 group membranes, after the cross-linking, membranes were completely stable, therefore, the morphologies were not clearly affected, besides, the densification effect was more efficient on the selective layer, for the macrovoid pores, densification can only affect the walls of the pores but not the pores themselves, so the morphology was similar to the membranes before cross-linking.

4.5.4 Separation performance

First, water permeability and thickness were studied on the original membranes and membranes cross-linked with two different methods.

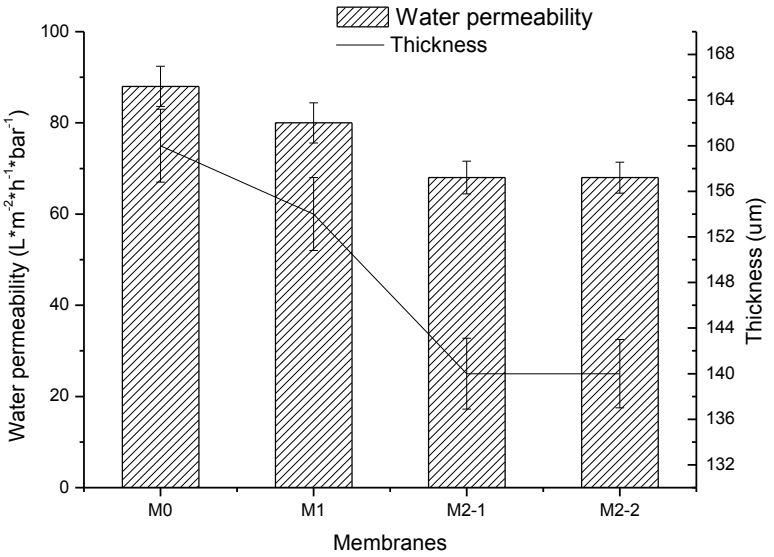

Fig. 4.24 Water permeability and thickness of membranes treated with different cross-linking process

After the cross-linking process, membranes were tested again in the filtration setup. Fig. 4.24 summarized the water permeability and thickness of unmodified membranes (M0) prepared from water only as non-solvent, membranes cross-linked with manlonyl dichloride (M1), membranes cross-linked with glutaraldehyde (M2-1) and membranes cross-linked with glutaraldehyde and PEG (M2-2). Slight decrease of both water permeability and thickness can be found from M0 to M2, this phenomenon has been already reported to be a result of densification of the membrane [181].

Because of the densification effect of cross-linking, the water permeability should be directly connected with cross-linking density, which means that with increasing cross-linking density, the water permeability decreased. It can be clearly observed from Fig. 4.24 and Fig. 4.25 that M2 had lower permeability than M1, besides membranes from M2 were more stable than that from M1, therefore, the cross-linking density of M2 group was mostly higher than that of M1 group. Furthermore, densification of membranes also leads to slight decrease in the pore size, therefore, the MWCO decreased as well after the cross-linking, and with increasing cross-linking density, the reduction in MWCO got higher.

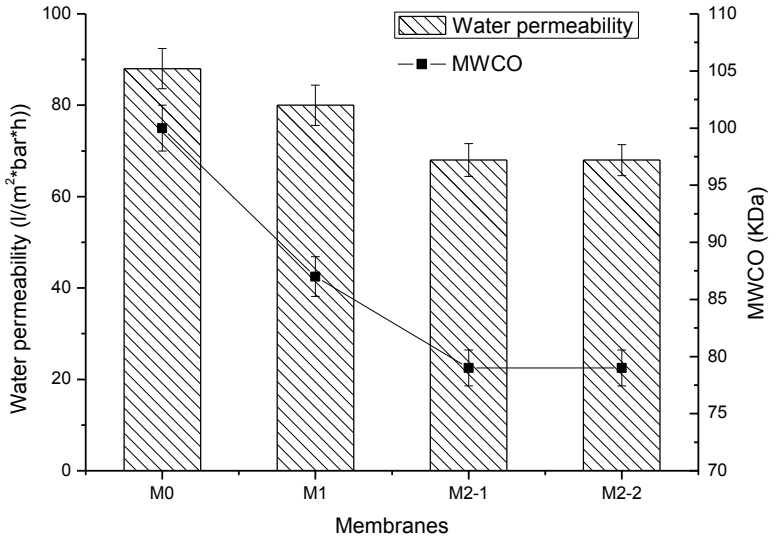

Fig. 4.25 Water permeability and MWCO in water of different membranes

4.5.5 Summary

It was proven via FT-IR measurement that the designed cross-linking reaction was possible to take place between all the cross-linkers and the membranes. After the cross-linking with two different processes, the membranes became more stable than before. Based on different cross-linking density, the resulting membranes showed difference in solvent resistance. Because of the densification effect of cross-linking process, the cross-linked membranes had lower water permeability and lower MWCO as well, higher cross-linking density lead to greater reduction in both permeability and MWCO. The resulting membrane had excellent solvent resistance, relatively high permeability and rejection properties as ultrafiltration membranes; so it is possible to apply them directly in solvent resistant ultrafiltration process, or as support materials for solvent resistant nanofiltration.

4.6 Conversion to nanofiltration membranes process

After the cross-linking process, the membranes were qualified for solvent resistant ultrafiltration or as support for solvent resistant nanofiltration. For direct application in organic solvent nanofiltration processes, the membranes were then treated with another

process to convert the membranes to nanofiltration types. Similar work has been done by J. Wang *et al.* [182], but the membrane material was PAN homo-polymer, and cross-linked membranes prepared from PAN-b-PEG-b-PAN were applied here in this study. Accordingly, conditions for the treatment were optimized for this block copolymer.

4.6.1 Parameters in the conversion

To achieve the best conversion result, according to the procedure described in Experimental part (cf. section 3.7), variation of various parameters was applied as following Table 4.15.

Table 4.15 Parameters applied in the conversion process

Parameters	Values			
Concentration of $ZnCl_2$	15%	30%	45%	60%
Temperature of heat treatment (°C)	100	110	120	130
Heat treatment time (h)	1	2	5	Over night

It was found that the solution of $ZnCl_2$ with 60% concentration was able to dissolve uncross-linked membranes; therefore no further experiments were carried out in 60% solution. Besides, after treated in zinc chloride solution, it was not possible to dry the membranes in the open air at room temperature, so the temperature of the heat treatment was 130°C, and the drying time was the longest --- over night, the membranes were dried in the oven till completely dry. Therefore, in the following discussion, variation was made exclusively on the concentration of zinc chloride.

4.6.2 Characterization via FT-IR/ATR

The resulting membranes were first characterized with IR, to check the conversion of functional groups.

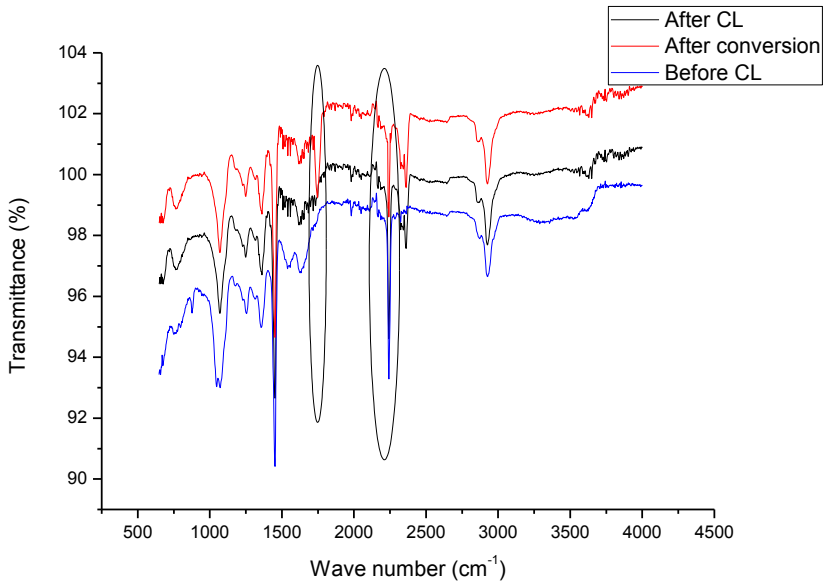

Fig. 4.26 IR spectra of membranes before and after different post treatments

Fig. 4.26 shows the ATR/FTIR spectra of the membranes modified with the conversion process. In this figure, the peak at around 1750 cm^{-1} corresponds to the –C=O stretching vibration. Before the conversion step, this peak was already there because of the cross-linker. After the conversion, this peak became much stronger, which indicated the introduction of the –COONa and $–CONH_2$ groups. Since the peak at 2243 cm^{-1} for nitrile group did not change significantly, only part of the nitrile groups were hydrolyzed.

4.6.3 Pore morphology

After conversion, morphologies of membranes were studied again via SEM. As all the membranes from different $ZnCl_2$ solutions had no visible pores in SEM, all the SEM images were similar to each other; therefore, only typical images are shown below (Fig. 4.27).

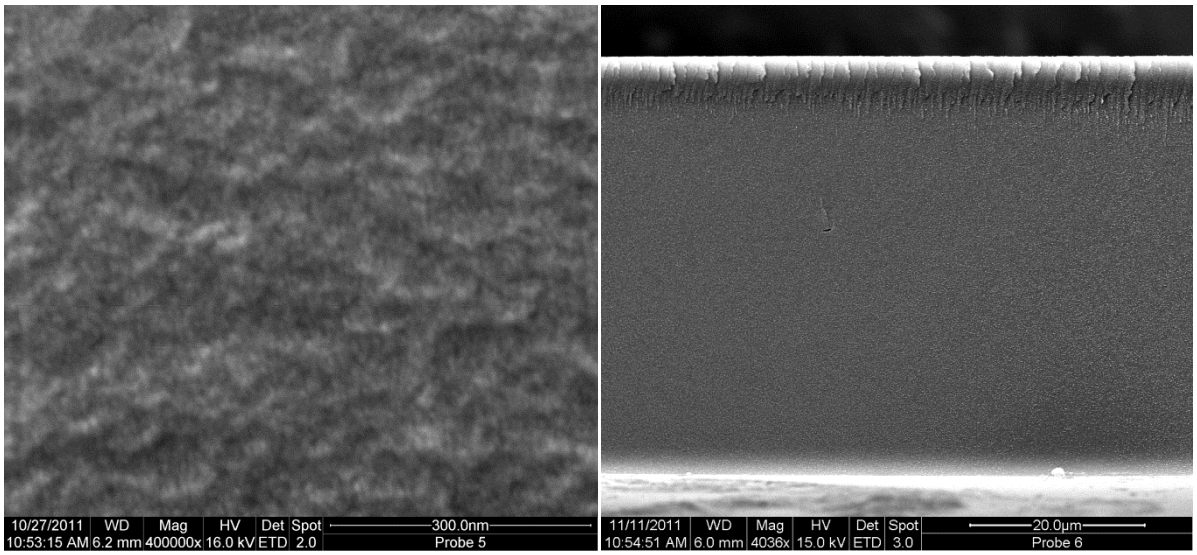

Fig. 4.27 SEM images (cross-section view) of membranes after conversion treatment

After the conversion step, morphologies of membranes were significantly changed, macro pores of the membranes support layer were largely declined and the resulting barrier layer pores were not observable in SEM.

4.6.4 Separation performance

After cross-linking and nanofiltration conversion process, membranes were tested again in the filtration setup. Fig. 4.28 illustrates the water permeability of unmodified membranes (M0) prepared from water only as non-solvent, cross-linked membranes (M2-2) and cross-linked membranes after nano-conversion (M3). Slight decrease of water permeability can be found from M0 to M2, which has been already discussed to be a result of densification of the membrane [181]. After the nano-conversion, both permeability and rejection of membranes were significantly changed as shown in Fig. 4.28, 4.29, 4.30 and 4.31. For the converted membranes, the water permeability increased with increasing $ZnCl_2$ concentration in the aqueous solutions. There are two main functions of $ZnCl_2$ in the conversion process, which were reported before [182]. First, because Lewis acids are able to form coordinate bonds with strong electronegative groups (e.g. nitrogen atoms in the nitrile groups, oxygen atoms in the unreacted hydroxyl groups), they anchor the nitrile groups on the pore surface even at elevated temperatures. When the temperature is higher than the Tg (glass transition temperature), in the absence of $ZnCl_2$, some nitrile groups would migrate from the pore surface to the bulk of the membrane. The migration will lead to fewer functional groups on

the pore surface. In addition, the complexation of $ZnCl_2$ causes severe reduction of pore size upon heating. Secondly, $ZnCl_2$ also acts as a filler to prevent a complete shrinkage of the pores upon heating, so increasing concentration of $ZnCl_2$ will lead to more pores in the membranes, which can probably explain the reason why water permeabilities increased with increasing $ZnCl_2$ concentration.

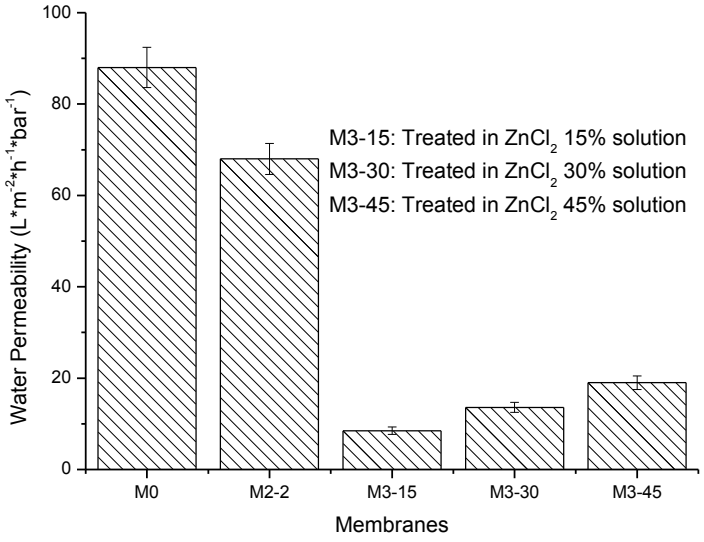

Fig. 4.28 Water permeability of membranes treated with different conditions

Permeabilities of other organic solvents through the membranes were also tested, as shown in Fig.4.29 Comparing with former tests, DMF was applied in the filtration tests on the cross-linked membranes. For M0, membranes are soluble in DMF, so no data were obtained. For cross-linked membranes, the permeability of DMF was much lower than other organic solvents, this is because of a high swelling of membranes in DMF as compared with other solvents, the swollen polymer chains occupied much free volume inside the membrane, thus declined the flux of solvents. Besides, the most important observation was the change in transport model: in ultrafiltration process, pore flow model dominates, as discussed before the permeability was strongly dependent on the viscosity; for nanofiltration processes, the commonly used model to describe the permeation is solution diffusion model, in this model, it is assumed that each permeating molecule dissolves in the membrane phase and diffuses through the membrane in response to the concentration gradient.

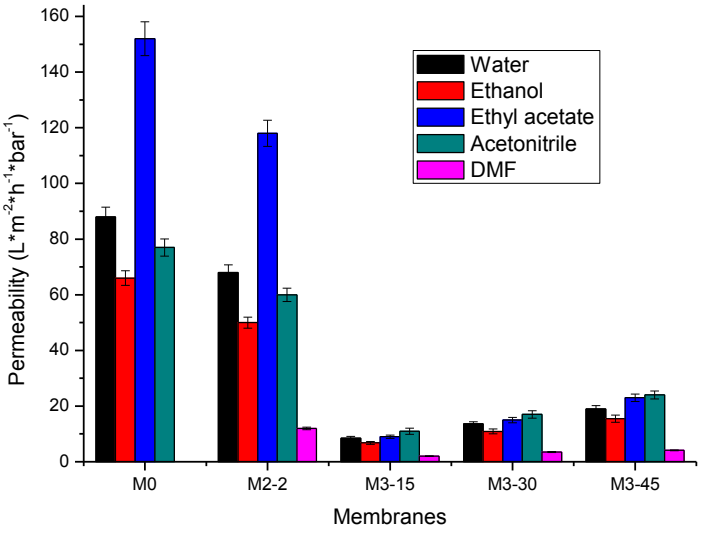

Fig. 4.29 Organic solvents permeability of membranes treated with different conditions

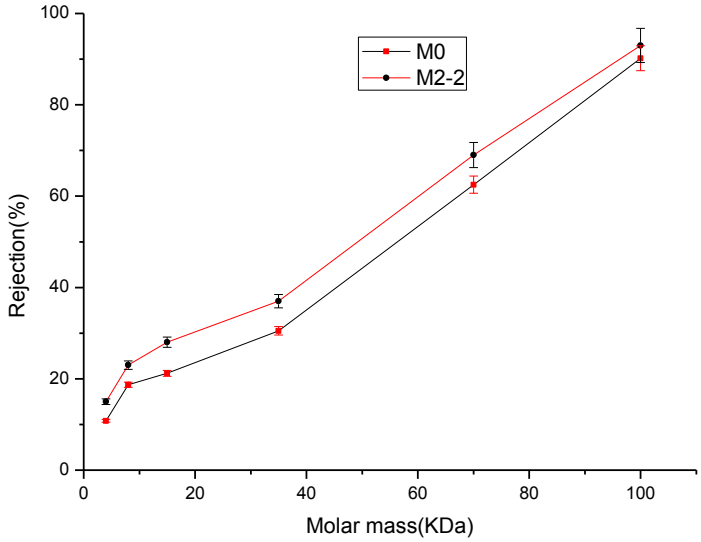

Fig. 4.30 Rejection curves of original and cross-linked membranes in aqueous condition

As the pore sizes decreased, the permeability declined as well, accordingly, rejection properties was expected to get better. In Fig. 4.30 and Fig. 4.31, the rejections of PEG with different molar masses in aqueous solution through different membranes were analyzed.

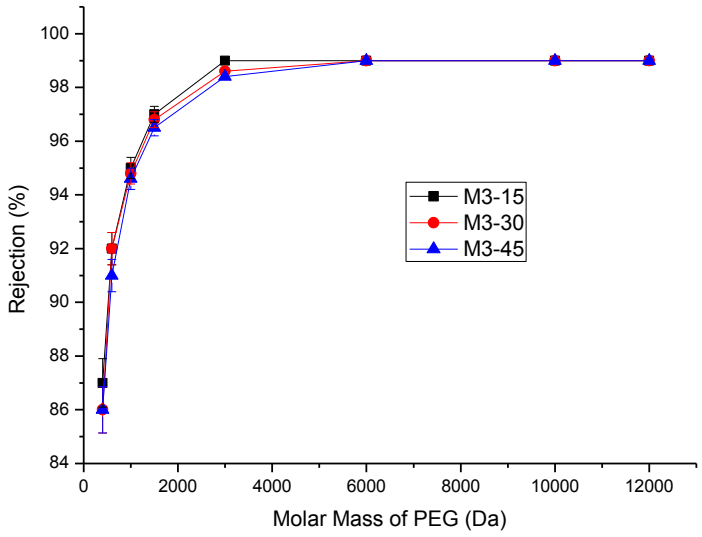

Fig. 4.31 Rejection curves of membranes treated in different $ZnCl_2$ solutions

In the fig. 4.30, it can be seen that for M0 and M2, the membranes had very low rejection of PEGs, which is due to their large pore sizes, and the growths of rejection curves were also quite stagnant, which was probably because a broad pore size distribution. Whereas, in Fig. 4.31, after the nano-conversion process, the rejection properties were significantly enhanced, the MWCO shifted from about 100 kDa to around 500 Da, as comparison with the slight loss of pure solvent permeability, the separation properties of membranes were greatly improved. Besides, after the conversion, all the membranes from M3 group had similar rejection curves. This can be still explained by the pore filler theory, higher $ZnCl_2$ concentration may lead to more tiny pores other than larger pores in the membranes. As a result, although the M3-45 membranes have higher permeability, the MWCO doesn't increase correspondingly. Furthermore, another phenomenon might result from the pore filler effect is that the rejection curves also increased fairly sharp after 400 Da, which indicated that, the conversion method can narrow the pore size distribution effectively. Consequently, membranes from M3-45 that has both high flux and high rejection were preferred.

An estimation of the pore sizes of the various membranes can be made with the help of Stokes radius of PEG molecules. The Stokes radius of a macromolecule can be derived from its diffusivity in a solution by using the following Stokes-Einstein equation:

$$D_{AB} = {kT}/{(6\pi\eta a)} \tag{4-5}$$

where D_{AB} is the diffusivity, k is Boltzmann's constant, η is the viscosity of the solvent and a is the Stokes radius. The diffusivity can be also calculated by the following equation [56]:

$$D_{AB} = \frac{2.5 \times 10^6 kT}{\{\eta(M[\eta])^{\frac{1}{3}}\}} \tag{4-6}$$

where M and $[\eta]$ are the molecular weight and the intrinsic viscosity of the polymer respectively. By combining the Eq. (4-5) and (4-6), the Stokes radius can be calculated by equation:

$$a = 2.122 \times 10^{-8}(M[\eta])^{1/3} \tag{4-7}$$

where a is in cm, M is in g/mol and $[\eta]$ is in dL/g. Intrinsic viscosity of a certain PEG of known molar mass can be calculated via the following equation [184]:

$$[\eta] = 4.9 \times 10^{-4} M^{0.672} \tag{4-8}$$

Intrinsic viscosities of PEGs of various molecular weights calculated from the empirical Eq. (4-8) are in very good agreement with the values determined in experiments [183,185]. Intrinsic viscosity for some of the PEG molecules were also given by Bessieres et al. [186], and they are also in very good agreement with the values calculated from the empirical Eq. (4-8). By substituting the expression for $[\eta]$ in Eq. (4-7), the Stokes radii of PEG molecules (in cm) can be obtained from their molecular weights with the following equation:

$$a = 16.73 \times 10^{-10} M^{0.557} \tag{4-9}$$

Thereafter, the following Table 4.16 can be made to give the estimation of the pore sizes as comparison with the values estimated from SEM images.

In Table 4.16, an agreement between estimations from SEM and from Stokes radius can be found as regards to M0 and M2-2 membranes. As for membranes from M3, as the pores were not visible in SEM measurements, there was no comparison with Stokes radius.

Table 4.16 Calculation of Stokes radii of PEGs of various molecular weights

	M0	M2-2	M3
MWCO (PEG)	100 kDa	95 kDa	500 Da
Stokes radii (nm)	10.2	9.9	0.53
Pore size estimated from SEM	10	9	n.a.

After the hydrolysis process, a certain amount of nitrile groups were converted to other functional groups like –COONa, $–CONH_2$. Thus the membranes became negatively charged in aqueous solutions, so in aqueous condition under nanofiltration, they were endowed with properties of rejection of salts that have much smaller molar mass than the MWCO which is around 500 Da here. In Fig. 4.32, the rejections of different salts through the resulting nanofiltration membranes were listed. As the original membranes had absolutely no rejection of any salts, the data for these membranes were not shown here.

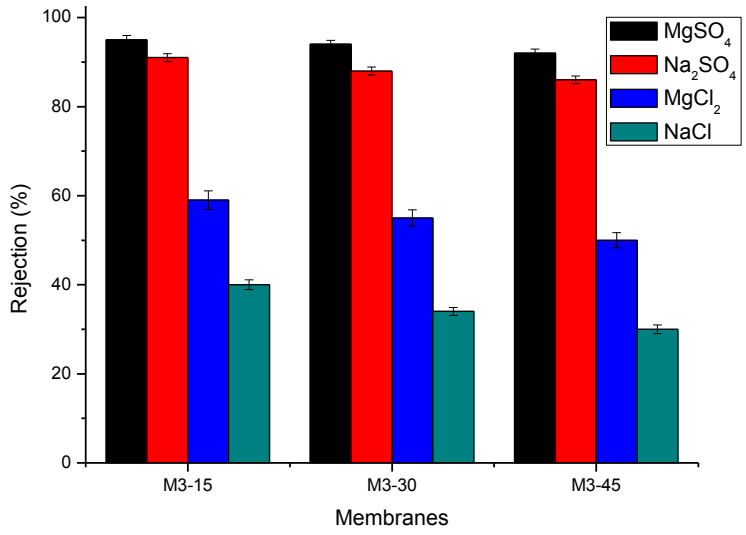

Fig. 4.32 Salt rejections of membranes treated with different $ZnCl_2$ solutions

As seen in fig. 4.32, the rejection of salts that have divalent anions was fairly high, this is because the nanofiltration membranes separate substances based mainly on the Donnan

exclusion effect and the steric hindrance effect [187], the membranes are thus more effective to reject divalent anions. But when it came to the mono-valent anions that were Cl^- here in this study, the rejection became much lower.

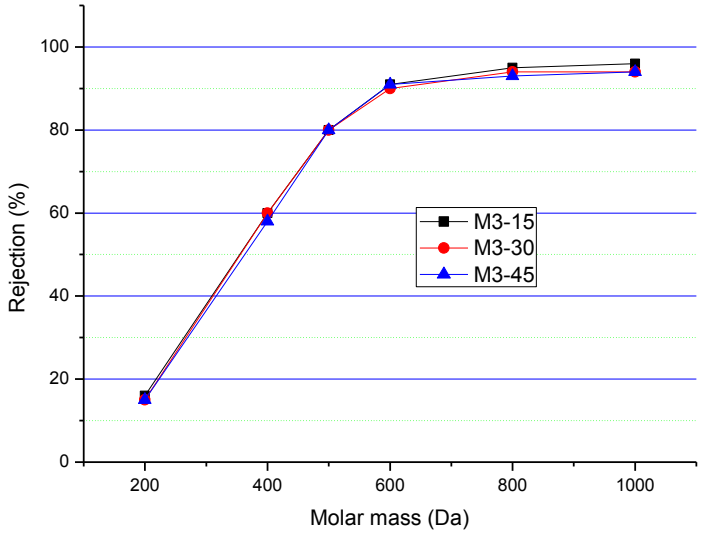

Fig. 4.33 Rejection of PS oligomers in DMF through the membranes treated with $ZnCl_2$ solution of different concentration

Rejection properties in organic solvents of the resulting membranes were also tested. As the membranes were also usable in solvents such as DMF or NMP and gave good separation within the NF range of 200-1000 g/mol. Extreme conditions such as in DMF was tested on the membranes, and the results were shown in Fig. 4.33. Comparing with the separation properties in aqueous solution, the MWCO in DMF was slightly increased, from 500 g/mol in aqueous to 600 g/mol in DMF. The variability of MWCO could be a result of different degrees of swelling of the polymer in the different solvents. In addition, the difference in size and shape (hydrodynamic radius [188]) of oligostyrenes and PEGs could also result in different observed MWCOs.

4.6.5 Summary

It was proven via FT-IR measurement that it was possible to convert the -CN groups in the membranes to –COONa or $–COONH_2$ groups via the designed conversion reaction. After the

conversion with different processes, the membranes became much tighter than before. No visible macrovoid pores still existed in the membranes, which can be observed from SEM images. As the pore morphologies of membranes changed completely, the resulting membranes had much lower solvent permeability and significantly improved rejection properties as well. Higher $ZnCl_2$ concentration led to better separation performance that meant larger solvent permeability and similar MWCO. Furthermore, the membranes were also endowed with properties to reject salts that have much smaller molecular weights than the MWCO, because of the conversion of –CN groups. The resulting membrane had excellent solvent resistance, relatively high permeability and desired rejection properties as nanofiltration membranes. So it is possible to apply them directly in solvent resistant nanofiltration processes, or in aqueous nanofiltration.

4.7 Comparison with state-of-the-art membranes

Table 4.17 compares the membranes prepared in this study with the commercially available MPF-50 membrane which is based on silicone rubber, and the cross-linked Lenzing P84 polyimide membranes prepared by Y.H. See Toh *et al.* [189]. In this table, PAN-PEG means the membranes prepared in this study.

Table 4.17 Characteristic parameters of different SRNF membranes

	Permeability (l/(m^2.h.bar))			MWCO (g/mol)		
	PAN-PEG	P84	MPF-50	PAN-PEG	P84	MPF-50
Water	8.5-19	2-16	0	500		700
DMF	2-4.1	1-8		600	250-400	700

For the MPF-50 membranes, it was reported that the pre-treatment has strong influence on the separation performance [190]. For example, Machado *et al*. [191] measured the flux of methanol through MPF-50 membrane at 30 bar as 175 L/(m^2.h), whereas Whu *et al*. [192]

measured it as 38 L/(m^2.h). So a standard pre-treatment is needed to achieve reproducible properties.

As regards to the cross-linked P84 polyimide membranes, although the DMF permeability was possible to reach up to 8 l/(m^2.h.bar), when the MWCO was in the range of 250-400, the permeability was even lower than 1 l/(m^2.h.bar). Comparing with other membranes, the membranes from cross-linked PAN-PEG have both high permeability and reasonable MWCO according to the permeability.

4.8 Conclusions for the block copolymers of AN and PEG

A novel block copolymer of AN and PEG was synthesized via water-phase precipitation copolymerization using Ce(IV)-PEG as a redox initiator system. Membranes were prepared by casting the solution of this copolymer in DMF or NMP with different concentrations and under different conditions. The membranes were successfully converted to solvent resistant nanofiltration membranes via cross-linking and nano-conversion process as post treatments and the resulting membranes were endowed with excellent solvent resistance, relatively high solvents permeability and high rejection of PEG, PS oligomers and salts with multi-valent anions. However, because of the limitation of Donnan exclusion mechanism, the membranes had low rejection of salts with mono-valent anions.

Chapter 5. Results and discussion for copolymers of PAN and AMPS

In this chapter, the experiment results and discussion on them are divided into two following parts: (I) characterization on the copolymers, (II) membrane performance in separation process.

5.1 Characterization of copolymers

As mentioned in last chapter, the composition and molar mass properties of copolymers can affect the performance of the ultimate membranes; therefore it is necessary to characterize the copolymers first in detail.

Table 5.1 Composition and parameters applied in the copolymerization

	C01-1	C01-2	C02-1	C02-2	C02-3	C03-1	C03-2
AN (g)	15	7	7	7	7	7	7
AMPS (g)	6	2.8	3.5	3.5	3.5	2.1	2.1
AIBN (g)	0.237	0.111	0.138	0.138	0.138	0.138	0.138
Reaction time (h)	2	1	0.5	1	2	2	4
Yields (%)	37	30	30	35	39	42	45

In Table 5.1, different ratios of two monomers and amount of initiators according to the content of AMPS were adjusted in these experiments to achieve more suitable copolymers for the membrane. Besides, to achieve the optimized condition, variation on the reaction time was also made. Following data will describe the effect of several important parameters.

5.1.1 FTIR/ATR, ^{1}H-NMR, element analysis and GPC results

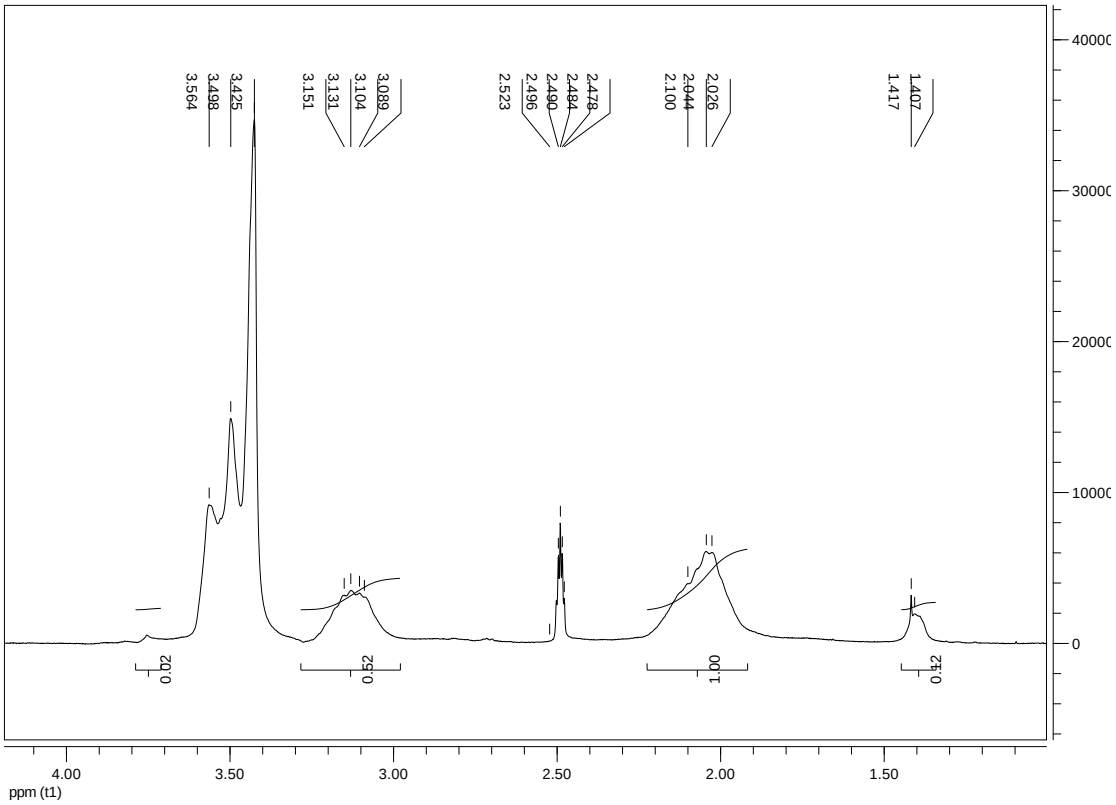

Fig. 5.1 ^{1}H NMR spectra of the copolymer from C03

Samples were dissolved in DMSO-d6. It can be observed from the spectrum that chemical shifts at 2.03 and 3.17 ppm are attributed to the hydrogen in -CH_2 and -CH in the PAN segments. A clear new peak at around 1.4 ppm appeared, it was probably due to the proton of -CH_3 group in the AMPS, at 3.59 ppm, the peak was the signal of –CH_2 group in AMPS, besides the chemical shift at 2.51 ppm corresponds to the solvent DMSO-d6.

Table 5.2 Mole ratio of AN calculated from NMR data

	C01-1	C01-2	C02-1	C02-2	C02-3	C03-1	C03-2
Mole ratio of AN in copolymer (%)	92.0	93.3	94.5	92.2	91.5	96.1	93.1
Mole ratio of AN in feed (%)	90.72	90.72	88.65	88.65	88.65	92.89	92.89

From the integration of the area under the peaks at 2.03 ppm and 1.42 ppm, absolute ratio of AN segments to AMPS units can be calculated, then mole ratio of AN in the copolymers were derived, which are summarized in Table 5.2.

Because of the obvious and constant characteristic peak of CN group in IR spectra, it is fairly convenient to judge the composition of the copolymer with FRIR/ATR. Figure 5.2 shows the IR spectrum of representative copolymers from C01 and C02. In the spectrum, the clear peak at 2243 cm^{-1} was due to the -CN group in AN, the broad peak at around 3500 cm^{-1} proved the existence of -NH in AMPS, the peak at 1680 cm^{-1} was from C=O double bonds in AMPS. The quantitative composition was estimated from relative peak ratios. The absorption of light was calculated via Beer-Lambert equation. Table 5.3 shows the absorbance of CN peak and C=O peak, and the relative ratio of them, then the mole ratio of AN in copolymers were calculated compared with the mole ratio of AN in feed.

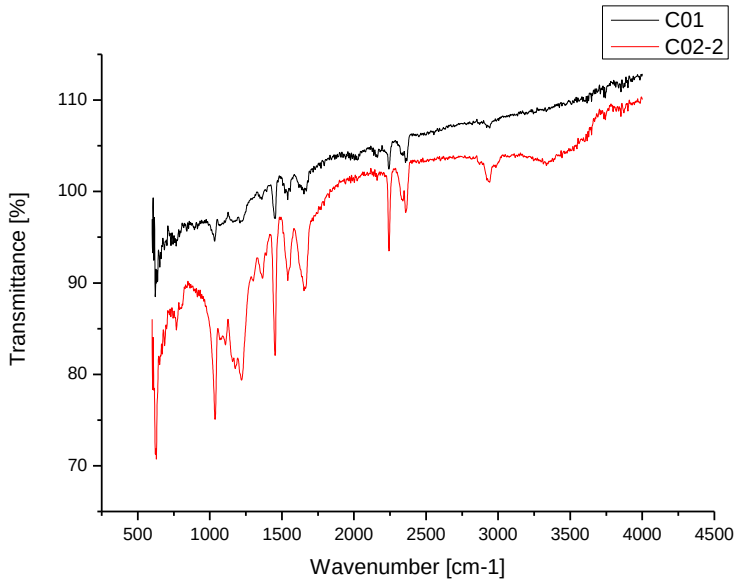

Fig. 5.2 IR spectrum of copolymers from C01 and C02

From the IR data, the absorbance of C=O double bonds in AMPS segments and -CN group in AN segments can be calculated via Beer-Lambert law which is same as in chapter 4. Table 5.3 shows the mole ratio of AN in the copolymers calculated from IR results in comparison with the values in feed.

Table 5.3 Mole ratio calculated from IR data

	C01-1	C01-2	C02-1	C02-2	C02-3	C03-1	C03-2
Mole ratio of AN in feed (%)	90.72	90.72	88.65	88.65	88.65	92.89	92.89
Mole ratio of AN in copolymer (%)	73.9	74.1	75.2	73.9	73.7	74.2	73.5

Molecular weight and distribution were derived by gel permeation chromatography (GPC), the results of which are listed in Table 5.4, in which M_n means number average molar mass, M_w represents weight average molar mass, and PDI for poly-dispersity index.

Table 5.4 Molar mass information of copolymers

Sample	C01-1	C01-2	C02-1	C02-2	C02-3	C03-1	C03-2
M_w (g/mol)	1.6E+06	3.2E+05	4.9E+04	1.6E+05	7.2E+05	6.6E+05	1.1E+06
M_n (g/mol)	8.8E+05	1.1E+05	1.2E+04	4.6E+04	2.7E+05	2.5E+05	5.7E+05
PDI	1.83	2.81	4.08	3.55	2.73	2.65	1.93

Table 5.5 illustrates the content of each element in the copolymers derived from element analysis and the mole ratio of AN in the copolymer calculated from the results, among these values, the content of sulfur directly represents the proportion of AMPS.

Table 5.5 Contents of each element in the copolymers from CHNS analysis

	C01-1	C01-2	C02-1	C02-2	C02-3	C03-1	C03-2
C (%)	60.19	60.12	59.55	58.86	58.56	61.65	60.59
N (%)	20.81	20.75	20.3	19.9	19.75	21.87	20.92
S (%)	4.44	4.51	5.09	5.18	5.36	3.58	4.06
O (%)	8.88	9.02	10.18	10.36	10.72	7.16	8.12
H (%)	5.68	5.6	4.88	5.7	5.61	5.74	6.31
Mole ratio of AN in copolymer (%)	90.60	90.45	88.84	88.56	88.01	92.83	91.63

5.1.2 Determination of reactivity ratio

Reactivity ratio is an important parameter in the copolymerization, as it can greatly affect the composition and conformation of copolymers. Although it can be looked up in the polymer handbook [193], different reaction conditions probably leads to different values, therefore experiments to determine the reactivity ratio of two monomers in real condition were performed. Copolymerization of AN-HEMA was performed in DMF using AIBN as initiator at 60°C.

Table 5.6 Parameters applied and results derived for the reactivity ratio determination

Mole fraction of AN in feed (M_1)	Reaction time (h)	Oxygen content (%)	Mole fraction of AN in copolymer (m_1)	Conversion (%)
0.8	5	14.91	0.808	20.5

0.667	5	20.12	0.677	18.3
0.333	5	27.26	0.344	25.6
0.2	5	28.97	0.208	19.1

Reactivity ratio r_1 and r_2 were calculated by the Kelen-Tudos method, which is expressed as

$$\eta = \left(r_1 + \frac{r_2}{a}\right)\xi - \frac{r_2}{a} \tag{5-2}$$

in which,

$$\eta = \frac{x(y-1)}{ay+x^2} \quad \xi = \frac{x^2}{ay+x^2}$$

$$x = \frac{M_1}{M_2} \quad y = \frac{m_1}{m_2} \quad a = \frac{x_{min}x_{max}}{\sqrt{y_{min}y_{max}}}$$

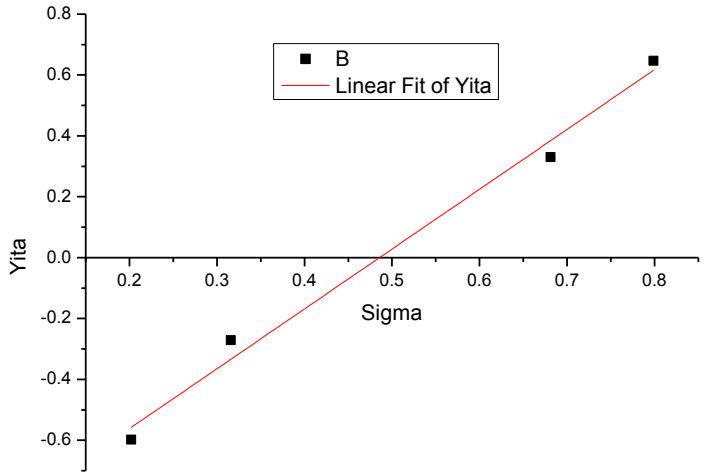

Fig. 5.3 Linear fit of parameters in Kelen-Tudos method

From the linear regression for the data, (r_1+r_2/a) and (r_2/a) can be determined by the slope of the plot, which were 1.966±0.138 and 0.959±0.077 separately, then r_1 and r_2 were calculated to be 1.006±0.215 and 0.912±0.073 respectively.

r_1 (AN) and r_2 (AMPS) are similar to each other, and both of them are around 1, which means monomer 1 (AN) will react same fast with another AN monomer or with monomer 2 (AMPS), and a random copolymer results.

The reactivity ratio of AN and AMPS can be looked up in a technical handbook [193], in which the value of r_1 and r_2 is 1.2 and 0.7 respectively. Comparing with the condition in this study, the copolymerization was carried out in dimethylformamide (DMF) in this handbook, which is different from water in this study. The solubility of AN in water is about 7 g in 100 ml water, which is much lower than that in DMF, therefore the influence of the solvent could be a crucial reason for the different reactivity ratios. Besides, the conversion in this study was much higher than other works, which was normally controlled to be below 12%.

5.1.3 Influence of reaction time

In free radical polymerizations, propagation of a certain polymer chain can finish within one second, so for a specific single chain, molecular weight or other properties are independent on reaction time. Whereas, as regarding to the whole reaction system, because new free radicals were continuously generated, the reaction can last much longer than several seconds, in the reaction process, the concentrations of monomers and initiators were decreasing with time, and because of different decreasing speed, the composition and molar mass of the copolymer are also expected to be changing with time. It can be seen in Table 5.1 that different reaction times were applied for each feed composition, in the following, the effect of reaction time will be discussed based on the data in section 5.1.1.

As shown in Fig. 5.4, Fig. 5.5, Fig. 5.6, for all the three groups of experiments, with increasing reaction time, there is quite clear tendency for mole ratio of AN in copolymers to decrease, which is found in all the three characterizations of NMR, FT-IR and element analysis. The only exception appeared in element analysis data, in which, group C01 shows a different trend, the mole ratio of AN increases with increasing reaction time, although the increase is very slight. This is probably because of the error in this analytical method, because in all the other characterizations, the C01 group shows same tendency as other groups.

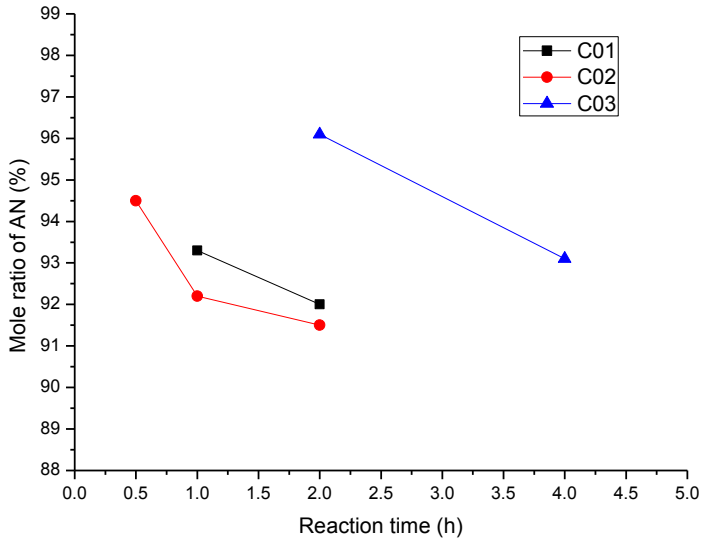

Fig. 5.4 Mole ratio of AN in copolymers calculated from NMR results

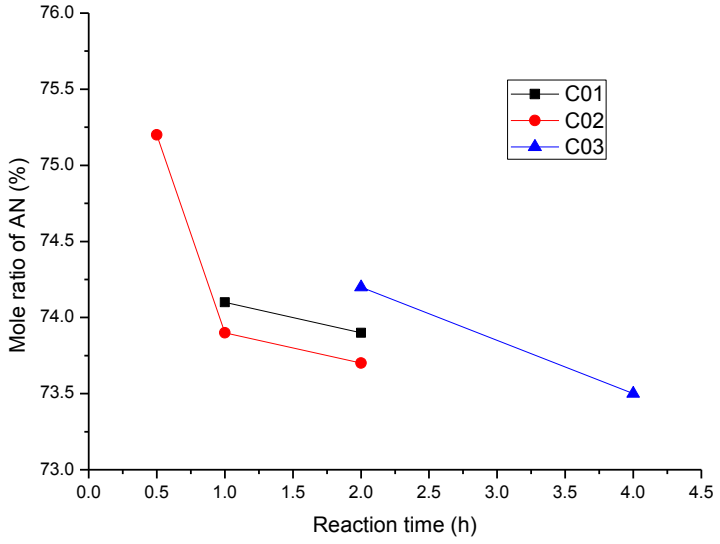

Fig. 5.5 Mole ratio of AN in copolymers based on IR spectra

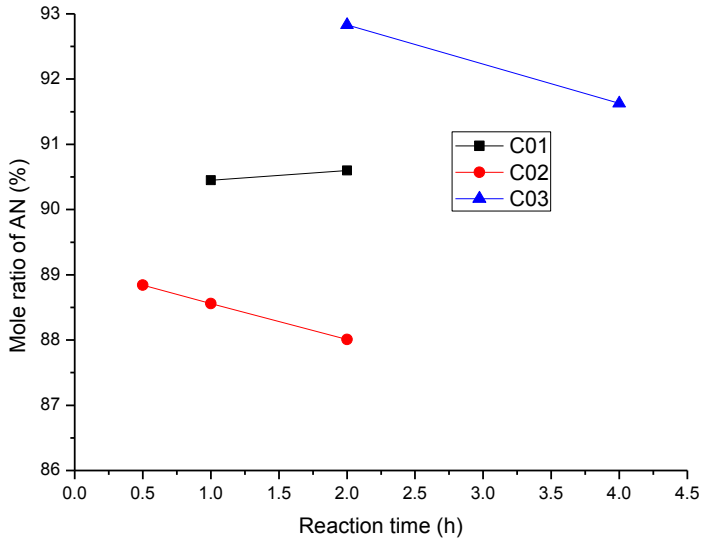

Fig. 5.6 Mole ratio of AN in copolymers according to element analysis data

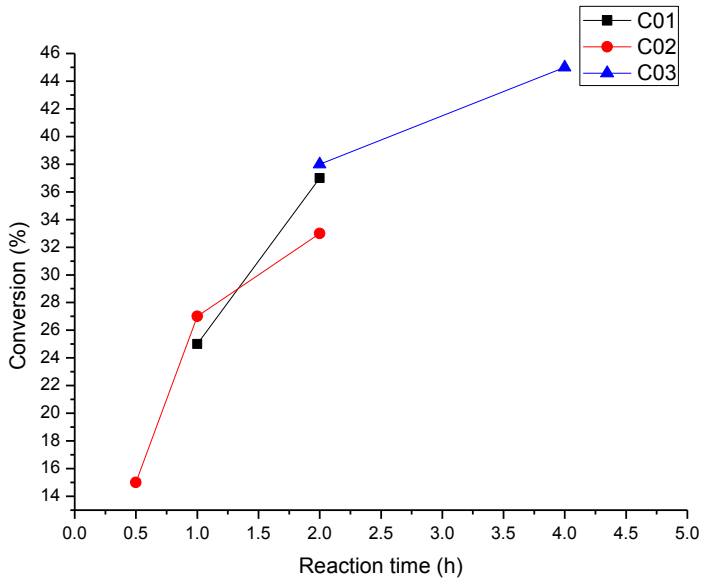

Fig. 5.7 Influence of reaction time on the conversion

In the reaction solution, the concentration of AN monomers was much higher than that of AMPS monomers, and the reactivity ratio of AN is also slightly higher than AMPS. So at the beginning of the reaction, the main contribution to chain propagation was made by AN, with increasing reaction time, the monomer concentration got lower. As the consumption of AN monomers was higher than AMPS, the concentration proportion of AN to AMPS also

declined, then more AMPS monomers were propagating on the growing polymer chains, therefore, the mole fraction of AN in the copolymers decreased with increasing time.

Another obvious observation was the dependency of conversion on the reaction time, in Fig. 5.7, clear increase of conversion with longer reaction time can be found. This makes agreement with the discussion before: with longer reaction time, new free radicals were continuously generated and thus new polymer chains were also formed, therefore conversion was also increasing with reaction time.

When it comes to the comparison with the result in section 5.1.2, because of similar reactivity ratio, if the reaction time were long enough (5 hours in that part), the mole ratio of AN in copolymers would tend to be close to a certain value -- the mole ratio in the feed. It can be predicted that, with longer reaction time, the reduction of AN mole fraction in the copolymers gets also less, the slope of the ratio curve tends to be flat. This tendency is already appearing in C-02 group, which can be observed in Fig. 5.4 and 5.5.

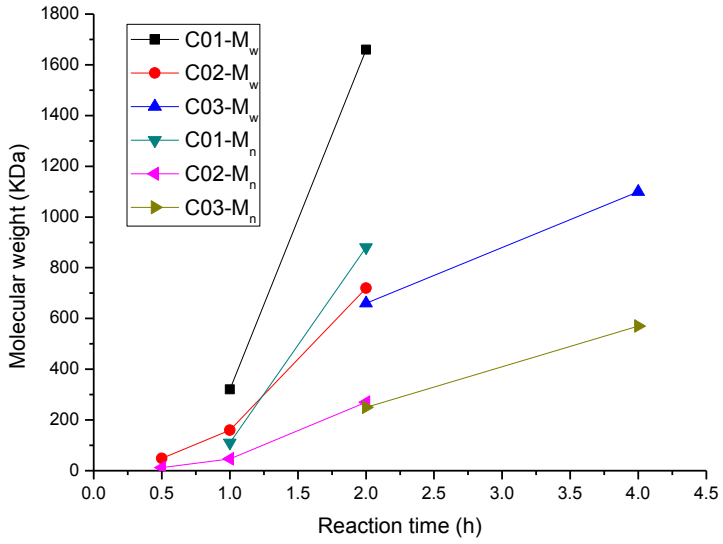

Fig. 5.8 Influence of reaction time on molecular weight

In Fig. 5.8, the dependency of weight and number average molecular weight on the reaction time was obviously identified. With increasing reaction time, both average molar masses increased significantly. Besides, the slopes of the M_w curve was fairly close to that of M_n curve for the same experiment series, which means for same additional reaction time, the

increase of M_w was almost same as that of M_n, but not proportional increasing. This can be more clearly seen in the following Fig. 5.7, commonly poly-dispersity index is defined as:

$$PDI = {M_w}/{M_n} \tag{5-3}$$

As the increase in M_w was less than proportional value of the increase in M_n, the ratio of M_w to M_n got lower, which was just defined as PDI. Therefore, as shown in Fig. 5.9, PDI value decreased with increasing reaction time.

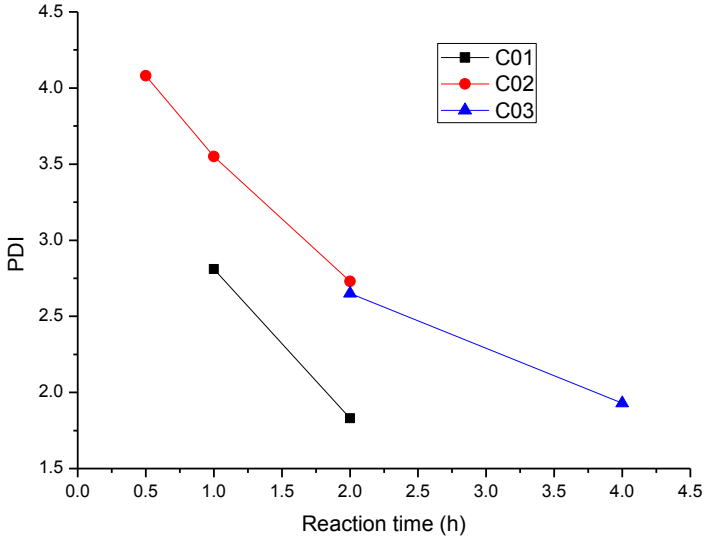

Fig. 5.9 Influence of reaction time on PDI

In the copolymerization reaction, the mole proportion of initiator to monomers can affect the molecular weight effectively. When the proportional value is high that means there are higher initiator fraction in the reaction solution, more radicals are generated so that there are more propagating polymer chains. Thus more but smaller polymers are synthesized, and average molecular weight is naturally low. Vice versus, when initiator fraction is low, less but larger polymers are formed, molar mass will be higher. With this theory, the increase of molar mass can be explained as following: at the beginning of the reaction, there were relatively higher concentration of activated initiators, so the molecular weight was low, with increasing reaction time, contents of both initiators and monomers decreased, but concentration of activated initiators decreased more than monomers, so after a certain

duration, initiators were not so sufficient as before, then larger molecules are formed, the molecular weight got larger as well.

5.1.4 Summary

Copolymers of PAN and AMPS were successfully synthesized via free radical copolymerization using AIBN as initiator. Detailed characterizations of the copolymers were carried out. Reactivity ratio of two monomers under the condition in this study was studied. It is possible to adjust the content of AMPS in the copolymer and molar mass of the copolymers to tune the properties of the resulting membranes. Optimized condition and composition were found out to synthesize appropriate copolymers.

5.2 Influence of concentration and drying methods

As discussed in chapter 4, it is possible to form membranes with distinct separation properties by changing concentration of the polymer solution or varying drying conditions. To find out the optimized condition for the membrane formation, the influence of these two most important parameters were studied.

In this chapter, the nomenclature of the samples was based on the preparation of the membranes, for example, in the name C03-WIP-5%, C03 refers to the copolymer group from which the membranes were prepared, WIP means the coagulation bath, in this chapter all the coagulation bathes were mixture of water and isopropanol with 1/1 volume fraction, and 5% corresponds to the concentration of the polymer solution. Besides, when comparing the properties of membranes from water and WIP as coagulation bathes, in the name C03-N-5% “N” means only that polymer solutions were prepared in NMP.

5.2.1 Thickness

In this part of experiments, membranes were casted with the thickness of 200 µm, then thicknesses before and after drying methods were measured, as presented in Table 5.7.

Table 5.7 Thicknesses of membranes before and after drying treatment

Concentration	Water			Solvent exchange		
	Before (μm)	After (μm)	Shrinkage (%)	Before (μm)	After (μm)	Shrinkage (%)
5%	53.75	50.44	6.16	51.84	48.56	6.32
6%	58.37	55.15	5.52	58.62	55.23	5.78

Overall, the drying treatments still lead to a certain content of shrinkage, but because the membranes were already rather dense, the shrinkage was fairly small as compare to that of the membranes in chapter 4. Besides, although all the membranes were dense, a slight difference resulted from concentration can be found, not only in the thickness, but also in the shrinkage, which indicated that the concentration could still affect the separation performance. Furthermore, judging from the thickness, drying methods had little influence on the membrane properties.

5.2.2 Pore morphology

To study the pore morphologies of the membranes, SEM images were taken with cross-section view. In this part, the SEM images were not taken in high vacuum condition, but with 50% humidity to detect the pore morphology that was closer to the wet state.

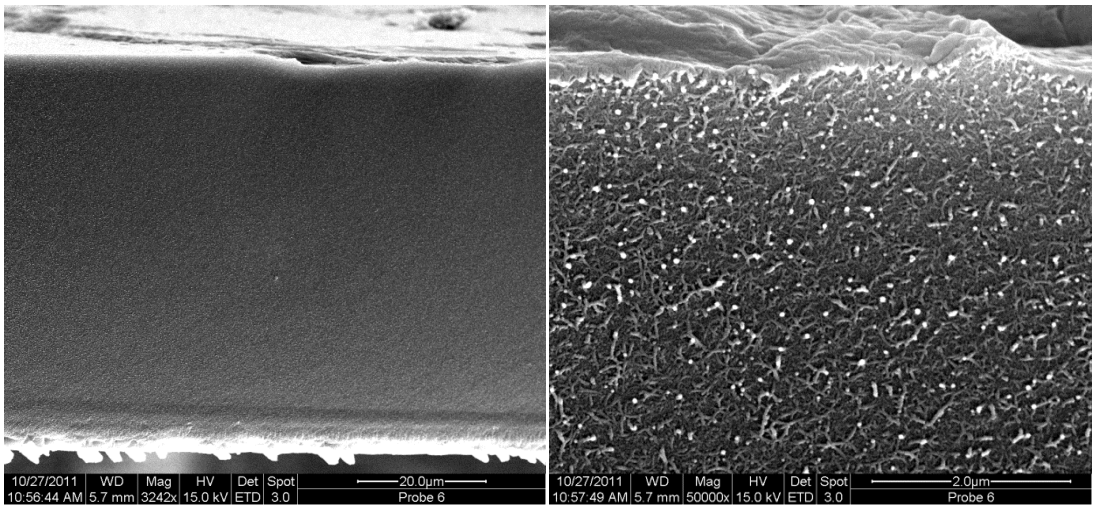

(a)

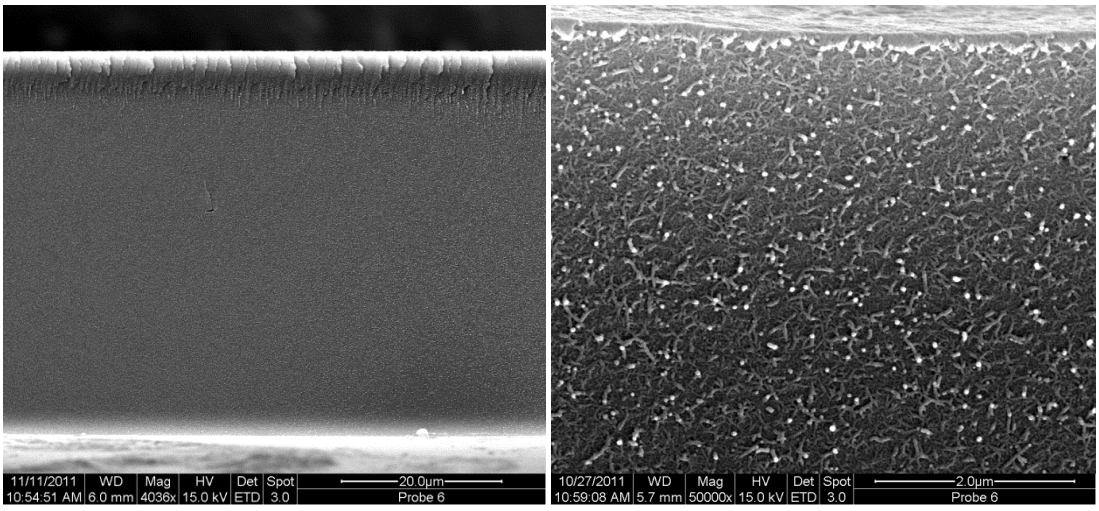

(b)

Fig. 5.10 SEM images of different membranes: (a), C03-WIP-5% at wet state;

(b), C03-W-5% at wet state

As seen in the SEM images, there were no cylindrical pores through the membranes from the cross-section view for all the groups. Typical images were shown in Fig. 5.10. As no pores were formed, no difference between membranes prepared from different concentration polymer solution can be found exclusively from the SEM images. The variation of coagulation bath didn't change the structure significantly either. Drying process changed the thickness, but still no obvious structural distinction was observed in the SEM images.

5.2.3 Separation performance

As shown in Fig. 5.11, the membrane prepared from the 5% polymer solution had much higher flux. Whereas either drying or using WIP as coagulation bath will decrease the permeability at a significant ratio, this may result from the free volume inside the membrane, both drying and slower precipitation can compress the free volume effectively thus induce lower flux. Besides, the reduction in permeability of C03-N-5% was more significant than that of C03-N-6%, which also proved the denser structure (less free volume) in C03-N-6%.

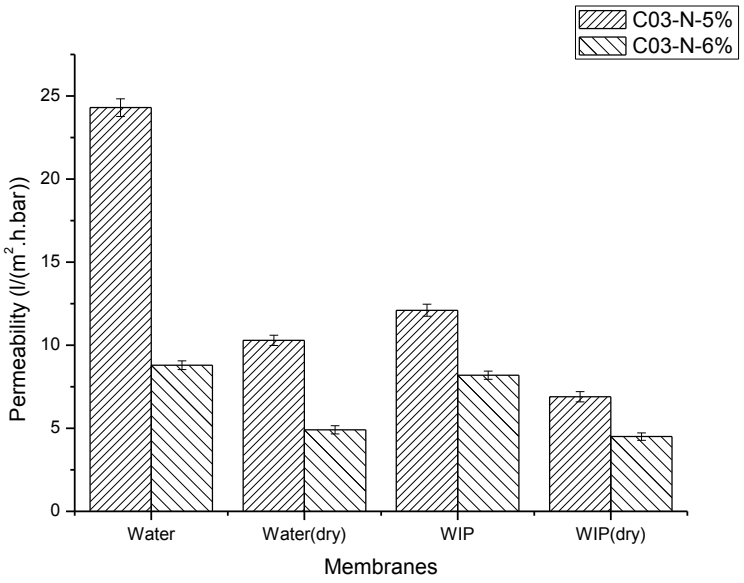

Fig. 5.11 Permeability of membranes from C-03 group

Filtration performance of the membranes with different AMPS content (prepared at the same concentration) was investigated, as shown in Fig. 5.12. All the membranes were endowed with similar water permeability at wet state, whereas, after drying with ethanol, the permeability decreased to certain content, and the reduction decreased with decreased AMPS content. This is mostly because of the hydrophilicity of the AMPS segment, in wet state, larger content of AMPS leads to higher swelling degree, during the drying process, the space that was occupied by water absorbed in the membrane would be compressed, thus the dried membranes with higher AMPS content got also denser structure after drying. In comparison with the membranes from Water/Isopropanol, the membranes were already rather dense and had few pores, so the coagulation bath had little effect on the membrane structure. This can explain the little difference in the permeability of membranes from water

and WIP, furthermore, after drying, all the membranes were converted to a dense layer as what happened to the membranes prepared from water, which is the reason why there was no difference between the membranes from water and WIP after drying.

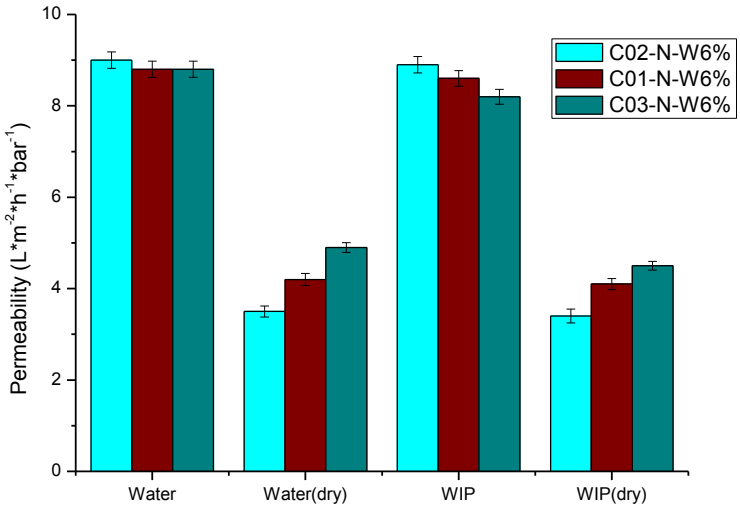

Fig. 5.12 Influence of coagulation bath and drying process on the permeability

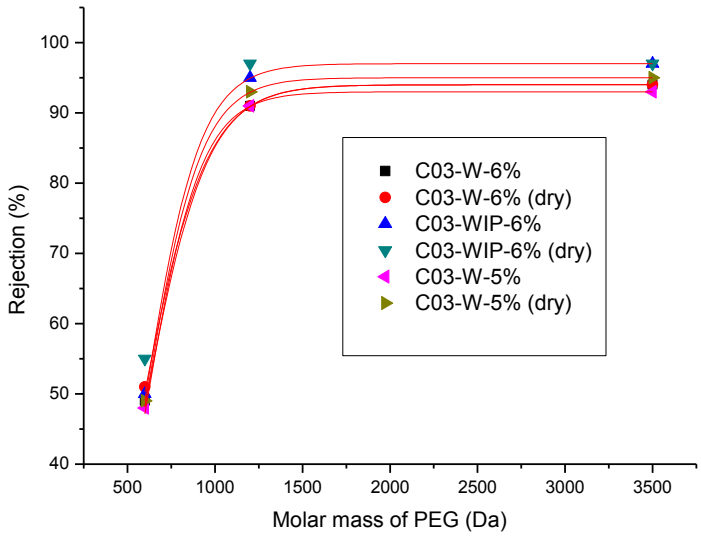

Fig. 5.13 Rejection curve of different membranes

Fig. 5.13 illustrated the rejection properties of six different membranes, in which, PEGs were tested as solutes. All the membranes were endowed with relatively low molecular weight

cut-off, the increase in rejection of molecules between 600 and 1200 Da was fairly sharp, after the rejection reached 90%, and the increase was not as fast as before. The membranes with this kind of rejection curve will be effective to separate mixture of molecules with similar molar mass, e.g. PEG 400 and PEG 1200.

The rejection of salts was also tested using magnesium sulfate as solute, results of which were shown in Fig. 5.14. As seen in this figure, the rejections of all the membranes were quite low. There are probably two reasons for that, first there are still certain amount of large pores in the membrane, so the salts can easily flow through it; second, also the most important reason was the relatively low charge density, as discussed before, the mole fraction of AMPS in the copolymers was only around 10%, rejection is expected to be higher when the content of AMPS increased. But when the mole fraction of AMPS in the feed was tuned to 1:1, the copolymers became water soluble, it was reported by M. Kumar *et al*. that the copolymer can be cross-linked thus stable in solvents using formaldehyde and polyvinyl alcohol as cross-linking agents [194].

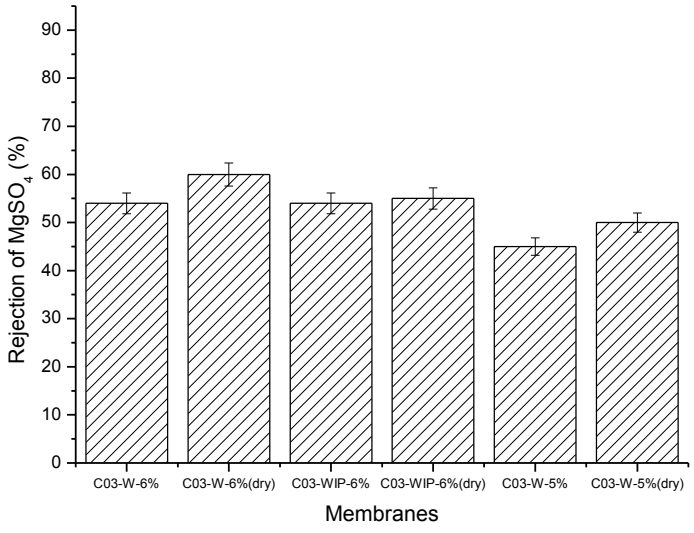

Fig. 5.14 Rejection of $MgSO_4$ of different membranes

5.2.4 Summary

Although it was not possible to prepare polymer solutions with higher concentration from the copolymer of AN and AMPS, the membranes derived from lower concentration (5% or

6%) had no visible pores in SEM images, which resulted in better performance in nanofiltration process. Comparing with former experiments, as the membranes were rather dense, neither drying methods nor coagulation bathes changed the properties significantly. But with lower polymer concentration, there was relatively large reduction in permeability after drying. Composition of copolymers can influence the permeability of resulting membranes, whereas the difference in rejection was not obvious. Finally, the rejection of salts was low, which was mainly because of low charge density.

5.3 Influence of non-woven support

As the membranes were rather thin and soft after formation, it was not so convenient to apply the membranes directly in the separation experiments; sometimes parts of the membranes folded under pressure thus inducing failure in experiments. Therefore, to make the membranes more applicable in real condition separation and to make sure that the results are reproducible, membranes were casted directly on non-woven supports to achieve good shape stability. Because the mesh size of the non-woven supports was extremely large, and for a better adhesion between membrane and support, no pore fillers were used.

5.3.1 SEM images

SEM images were first taken to observe the pore morphologies on the supports.

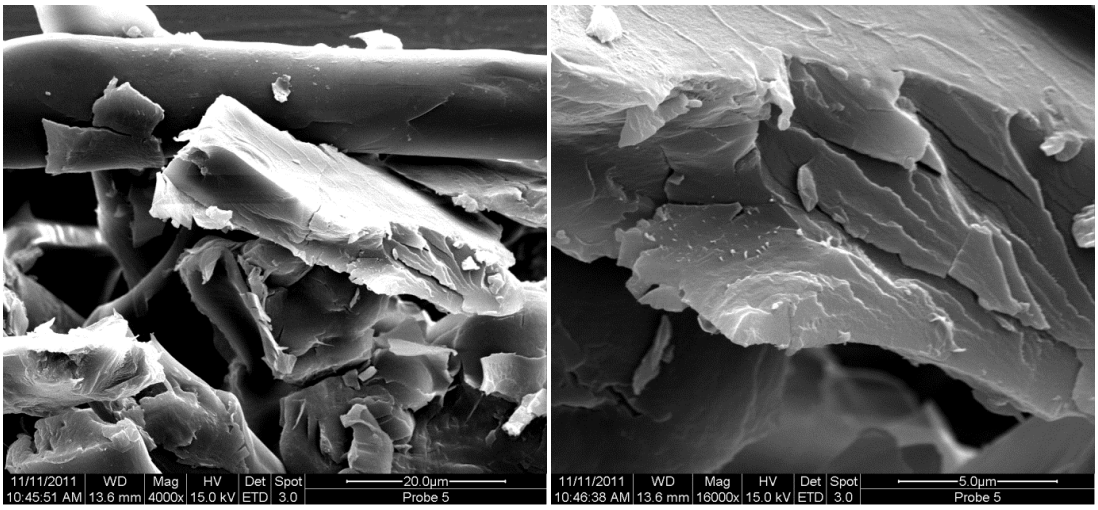

C03-2-N-W-5%(S)-1 cross-section

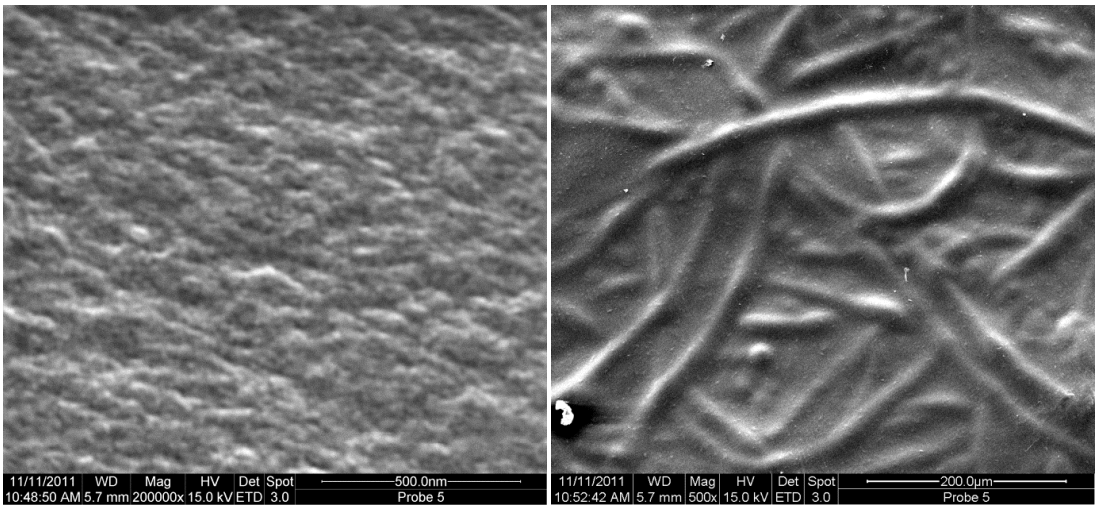

C03-2-N-W-5%(S)-1 surface

Fig. 5.15 SEM images of membranes with non-woven support

As the substrate is not easily cracked, it was not possible to crack the membrane in liquid nitrogen to prepare the cross-section samples, so the samples were prepared by simply scissoring. Therefore, in the cross section image of Fig. 5.15, some pieces of membranes that penetrate into the non-woven support can be found, but the cross section view of the dense layer can still be seen clearly, there were no pores either. Besides, from the surface view of the same group of membrane, with a lower magnification, clear fibers can be observed, which was because of the parameters of the support, the diameters of the fibers are relatively high and the pore sizes of the support are large as well. The reason why the non-

woven support was used is to get better shape stability, so it would be a matter if the substrate had influence on the separation properties, therefore the following discussion on separation was made.

5.3.2 Separation performance

The separation properties of membranes with non-woven support were evaluated in comparison with pure membranes. In Fig. 5.16, the membranes with support had slightly lower value of permeability, it could be due to the reduction of valid surface area because of the fiber in the support, but the influence was quite minor.

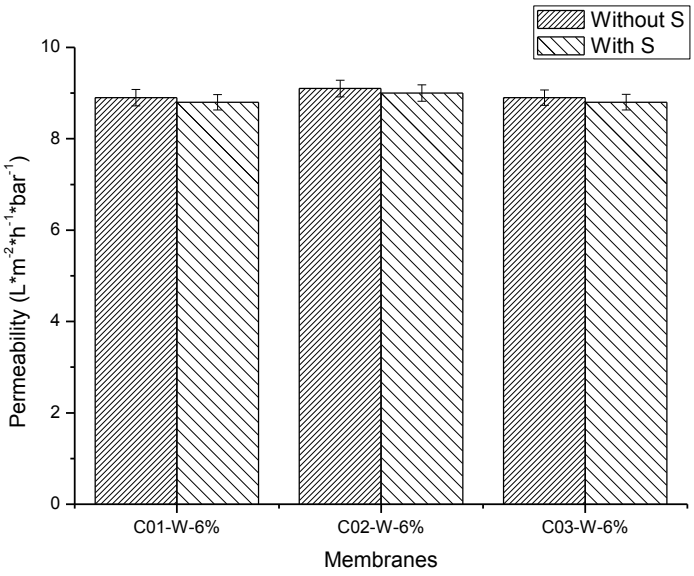

Fig. 5.16 Permeability of membranes with and without support

Similar things happened to the rejection properties as shown in Fig. 5.17. The membranes with and without non-woven supports had almost same rejection of PEGs.

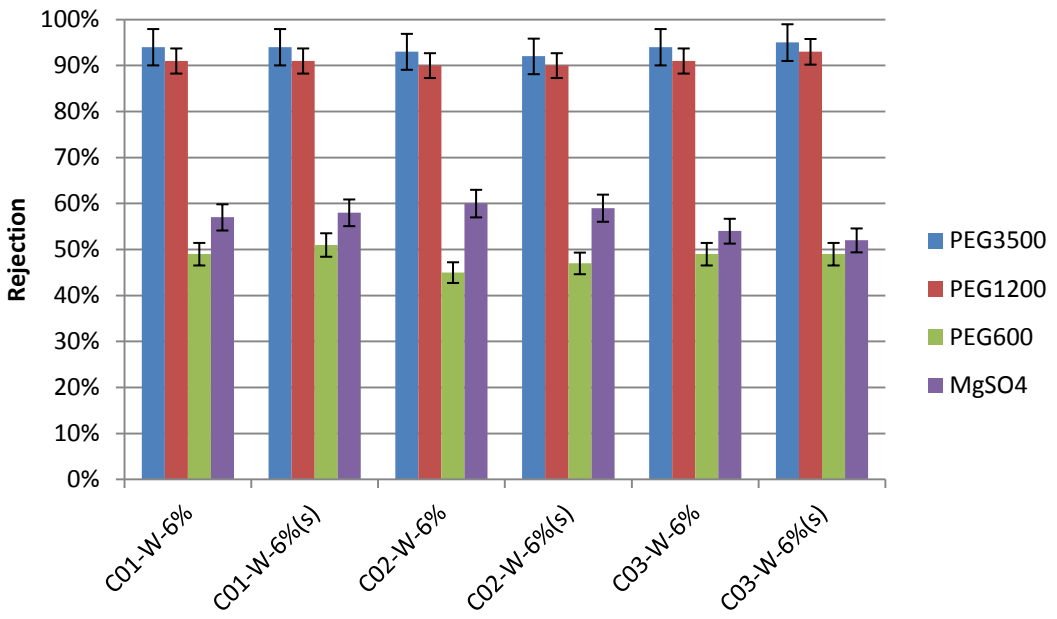

Fig. 5.17 Rejection of solutes in aqueous solution

When comparing membranes with and without supports, the rejection of a same PEG or salt was almost the same. Therefore, the influence of non-woven support on the separation properties can be almost ignored.

5.3.3 Summary

The introduction of the non-woven support can greatly enhance the mechanical stability of the resulting membranes, but didn't affect the separation performance obviously, therefore it is better to cast membranes directly on the non-woven supports for further experiments or storage.

5.4 Attempts on copolymers of AN and HEMA

Copolymers of AN and HEMA were also synthesized via free radical copolymerization using AIBN as initiator in DMF.

5.4.1 Overall observations on the copolymers

Variation of the parameters and compositions was also made to achieve the optimized copolymers. Among these parameters, the content of HEMA in feed was found to be most important.

Table 5.8 Composition and parameters used in the copolymerization

	B01	B02	B03	B14	B15	B16
DMF (ml)	50	50	50	50	50	50
HEMA (g)	4.94	4.94	4.94	2.12	1.62	1.12
AN (g)	3.5	3.5	3.5	7	7	7
AIBN (g)	0.0082	0.0164	0.0328	0.0146	0.0146	0.0146
Reacting time(hour)	10	10	10	10	10	10
t_b (min)	Few seconds	Few seconds	Few seconds	Few seconds	0	0

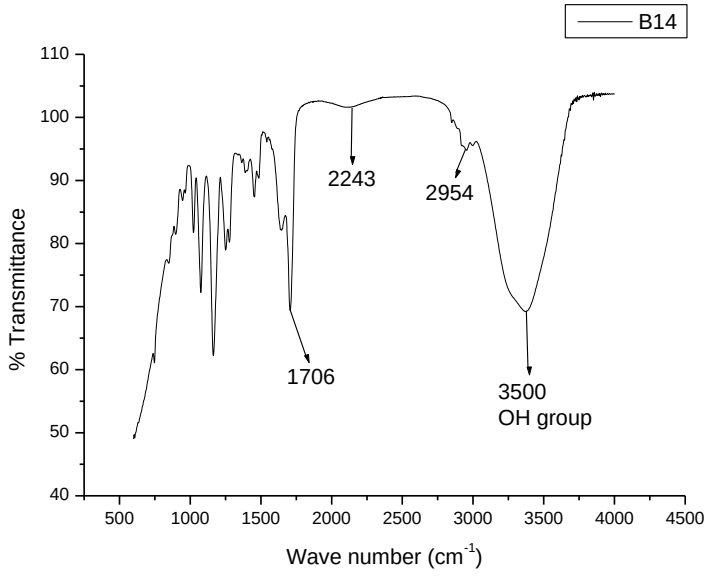

Fig. 5.18 IR spectra of copolymer B14

As shown in Fig. 5.18, in the copolymers of B14, the content of AN in the copolymer was quite low, this phenomenon was probably because of the reactivity ratio, the reactivity of

AN and HEMA pair is 0.2 and 1 respectively. This means that, in the initial stage of the copolymerization, HEMA was incorporated faster and the copolymer was rich in HEMA, when HEMA gets depleted, more AN segments were added. It can be also judged from the yield (not calculated), that only few copolymers were derived in the first several experiments. Besides, larger content of HEMA leads to poor solvent stability, the resulting membranes were so weak that even acetone vapor will deform them obviously. So higher content of AN is needed.

Whereas, when more AN monomers were added in the feed, the IR spectra of the resulting copolymer was shown in fig. 5.18. Content of –CN group was much higher than that in B14, but another problem came out, it was even not possible for the polymer to form a shape-stable membrane. Virtually, the membrane was so brittle that it fell into pieces by itself immediately after taken out from water bath. This phenomenon was mostly because of much too low molar mass of the copolymer. Because of the huge difference in reactivity ratio, when an AN monomer was activated, it tended largely to propagate with HEMA monomers, but in this case, the content of HEMA was too low to support enough propagation, therefore the molecular weight of copolymers was extremely low.

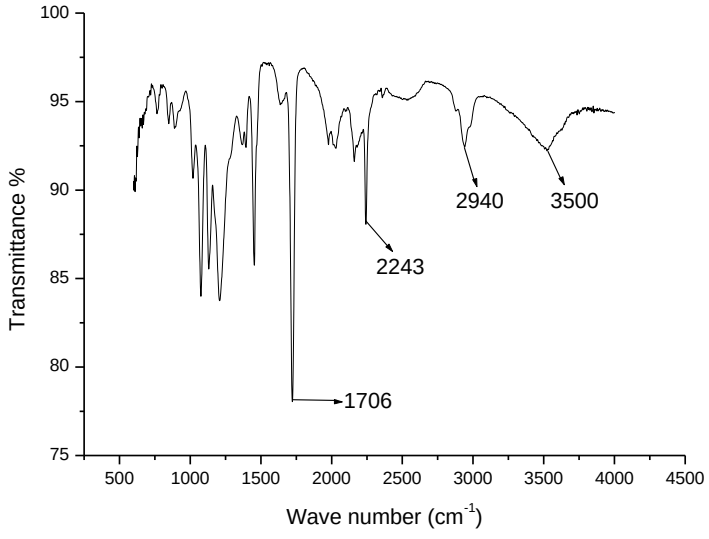

Fig. 5.19 IR spectra of copolymer B16

After the formation of so-called membranes from copolymer B16, one piece of broken membrane was treated with the second cross-linking procedure (with glutaraldehyde) as in

chapter 4, the membrane became stable both in shape and in solvent resistance; it was then put into DMF to check the stability and proved to be stable.

5.4.2 Summary

Copolymers of AN and HEMA were synthesized via free radical copolymerization. The resulting copolymers had several advantages over the block copolymer of AN and PEG, for instance: the solubility in DMF was much higher, so it was easier to prepare solutions with higher concentration thus denser membranes were formed. Besides, more OH groups are available for the post cross-linking process. But, it was not possible to control the composition of the copolymers freely, then either extremely low molar mass or extremely weak membranes was obtained, it was not possible to achieve the intermediate. Therefore, the copolymer itself was not valuable to prepare membranes directly, but the cross-linking attempts indicated that the cross-linking reaction was possible to take place on a piece of already-formed membrane under mild conditions.

5.5 Conclusions for the copolymers of AN and other monomers

Copolymers of PAN and AMPS were successfully synthesized via free radical copolymerization using AIBN as initiator. From detailed characterizations of the copolymers, the compositions of copolymers were studied, and it was possible to tune the composition and molar mass of the copolymers to achieve variation in separation properties of the resulting membranes. Even the membranes derived from lower polymer concentration (5% or 6%) had no visible pores in SEM images, which corresponded to better performance in nanofiltration process. As the membranes were rather dense, neither drying methods nor coagulation bathes affected the properties significantly, but with lower polymer concentration, drying still lead to reduction in permeability. Composition of copolymers can influence the permeability of resulting membranes, whereas the difference in rejection was not obvious. Rejection of salts was low, which was mainly because of low charge density. The introduction of the non-woven support can greatly enhance the mechanical stability of the resulting membranes, but didn’t affect the separation performance obviously.

Therefore the best condition to prepare membranes from copolymer of AN and AMPS was found to be: Polymer solution with concentration of 5% in NMP is casted on non-woven support, then precipitated in water, and it is better to avoid drying to store the membranes in water.

The attempts on the copolymers of AN and HEMA indicated that cross-linking as post-treatment is possible to take effect; the copolymer itself is not valuable for direct membrane preparation.

Chapter 6. Conclusions and Outlook

Block copolymers of PAN and PEG was successfully synthesized via water-phase precipitation copolymerization using Ce(IV)-PEG as a redox initiator system. It is possible to tune the content of PEG, the molar mass of the copolymer, and to change the molar mass of PEG segment, thus to tune the properties of the resulting membranes. Optimized condition and composition were worked out to synthesize appropriate copolymers.

After the comparison of various membranes treated with different drying methods, the membranes formed via NIPS from polymer concentration of 16% have the most appropriate pore sizes, and treatment with solvent exchange is better to maintain the properties of the membrane and to control both the pore size and pore structure. As for the filtration properties, the ultrafiltration membranes from 16% polymer solution were endowed with relatively high permeability and reasonable MWCO. But after drying treatment, the permeability of membranes declined from 661 to 88 L/(m^2*bar*h), and the reduction in MWCO was from 100 kDa to 70 kDa, which was not so significant as the reduction in permeability. Therefore, it is better to store the membranes in water other than dry them. Besides, the separation performance in non-aqueous condition was proved to be stable, and the pore flow model seems to dominate the transport through the membranes.

Because of the interaction between solvent and coagulation bath, addition of less polar solvent in the coagulation bath can lead to denser structure of the resulting membranes, thus lower permeability and better rejection properties. Whereas, compared with membranes from the coagulation bath with 50% isopropanol, membranes from 66% isopropanol was endowed with much lower pure solvent permeability but relatively less reduction in molecular weight cut-off. Therefore it is not a perfect way to reach better separation performance by continuously increasing the content of isopropanol in coagulation bath.

It was proved via FT-IR measurement that the two designed cross-linking reactions were possible to take place between all the cross-linkers and the membranes. After the cross-linking with different processes, the membranes became more stable than before, based on

different cross-linking density, the resulting membranes showed difference in solvent resistance. Because of the densification effect of cross-linking process, the cross-linked membranes had lower water permeability and lower MWCO as well, higher cross-linking density lead to greater reduction in both permeability and MWCO. The resulting membrane had excellent solvent resistance, relatively high permeability and rejection properties as ultrafiltration membranes; so it is possible to apply them directly in solvent resistant ultrafiltration process, or as support materials for solvent resistant nanofiltration membranes.

It was proved via FT-IR measurement that it was possible to convert the -CN groups in the membranes to –COONa or $–COONH_2$ groups via the designed conversion reaction. After the conversion with different process conditions, the membranes became much tighter than before, no visible macrovoid pores still existed in the membranes, which can be observed from SEM images. As the pore morphologies of membranes changed completely, the resulting membranes had much lower solvent permeability and significantly improved rejection properties as well. Higher $ZnCl_2$ concentration led to better separation performance that meant larger solvent permeability and similar MWCO. Furthermore, the membranes were also endowed with properties to reject salts that have much smaller molecular weights than the MWCO, because of the conversion of –CN to ionic groups. The resulting membrane had excellent solvent resistance, relatively high permeability and desired rejection properties as nanofiltration membranes; so it is possible to apply them directly in solvent resistant nanofiltration processes, or in aqueous nanofiltration.

The attempts on the copolymers of AN and HEMA indicated that cross-linking as post-treatment is possible to take effect; the copolymer itself is not valuable for direct membrane preparation.

Copolymers of PAN and AMPS were successfully synthesized via free radical copolymerization using AIBN as initiator. From detailed characterizations of the copolymers, the compositions of copolymers were studied, and it was possible to tune the composition and molar mass of the copolymers to achieve variation in separation properties of the resulting membranes. Even the membranes derived from lower polymer concentration (5% or 6%) had no visible pores in SEM images, which corresponded to better performance in nanofiltration process. As the membranes were rather dense, neither drying methods nor

coagulation bathes affected the properties significantly, but with lower polymer concentration, drying still lead to reduction in permeability. Composition of copolymers can influence the permeability of resulting membranes, whereas the difference in rejection was not obvious. Rejection of salts was low, which was mainly because of low charge density. The introduction of the non-woven support can greatly enhance the mechanical stability of the resulting membranes, but didn't affect the separation performance obviously. Therefore the best condition to prepare membranes from copolymer of AN and AMPS was found to be: Polymer solution with concentration of 5% in NMP is casted on non-woven support, then precipitated in water, and it is better to avoid drying to store the membranes in water. When the mole ratio of AMPS in the feed reached 50%, the resulting copolymers became water soluble, it is possible to cross-link it with post treatment to enhance solvent resistance, and membranes from the resulting polymer would be expected to have higher rejection of salts because of high charge density. Therefore, this work is worth continuous research.

References

[1] X. Lu, X. Bian, L. Shi, Preparation and characterization of NF composite membrane, J. Membr. Sci. 210 (2002) 3-11.

[2] L. P. Raman, M. Cheryan, N. Rajagopalan, Consider nanofiltration for membrane separations, Chem. Eng. Prog. 90 (1994) 68-74.

[3] M. E. Williams, J. A. Hesyekin, C. N. Smothers, D. Bhattacharayya, Separation of organic pollutants by reverse osmosis and nanofiltration membranes, Ind. Eng. Chem. Res. 38 (1999) 3683-3695.

[4] B. Van der Bruggen, J. Geens, C. Vandecasteele, Influence of organic solvents on the performance of polymeric nanofiltration membranes, Sep. Sci. Technol. 37 (2002) 783-797.

[5] D. A. Musale, A. Kumar, Solvent and pH resistance of surface crosslinked chitosan/poly(acrylonitrile) composite nanofiltration membranes, J. Appl. Polym. Sci. 77 (2000) 1782-1793.

[6] J.A. Whu, B.C. Baltzis, K.K. Sirkar, Modeling of nanofiltration-assisted organic synthesis, J. Membr. Sci. 163 (1999) 319-331.

[7] J.T. Scarpello, D. Nair, L.M. Freitas dos Santos, L.S. White, A.G. Livingston, The separation of homogeneous organometallic catalysts using solvent resistant nanofiltration, J. Membr. Sci. 203 (2002) 71-85.

[8] L.S. White, A.R. Nitsch, Solvent recovery from lube oil filtrates with a polyimide membrane, J. Membr. Sci. 179 (2000) 267-274.

[9] S. Han, H.T. Wong, A.G. Livingston, Application of organic solvent nanofiltration to separation of ionic liquids and products from ionic liquid mediated reactions, Chem. Eng. Res. Des. 83 (2005) 309-316.

[10] J.A. Whu, B.C. Baltzis, K.K. Sirkar, Nanofiltration studies of larger organic microsolutes in methanol solutions, J. Membr. Sci. 170 (2000) 159-172.

[11] J.P. Sheth, Y. Qin, K.K. Sirkar, B.C. Baltzis, Nanofiltration-based diafiltration process for solvent exchange in pharmaceutical manufacturing, J. Membr. Sci. 211 (2003) 251-261.

[12] D. Bhanushali, D. Bhattacharyya, Advances in solvent-resistant nanofiltration membranes: experimental observations and applications, Ann. N. Y. Acad. Sci. 984 (2003) 159-177.

[13] D. Bhanushali, S. Kloos, D. Bhattacharyya, Solute transport in solvent-resistant nanofiltration membranes for non-aqueous systems: experimental results and the role of solute-solvent coupling, J. Membr. Sci. 208 (2002) 343-359.

[14] W. Zhang, G. He, P. Gao, Y.K. Chen, Development and characterization of composite nanofiltration membranes and their application in concentration of antibiotics, Sep. Purif. Technol. 30 (2003) 27-35.

[15] M. Cheryan, Ultrafiltration and Microfiltration Handbook, Technomic, Lancaster, PA, 1998.

[16] M.H. Nguyen, M.M.A. Khan, K. Kailasapathy, J.A. Hourigan, Use of membrane concentrated cottage cheese whey in ice-creams, Aust. J. Dairy Technol. 52 (2) (1997) 75-78.

[17] V. Nwuha, Novel studies on membrane extraction of bioactive components of green tea in organic solvents, Part 1, J. Food Eng. 44 (2000) 233-238.

[18] Y.K. Guu, C.H. Chiu, J.K. Young, Processing of soybean soaking water with a NF-RO membrane system and lactic-acid fermentation of retained solutes, J. Agric Food Chem. 45 (10) (1997) 4096-4100.

[19] D. Bo, Z. Kun, Preparation and peoperties of polyimide ultrafiltration membranes, J. Membr. Sci. 60 (1991) 63-73.

[20] K.V. Peinemann, K. Ebert, H.G. Hicke, N. Scharnagl, Polymeric composite ultrafiltration membranes for non-aqueous applications, Environ. Prog. 20 (1) (2001) 17.

[21] L.S. White, Transport properties of a polyimide solvent resistant nanofiltration membrane, J. Membr. Sci. 205 (2002) 191-202.

[22] M.H.V. Mulder, Basic Principles of Membrane Technology

[23] P.T. Anastas, J.C. Warner, Green Chemistry - Theory and Practic. Oxford Unversity Press, 1998

[24] A. Lambert, P. Plucinski and I. Kozhevnikov, Polyoxometalate epoxidation of 1-octene with hydrogen peroxide in micro emulsion coupled with ultrafiltration, Chem. Commun. (2003), 714-715.

[25] I.F.J. Vankelecom, Polymeric membranes in catalytic reactor, Chem. Rev. 102 (2002), 3779-3810.

[26] M.T. Westaway and G. Walker, Catalyst ultrafiltration process, US Pat. 3,617,553 (1969).

[27] H. Bahrmann, M. Haubs, W. Kreuder and T. Muller, Process for separating organometallic compounds and/or metal carbonyls from their solutions in organic media, US Pat. 5,174,899.

[28] J.F. Miller, D.R. Robert, K.L. Hoy, N.E. Kinkade and R.H. Zanapalidou, Membrane separation process, US Pat. 5,681,473 (1997).

[29] J.T. Scarpello, D. Nair, L.M. Freitos dos Santos, L.S. White and A.G. Livingston, The separation of homogeneous organometallic catalysts using solvent resistant nanofiltration, J. Membr. Sci., 203 (2002), 71-85.

[30] D. Turlan, E.P. Urriolabeitia, R. Navarro, C. Royo, M. Menendez and J. Santamaria, Separation of Pd complexes from a homogeneous solution using zeolite membranes, Chem. Commun. (2001), 2608-2609.

[31] D. Nair, S.S. Luthra, J.T. Scarpello, L.S. White, L.M. Freitos dos Santos and A.G. Livingston, Homogeneous catalyst separation and re-use through nanofiltration of organic solvents, Desalination, 147 (2002), 301-306

[32] K. De Smet, S. Aerts, E. Ceulemans, I.F.J. Vankelecom and P.A. Jacobs, Nanofiltration coupled catalysis to combine the advantages of homogeneous and heterogeneous catalysis, Chem. Commun. 2001, 597.

[33] D.L. Wernick, Preparation of cellulose acetate membrane and its use for polar solvent-oil separation, US Pat. 4,678,555 (1987).

[34] L.E. Black, Interfacially polymerized membranes and reverse-osmosis of organic solvent solutions using them, EP 421676 (1991).

[35] H.F. Shuey and W. Wan, Asymmetric polyimide reverse osmosis membrane, method for preparation of same and use thereof for organic liquid separations, US Pat. 4,532,041 (1985).

[36] B.P. Anderson, Ultrafiltration polyimide membrane and its use for recovery of dewaxing aid, US Pat. 4,963,303 (1990).

[37] L.S. White and A.R. Nitsch, Solvent recovery from oil filtrates with a polyimide membrane, J. Membr. Sci. 179 (2000), 267-274

[38] R.M. Gould, L.S. White and C.R. Wildemuth, Membrane separation in solvent dewaxing, Env. Progress 20 (2001), 12-16.

[39] L.S. White, I.F. Fan and S. Minhas, Polyimide membrane for the separation of solvent from lube oil, US Pat. 5,429,748 (1995).

[40] J.L. Feimer, D.W. Kraemer, J. Mann and G.L. Wagner, Membrane process to remove elemental sulphur from gasoline, CA2111176 (1994).

[41] H.-D. Belitz and W. Grosch, Food Chemistry, Springer-Verlag, Germany (1999).

[42] S. Gupta and K. Achintya, Refining, US Pat. 4,533,501 (1985).

[43] S. Gupta and K. Achintya, Process for refining crude glyceride oil by membrane filtration, US Pat. 4,062,882 (1977).

[44] A.K. Iwama and N.K. Yoshiyasu, Purification of crude glyceride oil compositions, EP302766 (1983).

[45] L. Lin, K.C. Rhee and S.S. Koseoglu, Bench-scale membrane degumming of crude vegetable oil: Process optimization, J. Membr. Sci. 134 (1997), 101-108.

[46] N. Ochoa, C. Pagliero, J. Marchese and M. Mattea, Ultrafiltration of vegetable oils: degumming by polymeric membranes, Separation and Purification Technology 22-23 (2001), 417-422.

[47] S.S. Köseoglu, J.T. Lawbon and E.W. Lusas, Membrane processing of crude vegetable oils: Pilot plant scale removal of solvent from oil miscellas, J. Am. Oil Chem. Soc., 67 (1990), 315-322.

[48] M. Schmidt, K.-V. Peinemann, N. Scharnagl, K. Friese and R. Schubert, Radiation-modified siloxane composite membranes for ultrafiltration of solutes from organic solvents, DE19507584 (1996).

[49] N. Stafie, D.F. Stamatialis and M. Wessling, Insight into the transport of hexane-solute systems through tailor-made composite membranes, J. Membr. Sci. 228 (2004), 103-106.

[50] J.P. Sheth, Y. Qin, K.K. Sirkar, B.C. Saltzis, Nanofiltration-based diafiltration process for solvent exchange in pharmaceutical manufacturing, J. Membr. Sci. 211 (2003), 251-261.

[51] A.G. Livingston, Method; 2 WO02076588 (2002).

[52] U. Razdan, S.V. Joshi, V.J. Shah, Novel membrane processes for separation of organics, Curr. Sci. India 85 (2003), 761.

[53] R.A. Hayes, Polyimide gas separation membranes, US 4,717,393 (1988).

[54] H. Kita, T. Inada, K. Tanaka, K.I. Okamoto, Effect of photocrosslinking on permeability and permselectivity of gases through benzophenone-containing polyimide, J. Membr. Sci. 87 (1994), 139.

[55] P.S. Tin, T.S. Chung, Y, Liu, R. Wang, S.L. Liu, K.P. Pramoda, Effects of cross-linking modification on gas separation performance of Matrimid membranes, J. Membr. Sci. 225 (2003), 77.

[56] T.S. Chung, L. Shao, P.S. Tin, Surface modification of polyimide membranes by diamines for H_2 and CO_2 separation, Macromol. Rapid Commun. 27 (2006), 998.

[57] J.H. Kim, W.J. Koros, D.R. Paul, Effects of CO_2 exposure and physical aging on the gas permeability of thin 6FDA-based polyimide membranes: Part 2. With crosslinking, J. Membr. Sci. 282 (2006), 32.

[58] C.K. Kim, J.H. Kim, I.J. Roh, J.J. Kim, The changes of membrane performance with polyamide molecular structure in the reverse osmosis process, J. Membr. Sci. 165 (2000), 189-199.

[59] I.J. Roh, S.Y. Park, J.J. Kim, C.K. Kim, Effects of the polyamide molecular structure on the performance of reverse osmosis membranes, J. Polym. Sci. Part B-Polym. Phys 36 (1998), 1821-1830.

[60] J.E. Tomaschke, Interfacially polymerized bipiperidine-polyamide membranes for reverse osmosis and/or nanofiltration and process for making the same (2000), EP 1,060,785.

[61] M.M. Jayarani, S.S. Kulkarni, Thin-film composite poly (esteramide)-based membranes, Desalination 130 (2000), 17-30.

[62] S.Y. Kwak, C.K. Kim, J.J. Kim, Effects of bisphenol monomer structure on the surface morphology and reverse osmosis (RO) performance of thin-film composite membranes composed of polyphenyl esters, J. Polym. Sci.: Part B: Polym. Phys. 34 (1996), 2201-2208.

[63] A.K. Pandey, R.F. Childs, M. West, J.N.A. Lott, B.E. McCarry and J.M. Dickson, Formation of pore filled ion-exchange membranes with *in situ* cross-linking: poly(vinylbenzyl) ammonium salt)-filled membranes, J. Polym. Sci.: Part A: Polym Chem. 39 (2001), 807-820.

[64] L. Costa, Catalyst mediated method of interfacial polymerisation on a microporous support, and polymers, fibers, films and membranes made by such a method (1997), US 5,693,227.

[65] W. Mickols, Composite membrane and method for making same (2001), WO 01/78882.

[66] J. E. Tomaschke, Amine monomers and their use in preparing interfacially synthesised membranes for reverse osmosis and nanofiltration (1999), US 5,922,203.

[67] D.M. Koenhen and A.H.A. Tinnemans, Semipermeable composite membrane, a process for the manufacture thereof, as well as application of such membranes for the separations of components in an organic liquid phase or in the vapor phase (1993), US 5,274,047.

[68] D.M. Koenhen and A.H.A. Tinnemans, Process for the separation of components in an organic liquid medium and a semi-permeable composite membrane (1994), US 5,338,455.

[69] D.M. Koenhen and A.H.A. Tinnemans, Semi-permeable composite membrane and process for manufacturing same (1993), US 5,207,908.

[70] N.W. Oh, J. Jegal, K.H. Lee, Preparation and characterisation of nanofiltration composite membranes using polyacrylonitrile (PAN). II. Preparation and characterisation of polyamide composite membranes, J. Appl. Polym. Sci. 80 (2001), 2729-2736.

[71] K.-R. Lee, M.-Y. Teng, H.-H. Lee and J.-Y. Lai, Dehydration of ethanol/water mixures by pervaporation with composite membranes of polyacrylic acid and plasma-treated polycarbonate, J. Membr. Sci. 164 (2000), 13-23.

[72] M.L. Sforca, S.P. Nunes, K.V. Peinemann, Composite nanofiltration membranes prepared by a *in situ* polycondensation of amines in a poly(ethylene oxide-*b*-amide) layer, J. Membr. Sci. 135 (2) (1997), 179-186.

[73] C. Linder, M. Perry and R. Kotraro, Semipermeable composite membranes, their manufacture and their use, US Pat. 4,753,725 (1988).

[74] L.E. Black, Interfacially polymerized membranes and reverse-osmosis of organic solvent solutions using them, EP 421676 (1991).

[75] S.C. Williams, B. Bikson, J.K. Nelson and R.D. Burhesky, Method for preparing composite membranes for enhanced gas separation, US Pat. 4,840,819 (1989).

[76] H.J. Kim and S.S. Nah, A new technique of preparation of PDMS pervaporation membrane for VOC removal, Adv. Env. Res. 6 (2002), 255-264.

[77] C. Linder, M. Nemas, M. Perry and R. Katraro, Silicon-derived solvent stable membranes, US Pat. 5,205,934 (1993).

[78] C. Linder, M. Nemas, M. Perry and R. Katraro, Silicon-derived solvent stable membranes, US Pat. 5,265,734 (1993).

[79] G. Golemme and E. Drioli, Polyphosphazene Membrane Separations-Review, J. inorganic and organometallic polymers 69 (1996), 341-365.

[80] C. Bardot, M. Carles, R. Desplantes, L. Shrive, Reverse osmosis or nanofiltration membrane and its production process (1994), US 5,342,521.

[81] K. Lang, S. Sourirajan, T. Matsuura, G. Chowdhury, A study on the preparation of polyvinyl alcohol thin-film composite membranes and reverse osmosis testing, Desalination 104 (3) (1996), 185-196.

[82] W. Stone, P.A. Cantor B.S. Fischer and W.S. Highley, Dry polycarbonate membranes, EP 46,817 (1982).

[83] R.J. Petersen, Composite Reverse Osmosis and Nanofiltration Membranes, J. Membr. Sci. 83 (1993), 81-150.

[84] A. Kumar and D. Musale, Composite solvent resistant nanofiltration membranes, US Pat. 6,113,794 (2000).

[85] A. Kumar and D. Musale, Effects of surface cross-linking on sieving charatersitics of citosan/poly(acrylonitrile) composite nanofiltration membranes, Separation and Purification Tech. 21 (2000), 27-38.

[86] D. Musale and A. Kumar, Solvent and pH resistance of surface cross-linked chitosan/(polyacrylonitrile) composite membranes, J. Appl. Polym. Sci. 77 (2000), 1782-1793.

[87] K. Lang, G. Chowdhurry, T. Matsuura and S. Sourirajan, Reverse osmosis of modified polyvinylalcohol thin-film composite membranes, J. Colloid and Interface Sci. 166 (1994), 239-244.

[88] J. Jegal and K.-H. Lee, Nanofiltration membranes based on poly(vinylalcohol) and ionic polymers, J. Appl. Pol. Sci. 72 (1999), 1755-1762.

[89] H. Ohya, M. Shibata, Y. Negishi, Q.H. Guo and H.S. Choi, The effect of molecular weight cut-off of PAN ultrafiltation support layer of water-ethanol mixtures through pervaporation with PAA-PAN composite membranes, J. Membr. Sci. 90 (1994), 91-100.

[90] J. Huang, Q. Guo, H. Ohya, J. Fang, The characteristics of cross-linked PAA composite membranes for the separation of aqueous organic solutions by reverse osmosis, J. Membr. Sci. 144 (1998), 1-11.

[91] M. Pasternak, Membrane process for treating a charge containing dewaxing solvent and dewaxed oil, US Pat. 5,093,002 (1992).

[92] J.G.A. Bitter and J.P. Haan, Process for separating a fluids feed mixture containing hydrocarbon oil and an organic solvent, US Pat. 4,810,366 (1989).

[93] C. Linder, R. Katraro, M. Nemas and M. Perry, Solvent stable membranes, EP0392982 (1990).

[94] C. Linder and M. Perry, Reverse osmosis of modified ultrafiltration polyacrylonitrile modified membrane, US Pat. 4,584,103 (1986).

[95] C. Linder, R. Katraro, and M. Perry, Composite membranes and processes using them, US Pat. 5,024,765 (1991).

[96] C. Linder, R. Katraro, A. Gershon and M. Perry, Chemically modified semipermeable membranes and their use in reverse osmosis and ultrafiltration, US Pat. 4,690,765 (1987).

[97] M. Perry , H. Yacubowicz, C. Linder, M. Nemas and R. Katraro, Polyphenylene oxide-derived for separation in organic solvents, US Pat. 5,151,182 (1992).

[98] M.L. Stone, Method of dye removal for the textile industry, US Pat. 6,093,325 (2000).

[99] E.S. Peterson, C.J. Orme and M.L. Stone, Method for preparing membranes with adjustable separation performance, US Pat. 5,385,672 (1995).

[100] A. Boye, A. Grangeon, C. Guizard, Composite nanofiltration membrane (1993) US 5,266,207.

[101] M. Pasternak, Membrane process for treating a charge containing dewaxing solvent and dewaxed oil, US Pat. 5,234,579 (1993).

[102] K. Ebert, Thin film composite membranes of glassy polymers for gas separation – preparation and characterisation, PhD dissertation, University Twente, the Netherlands, (1995)

[103] C. Linder, R. Katraro and M. Perry, Novel membranes and process for making them, US Pat. 4,761,233 (1988).

[104] K.J. Kim, G. Chowdhury, T. Matsuura, Low pressure reverse omosis performances of sulfonated poly (2,6-dimethyl-1,4phenylene oxide) thin-film composite membranes: effect of coating conditions and molecular weight of polymer, J. Membr. Sci. 179 (1-2) (2000), 43-52.

[105] GELEST catalogue

[106] S.O. Hammouch, G.J. Beinert and J.E. Herz, Contribution to a better knowledge of the cross-linking reaction of polydimethylsiloxane (PDMS) by end-linking: the formation of star-branched PDMS by the hydrosilylation reaction, Polymer 37 (1996), 3353-3360.

[107] M. Schmidt, K.-V. Peinemann, N. Scharnagl, K. Friese and R. Schubert, Radiation-modified siloxane composite membranes for ultrafiltration of solutes from organic solvents, DE19507584 (1996).

[108] S. Loeb, S. Sourirajan, Seawater demineralisation by means of an osmotic membrane, Adv. Chem. Ser. 38 (1963), 117.

[109] M. Mulder, Basic Principles of Membrane Technology, Kluwer Academic, Dordrecht, The Netherlands (1991), 89-140.

[110] I. Pinnau and W. Koros, A qualitative skin layer formation mechanism for membranes made dry/ wet phase inversion, J. Pol. Sci.: Part B: Pol. phys., 31 (1993), 419-427.

[111] C. Dias, M. Rosa and M. de Pinho, Structure of water in asymmetric cellulose ester membranes – an ATR-FTIR study, J. Membr. Sci. 138 (1998), 259-267.

[112] D. Stamatialis, C. Dias and M. de Pinho, Atomic force microscopy of dense and asymmetric cellulosebased membranes, J. Membr. Sci., 160 (1990), 235-242.

[113] S. Konagaya, M. Tokai and H. Kuzumoto, Reverse osmosis performance and chlorine resistance of new ternary aromatic copolyamides comprising 3,3'- diaminodiphenylsulfone and a comonomer with a carboxyl groups, J. Appl. Pol. Sci. , 80 (2001), 505-513.

[114] S. Konagaya, H. Kuzumoto and O. Watanabe, New reverse osmosis membrane materials with higher resistance to chlorine, J. Appl. Pol. Sci. , 75 (2000), 1357-1364.

[115] S. Konagaya and M. Tokai, Synthesis of ternary copolyamides from aromatic diamines (mphenylenediamine, diaminodiphenylsulfone), aromatic diamine with carboxyl groups or sulfonic group (3,5-diaminobenzoic acid, 2,4-diaminobenzenesulfonic cid), and iso- or terephthaloyl chloride, J. Appl. Pol. Sci., 76 (2000), 913-920.

[116] P. Dvornic, Wholly aromatic polyamide-hydrazides: 5. Preparation and properties of semi-permeable membranes from poly [4-terephthaloylamino) benzoic acid hydrazide, J. Appl. Pol. Sci. 42 (1991), 957-972.

[117] C. Tsay and A. McHugh, Mass transfer modelling of asymmetric membranes formation by phase inversion, J. Pol. Sci.: Part B: Pol. Phys., 28 (1990), 1327-1365.

[118] Y. Dai, X. Jin, S. Zhang and M Guiver, Thermostable ultrafiltration and nanofiltration membranes from sulfonated poly(phthalazinone ether sulfone ketone), J. Membr. Sci., 188 (2001), 195-203.

[119] X. Jian, Y. Dai, G. He and G. Chen, Preparation of UF and NF poly(phthalazinone ether sulfone ketone) membranes for high temperature application, J. Membr. Sci., 161 (1999), 185-191.

[120] L. White, Polyimide membranes for hyperfiltration recovery of aromatic solvents, U.S. Pat. 6,180,008. (2001).

[121] S. Nunes and K. Peinemann, Membrane technology in the chemical industry, Wiley-VCH, Weinheim, Germany (2001), 7-11.

[122] N. Mohamed, Novel wholly aromatic polyamide-hydrazides: 6. Dependence of membrane reverse osmosis performance on processing parameters and polymer structural variations, Polymer 38 (1997), 4705-4713.

[123] R. Bindal, M. Hanra and B. Misra, Novel solvent exchange cum immersion precipitation technique for the preparation of asymmetric polymeric membrane, J. Membr. Sci. 118 (1996), 23-29.

[124] M. Satre, N. Ghatge and M. Ramani, Aromatic polyamide-hydrazides for water desalination: 1. Syntheses and RO membrane performance, J. Appl. Pol. Sci. 41 (1990), 697-712.

[125] W. Bowen, T. Doneva and H. Yin Polysulfone – sulfonated poly (ether ether) ketone blend membranes: systematic synthesis and characterisation, J. Membr. Sci. 181 (2001), 253-263.

[126] J.-H. Kim and K.-H. Lee, Effect of PEG additive on membrane formation by phase inversion, J. Membr. Sci. 138 (1998), 153-163.

[127] C. Linder, M. Perry and R. Ketraro, Novel membranes and process for making them, US Pat. (1988), 4,761,233

[128] K. Gupta, Synthesis and evaluation of aromatic polyamide membranes for desalination in reverseosmosis technique, J. Appl. Pol. Sci. 66 (1997), 643-653.

[129] K. Nakamae and N. Mohamed, Novel wholly polyamide-hydrazide: 2. Preparation and properties of membranes for reverse osmosis separation, J. Appl. Pol. Sci. Appl. Pol. Symp. 52 (1993), 307-317.

[130] R. McKinney and J. Rhodes, Aromatic polyamide membranes for reverse osmosis separations, Macromolecules 4 (1971), 633-637.

[131] X. Jian, Y. Dai, G. He and G. Chen, Preparation of UF and NF poly(phthalazinone ether sulfone ketone) membranes for high temperature application, J. Membr. Sci., 161 (1999), 185-191.

[132] A. Bottino G. Capannelli and S. Munari., Effect of coagulation medium on properties of sulfonated polyvinylidene fluoride membranes, J. Appl. Pol. Sci. 30 (1985), 3009-3022.

[133] M.A.M. Beerlage, Polyimide membranes for non-aqueous systems, Thesis, University Twente, 1994.

[134] H. Colquhoun, A. Simpson and K. Roberts, Production of membranes, WO 95/15808 (1995).

[135] H.G. Hicke, I. Lehmann, G. Malsch, M. Ulbricht and M. Becker, Preparation and characterization of a novel solvent-resistant and autoclavable polymer membrane, J. Membr. Sci., 198 (2002), 187-196.

[136] T. Sano, T. Shimomura, M. Sasaki and I. Murase, Semipermeable membranes based on acrylonitrile polymers, US Pat. 4,272,378 (1981).

[137] G.S. Misra, VDN. Bajpai, Redox polymerization, Prog. Polym. Sci. 8 (1982) 61-131.

[138] G.S. Misra, Encyclopedia Polym. Sci. 8 (1985-1989), 61-131.

[139] J.W. Vanderhoft, In: G.E. Ham, editor, Vinyl polymerization, New York: Marcel Dekker, 1969 [Chapter 1].

[140] V.S. Ananthanarayanan, M. Santappa, J. Appl. Polym. Sci. 9 (1965), 2347.

[141] S.B. Hanna, W.R. Carrol, S. Attiga, W.H. Webb, Z Naturforsch, B Anorg Chem 30 (1975), 409.

[142] G. Renders, G. Broze, R. Jerome, Ph. Teyssie, J. Macromol. Sci. Chem. A 16 (1981), 1399.

[143] M. Fernandez, T. Fernandez, M.J. Fernandez, G.M. Guzman, Polymerization of methyl methacrylate initiated by a ceric ion-isopropyl alcohol redox system, J. Polym. Sci. Chem. Ed 22 (1984), 2729.

[144] K.C. Gupta, K. Behari, Cerium (IV)-2-chloroethanol redox-pair initiated polymerization of arylamide in aqueous medium, J. Polym. Sci. 24 (1986), 767.

[145] M.N. Fernandez, G.M. Guzman, Aqueous polymerization of methyl methacrylate initiated by Ce(IV)-alcohol redox system: Effect of acid concentration and additives, J. Polym. Sci. 27 (1989), 2427.

[146] M.N. Fernandez, G.M. Guzman, Aqueous polymerization of methyl methacrylate initiated by Ce(IV)-isopropyl alcohol. Kinetics and molecular weight, J. Polym. Sci. 27 (1989), 3703.

[147] M.N. Fernandez, A. Pelayo, T.F. Otero, G.M. Guzman, J. Polym. Sci., Polym. Lett. Ed. 23 (1985), 79.

[148] N. Mohanty, B. Pradhan, M.C. Mohanta, Eur. Polym. J. 15 (1979), 743.

[149] N. Mohanty, B. Pradhan, M.C. Mohanta, J. Macromol. Sci. A 19(2) (1983), 283.

[150] A. Jayakrishnan, M. Haragopal, V. Mahadevan, J. Polym. Sci. 19 (1981), 1147.

[151] A. Rout, S.P. Rout, B.C. Singh, M. Santappa, Makromol. Chem. 178 (1977), 639.

[152] S.V. Subramanian, M. Santappa, Makromal. Chem. 112 (1968), 1.

[153] S.V. Subramanian, M. Santappa, J. Polym. Sci., Part A-1 6 (1968), 493.

[154] S.K. Saha, A.K. Chaudhuri, J. Polym. Sci. Polym. Chem. Ed. 10 (1972), 797.

[155] A.S. Sarac, H. Basak, A.B. Soydan, A. Akar, Die Angew. Makromol. Chem. 198 (1992), 191.

[156] C. Erbil, B. Ustamehmetoglu, G. Uzelli, A.S. Sarac, Eur. Polym. J. 30 (1994), 149.

[157] A.S. Sarac, B. Ustamehmetoglu, C. Erbil, Polym. Bull 32 (1994), 91.

[158] S. Bayulken, A.S. Sarac, Zeit fuer Phys. Chem. 205 (1998), 181.

[159] C. Erbil, A.B. Soydan, A.Z. Aroguz, A.S. Sarac, Die Angew. Makromol. Chem. 213 (1993), 55.

[160] C. Erbil, C. Cin, A.B. Soydan, A.S. Sarac, J. Appl. Polym. Sci. 47 (1993), 1643.

[161] A.S. Sarac, C. Erbil, A.B. Soydan, J. Appl. Polym. Sci. 44 (1992), 877.

[162] U.D.N. Bajpai, A. Ahi, Appl. Polym. Sci. 40 (1990), 359.

[163] M.D. Fernandez, G.M. Guzman, J. Polym. Sci. Part A: Polym. Chem. 27 (1989), 2427.

[164] R.K. Samal, M.C. Nayak, G.V. Suryanarayan, G. Panda, D.P. Das, J. Polym. Sci. Polym. Chem. Ed. 9 (1981), 2759 and references cited therein.

[165] R. Shulz, G. Renner, A. Henglein, W. Kern, Makromol. Chem. 12 (1954), 20.

[166] C.H. Bamford, A.D. Jenkins, R. Johnston, Proc. R. Soc. London Ser. A, 239 (1957), 214.

[167] M.M. Hussain, A. Gupta, Makromol. Chem. 29 (1977), 178.

[168] K. Kishore, V.A. Bhanu, J. Polym. Sci. Polym. Chem. Ed. 24 (1986), 379 and references cited therein.

[169] Y. Tatsukami, H. Yoshioka, Makromol. Chem. 181 (1980), 1107.

[170] J. Furukawa, T. Tsuruta, J. Polym. Sci. 28 (1958), 227.

[171] G.G. Reddy, T. Nagbhushanam, V.K. Rao, M. Santappa, Polymer 22 (1980), 1692.

[172] Goldfinger G, Gilbert RD. In: Mark HF, Gaylond NG, editors. Inhibition and retardation; encyclopedia of polymer science and technology, vol. 7. New York: Wiley Interscience, (1969).

[173] V.A. Bhanu, K. Kishore, A demonstration of the inhibitory role of oxygen during the room temperature radical polymerization of styrene initiated by cobalt (II)-sodium borohydride redox system, Macromolecules 22 (1989), 3491.

[174] G. M. Cruise, D. S. Scharp, J. A. Hubbell, Characterization of permeability and network structure of interfacially photopolymerized poly(ethylene glycol) diacrylate hydrogels, Biomaterials 19 (1998), 1287.

[175] S. H. Kim, C. Y. Won, C. C. Chu, Synthesis and Characterization of Dextran-maleic acid based Hydrogel, J. Biomed. Mater. Res., 46 (1999), 160.

[176] S. Jo, H. Shin, A. K. Shung, J. P. Fisher, A. G. Mikos, Synthesis and Characterization of Oligo(Poly(Ethylene Glycol) Fumarate) Macromer, Macromolecules, 34 (2001), 2839.

[177] H. Y. Kweon, M. K. Yoo, I. K. Park, T. H. Kim, H. C. Lee, H. S. Lee, J. S. Oh, T. Akaike, C. S. Cho, A novel degradable polycaprolactone network for tissue engineering, Biomaterials, 24 (2003), 801.

[178] E. Jabbari, S. Wang, L. Lu, J. A. Gruetzmacher, S. Ameenuddin, T. E. Hefferan, B. L. Currier, A. J. Windebank, M. J. Yaszemski, Synthesis, material properties, and biocompatibility of a novel self-cross-linkable poly(caprolactone fumarate) as an injectable tissue engineering scaffold, Biomacromolecules, 6 (2005), 2503.

[179] T. Ono, T. Sugimoto, S. Shinkai, K. Sada, Lipophilic polyelectrolyte gels as super-absorbent polymers for nonpolar organic solvents, Nat. Mater. 6 (2007), 429.

[180] L. Cai, S. F. Wang, Elucidating Colorization in the Functionalization of Hydroxyl-Containing Polymers Using Unsaturated Anhydrides/Acyl Chlorides in the Presence of Triethylamine, Biomacromolecules 11 (2010), 304.

[181] X. Qiao, T.S. Chung, K.P. Pramoda, Fabrication and characterization of BTDA-TDI/MDI (P84) co-polyimide membranes for pervaporation dehydration of isopropanol, J. Membr. Sci. 264 (2005), 176.

[182] J. Wang, Z. Yue, J. S. Ince, J. Economy, Preparation of nanofiltration membranes from polyacrylonitrile ultrafiltration membranes, J. Membr. Sci. 286 (2006), 333.

[183] F.U. Hsieh, T. Matsuura, S. Sourirajan, Reverse osmosis separation of polyethylene glycols in dilute aqueous solution using porous cellulose acetate membranes, J. Appl. Polym. Sci. 23 (1979), 561-573.

[184] M. Meireles, A. Bessieres, I. Rogissart, P. Aimar, V. Sanchez, An appropriate molecular size parameter for porous membranes calibration, J. Membr. Sci. 103 (1995), 105-115.

[185] F.-U. Hsieh, T. Matsuura, S. Sourirajan, Analysis of Reverse osmosis data for the system polyethylene glycol-water-cellulose acetate membrane at low operating pressures, Ind. Eng. Chem. Process Des. Dev. 18 (1979), 414-423.

[186] A. Bessieres, M. Meireles, R. Coratger, J. Beauvillain, V. Sanchez, Investigations of surface properties of polymeric membranes by near field microscopy, J. Membr. Sci. 109 (1996), 271-284.

[187] B. Van der Bruggen, J. Schaep, D. Wilms, C. Vandecasteele, Influence of molecular size, polarity and charge on the retention of organic molecules by nanofiltration, J. Membr. Sci. 156 (1999), 29-41.

[188] M.A.M. Beerlage, Polyimide ultrafiltration membranes for non-aqueous systems, Ph.D. Thesis, University of Twente Enschede, 1994.

[189] Y.H. See Toh, F.W. Lim, A.G. Livingston, Polymeric membranes for nanofiltration in polar aprotic solvents, J. Membr. Sci. 301 (2007), 3-10

[190] E. Gibbins, M. D'Antonio, D. Nair, Obervations on solvent flux and solute rejection across solvent resistant nanofiltration membranes, Desalination 147 (2002), 307-313.

[191] D.R. Machado, D. Hasson and R. Semiat, Effect of solvent properties on permeate flow through nanofiltration membranes. Part I. Investigation of parameters affecting solvent flux, J. Membr. Sci., 163 (1999), 93–102.

[192] J.A. Whu, B.C. Baltzis and K.K. Sirkar, Nanofiltration studies of larger organic microsolutes in methanol solutions, J. Membr. Sci., 170 (2000), 159–172.

[193] J.Brandrup, E.H.Immergut, E.A. Grulke, Polymer Handbook 4th edition, (1999).

[194] M. Kumar, S. Singh, V.K. Shahi, Cross-Linked poly(vinyl alcohol)-poly(acrylonitrile-co-2-dimethylamino ethylmethacrylate) based anion-exchange membranes in aqueous media, J. Phys. Chem. B, 114 (2010), 198-206.

[195] C.M. Hansen, Hansen Solubility Parameters, (2007)

[196] adapted from the website www.kochmembrane.com

Appendix-1
List of abbreviations

AN	acrylonitrile
CTA	cellulose triacetate
HEMA	hydroxylethyl methacrylate
AMPS	2-acrylamido-2-methyl-propanesulfonic acid
AIBN	azobisisobutyronitrile
CL	cross-linker
DMF	dimethylformamide
DMAc	dimethylacetamide
NMP	N-methylpyrrolidone
DMOS	dimethyl sulfoxide
EA	ethyl acetate
MF	microfiltration
UF	ultrafiltration
NF	nanofiltration
RO	reverse osmosis
SRNF	solvent resistant nanofiltration
PAN	polyacrylonitrile
PAH	poly(amide hydrazide)
PC	polycarbonate
PEG	poly(ethylene glycol)

PEO	poly(ethylene oxide)
PES	poly(ether sulfone)
PI	polyimide
PS	polystyrene
PVA	poly(vinyl alcohol)
PVDF	poly(vinylidene fluoride)
PP	polypropylene
NIPS	non-sovlent induced phase separation
PSf	polysulfone
MDC	malonyl dichloride´
PDI	polydispersity index
MWCO	molecular weight cut-off
TOABr	tetraoctylammoniumbromide
TBABr	tetrabutylammoniumbromide

Appendix-2
List of conferences

2011 ICOM 2011, Amsterdam, Netherlands.

"Novel cross-linkable polymeric membranes for organophilic ultra- and/or nanofiltration" (poster paper)

2009 Euromembrane 2009, Montpellier, France

"Novel cross-linkable copolymer membranes for organophilic ultra- and nanofiltration" (poster paper)

Appendix-3
Curriculum Vitae

Name: Zhaoqing Pei

Place/Date of Birth: Hebei, China/29, Oct, 1982

Educational Background

2008-2012 (Ph.D): Technical Chemistry, University of Duisburg-Essen, Germany.

Advisor: Prof. Dr. Mathias Ulbricht

2005-2008 (M.Sc.): Material Science, Northwestern Polytechnical Univeristy, Xi'an, China.

Advisor: Prof. Dr. Rumin Wang

2001-2005 (B.Sc.): Polymer Science and Technology, Northwestern Polytechnical University, Xi'an, China